Copy 6
RM L55F06

NACA RM L55F06

NACA

RESEARCH MEMORANDUM

EFFECTS OF LEADING-EDGE RADIUS ON THE LONGITUDINAL STABILITY OF TWO 45° SWEPTBACK WINGS AS INFLUENCED BY REYNOLDS NUMBERS UP TO 8.20×10^6 AND MACH NUMBERS UP TO 0.303

By Gerald V. Foster and William C. Schneider

Langley Aeronautical Laboratory
Langley Field, Va.

NATIONAL ADVISORY COMMITTEE
FOR AERONAUTICS

WASHINGTON
July 28, 1955

NACA RM L55F06

NATIONAL ADVISORY COMMITTEE FOR AERONAUTICS

RESEARCH MEMORANDUM

EFFECTS OF LEADING-EDGE RADIUS ON THE LONGITUDINAL STABILITY OF TWO 45° SWEPTBACK WINGS AS INFLUENCED BY REYNOLDS NUMBERS UP TO 8.20×10^6 AND MACH NUMBERS UP TO 0.303

By Gerald V. Foster and William C. Schneider

SUMMARY

An investigation to show the effects of systematic changes of leading-edge radius, aspect ratio, Reynolds number, and Mach number on the static longitudinal aerodynamic characteristics of sweptback wings has been conducted in the Langley 19-foot pressure tunnel. As a part of this investigation, tests have been completed on several wings of aspect ratios 3 and 5 having 45° sweepback of the quarter-chord line and 9-percent-thick symmetrical airfoil sections. The range of Reynolds numbers obtained for these tests were 0.76×10^6 to 5.50×10^6 at atmospheric pressure and 1.74×10^6 to 8.20×10^6 at 33 pounds per square inch absolute; corresponding ranges of Mach number were 0.057 to 0.303 and 0.041 to 0.193, respectively.

In general, the results tend to indicate that, for a sweepback angle of 45°, the boundary between a leading-edge type of separation and a trailing-edge type of separation (as expressed in terms of leading-edge radius and sweep angle) is somewhat broader than is indicated in NACA RM L52D16.

A decrease in leading-edge radius for either the aspect-ratio-3 wing or the aspect-ratio-5 wing (within the limits of the investigation) hastened the onset of changes in the longitudinal stability characteristics associated with flow separation.

For a given Mach number, the lift coefficient associated with marked changes of stability increased with Reynolds number, whereas an increase in Mach number (for a constant Reynolds number) had an adverse effect and tended to decrease the inflection lift coefficient.

INTRODUCTION

Sweepback generally produces nonlinear pitching-moment characteristics, below the maximum lift coefficient, which are associated with the processes of boundary-layer thickening and separation. Swept-wing boundary layers have a greater complexity than those of unswept wings because of a pressure gradient normal to the main stream and a curvature of the streamlines of the nonviscous flow in the lateral plane. Reference 1 has indicated that the flow separation experienced on swept wings is influenced mainly by leading-edge radius, leading-edge sweep angle, aspect ratio, and Reynolds number. In order to gain further knowledge of the influence of these parameters on the longitudinal aerodynamic characteristics of wings, a series of wings designed to have a systematic variation of leading-edge radius and aspect ratio has been tested in the Langley 19-foot pressure tunnel at various Mach numbers and Reynolds numbers.

This report shows the effects of these variables on the static longitudinal stability characteristics of several uncambered wings having aspect ratios of 3 and 5. The wings had 45° sweepback, a maximum thickness ratio of 9 percent chord, and leading-edge radii of 0.89, 0.50, and 0.25 percent chord. Tests were conducted at tunnel pressures of 14.7 and 33 pounds per square inch absolute, which permitted ranges of Reynolds number from 0.76×10^6 to 5.50×10^6 (Mach numbers from 0.057 to 0.303) and from 1.74×10^6 to 8.20×10^6 (Mach numbers from 0.041 to 0.193), respectively.

SYMBOLS

C_L	lift coefficient, Lift/qS
$C_{L_{inf}}$	inflection lift coefficient
C_m	pitching-moment coefficient about $0.25\bar{c}$, $\frac{\text{Pitching moment}}{q\bar{c}S}$
S	wing area, sq ft
$\bar{c}$	mean aerodynamic chord, $\frac{2}{S}\int_0^{b/2} c^2 dy$, ft
c	local wing chord parallel to plane of symmetry, ft

y	spanwise ordinate normal to plane of symmetry, ft
b	wing span, ft
q	free-stream dynamic pressure, $\frac{1}{2}\rho V^2$, lb/sq ft
ρ	density of air, slugs/cu ft
V	free-stream velocity, ft/sec
R	Reynolds number
M	Mach number
$\Lambda_{c/4}$	sweepback of quarter-chord line, deg
A	aspect ratio, b^2/S
x	chordwise ordinate of airfoil section, ft
z	vertical ordinate of airfoil section, ft

Subscripts:

s	stable break
u	unstable break

MODEL

Six wings were tested during this investigation. The principal dimensions of the wings are shown in figure 1 and the principal geometric characteristics of these wings are given in the following table:

Wing	$\Lambda_{c/4}$	Aspect ratio	Taper ratio	Leading-edge radius	Airfoil Section
1	45°	5	0.286	0.0089c	NACA 0009-63
2	45°	3	.500	.0089c	NACA 0009-63
3	45°	5	.286	.0050c	NACA 0009-(4.53)3
4	45°	3	.500	.0050c	NACA 0009-(4.53)3
5	45°	5	.286	.0025c	NACA 0009-(3.18)3
6	45°	3	.500	.0025c	NACA 0009-(3.18)3

It should be pointed out that the aspect ratio was changed by removing the wing tips. Thus, the taper ratio for the aspect-ratio-5 wing differs from that of the aspect-ratio-3 wing. The NACA four-digit-series airfoil section parallel to the air stream was chosen since there was a systematic procedure for varying the leading-edge radius, the location and the magnitude of the maximum thickness constant (ref. 2) being kept constant.

TESTS AND CORRECTIONS

Tests

Tests were conducted at stagnation pressures of 14.7 and 33 pounds per square inch absolute through a large part of the tunnel speed range. This permitted Reynolds number and Mach number variations as follows:

Stagnation pressure, lb/sq in. abs	R		M	
	A = 5	A = 3	A = 5	A = 3
14.7	0.76×10^6 to 5.39×10^6	1.63×10^6 to 5.50×10^6	0.057 to 0.303	0.079 to 0.280
33	1.74×10^6 to 7.97×10^6	3.01×10^6 to 8.20×10^6	0.041 to 0.193	0.063 to 0.180

The model was supported on the normal two-support system of the Langley 19-foot pressure tunnel.

The contours of the wing were carefully constructed so that the airfoils are believed to be very accurate. Particular emphasis was placed on the coordinates near the leading edge, where the accuracy is within 0.05 percent of the chord.

CORRECTIONS

The pitching-moment data and values of angle of attack have been corrected for tunnel wall effects by the method of reference 3. Inasmuch as interest in these data rested primarily in the variations of lift and pitching moment rather than in the absolute values, tests to determine the model-support tare and interference effects were not conducted. The zero-lift pitching-moment coefficient gave an indication of the combined effects of model-support tare and interference, and model asymmetry.

The curves of pitching-moment coefficient against lift coefficient were shifted toward the origin by a constant increment in pitching-moment coefficient equal to the average of the values obtained at zero lift. This correction involves the assumption that the support tare and interference remains constant with lift coefficient. The following equations indicate the magnitude and manner of application of these corrections: For an aspect ratio of 3

$$C_m = C_{m_{gross}} + 0.0020C_L + (-0.004)$$

For an aspect ratio of 5

$$C_m = C_{m_{gross}} + 0.0055C_L + (-0.007)$$

The jet-boundary correction to the pitching-moment coefficient is a function of lift coefficient as can be seen in the above equations.

In most cases values of zero lift angle of attack were close to a mean value of 0.1° which was added to values of angle of attack to correct for airstream misalinement.

RESULTS AND DISCUSSION

The lift and pitching-moment characteristics obtained for the wings having NACA 0009-63, NACA 0009-(4.53)3, and NACA 0009-(3.18)3 airfoil sections are presented in figures 2 to 7 for the wings of aspect ratio 3, and figures 8 to 13 for the wings of aspect ratio 5. The effects of leading-edge radius on the static longitudinal stability characteristics are presented in figures 14 and 15. Results showing the interdependent effects of Reynolds number and Mach number on the longitudinal stability characteristics are presented in figures 16 to 19. (For simplicity nominal values of Reynolds number, or Mach number, or both, have been used in figures 16 to 19.) The variation of inflection lift coefficient with Reynolds number and Mach number is presented in figures 20 to 22 for wings of aspect ratio 5 and 3. The term "inflection" lift coefficient is used to designate the lift coefficient beyond which there is a marked change in the pitching-moment characteristics. Unstable inflection lift $C_{L_{inf_u}}$ is defined as the lift coefficient beyond which the change is destabilizing, while stable inflection lift $C_{L_{inf_s}}$ denotes a stabilizing change.

Effect of Leading-Edge Radius and Aspect Ratio

On the basis of the results of references 1 and 4, a change in wing leading-edge radius from 0.89 to 0.25 percent chord would be expected to result in a change from a trailing-edge type of separation to a leading-edge bubble type of separation. These types of separation are generally thought to have markedly different effects on the longitudinal stability characteristics of sweptback wings. Trailing-edge separation is commonly associated with pitch-up tendencies at or prior to maximum lift; whereas leading-edge separation can, for certain aspect ratios, be associated with a marked increase in longitudinal stability accompanied by an increase in lift-curve slope prior to maximum lift.

Within the range of the leading-edge radii investigated, characteristic pitching-moment curves were obtained for each aspect ratio. The pitching-moment curves of the aspect-ratio-3 wing (fig. 14) indicated stability changes which were previously mentioned as characteristic of leading-edge separation. In the case of the 0.25-percent-chord leading-edge radius, the lift curves also indicate the presence of this type of separation for Reynolds number of less than 6.63×10^6. (See figs. 6(a) and 6(b).) The lift characteristics for the two wings of aspect ratio 3 with larger leading-edge radii indicate a general tendency toward a loss in lift prior to the initial increase in stability; this loss in lift may arise from the effects of mixed type of separation. Exceptions to this, however, tend to occur with 0.50-percent-chord leading-edge radius at the lower Reynolds numbers of the investigation (figs. 4(a) and 4(b)).

Decreasing the leading-edge radius, within the limits of the investigation, hastened the onset of leading-edge separation. For example, at a Reynolds number of 3.1×10^6 and a Mach number of 0.148, decreasing the leading-edge radius of the wing of aspect ratio 3 from 0.89 to 0.25 percent chord resulted in a decrease in the inflection lift coefficient from about 0.68 to 0.52. (See fig. 14.)

At lift coefficients beyond the stable break in the pitching-moment curves for these aspect-ratio-3 wings, a point of destabilizing moment was reached $\left(C_{L_{inf_u}}\right)$ as the area of separated flow increased. In general, $C_{L_{inf_u}}$ increased with an increase in leading-edge radius.

An examination of the pitching-moment characteristics of the aspect-ratio-5 wings reveals that these wings exhibited destabilizing changes which were larger than those found for the wing of aspect ratio 3. Similarly, the stabilizing shift (where they are present) are of a much smaller and milder nature. The increase in aspect ratio, for a constant leading-edge radius, apparently promotes trailing-edge separation at the wing tips

which nullifies the effects of any leading-edge separation. This manifests itself as a destabilizing shift in the pitching-moment curves with a gradual decrease in lift-curve slope.

Decreasing the leading-edge radius of the aspect-ratio-5 wing resulted mainly in a decrease in the unstable inflection lift coefficient. This decrease is a result of the effect of nose shape on both leading- and trailing-edge-type separation. The effect of radius on leading-edge separation is, of course, obvious. The effect of radius on the trailing-edge type of separation is such that the loss in lift due to the thickening of the boundary layer counterbalances any increase in lift due to a leading-edge bubble. As an example of the effect of the decrease in leading-edge radius, figure 15(a) compares the data obtained at a Reynolds number of about 3.0×10^6 and a Mach number of 0.16. Decreasing the leading-edge radius from 0.89 to 0.25 percent chord caused a decrease in $C_{L_{inf_u}}$ from about 0.83 to 0.63.

In general, interpretation of the data presented herein for both the aspect-ratio-3 wing and the aspect-ratio-5 wing in terms of flow separation indicates that the boundary between the leading-edge type of separation and the trailing-edge type of separation (as expressed in terms of leading-edge radius and sweep angle) is somewhat broader for a sweepback angle of 45° than is shown in figure 5 of reference 1; thus, a wide region of mixed separation is indicated.

Effects of Reynolds Number and Mach Number

A comparison of the pitching-moment characteristics (figs. 16 to 19) for a wing of given aspect ratio and leading-edge radius indicates that the interrelated effects of Reynolds number and Mach number can have an important bearing on an analysis of flow separation. The results presented in figures 16 and 18 indicate that, in general, an increase in Reynolds number at a constant Mach number (within the limits of the investigation) delayed the changes in the pitching-moment characteristics associated with flow separation for the wings of aspect ratio 3 and 5. For example, at a Mach number of about 0.14, the lift coefficient at which marked unstable changes occurred for the wing of aspect ratio 5 and leading-edge radius of 0.25-percent chord (fig. 18(c)) increased from 0.62 to 0.75 with an increase in Reynolds number from 2.75×10^6 to 6.10×10^6. On the other hand, increasing the Mach number (within the limits of the investigation) tended to hasten the onset of flow separation (figs. 17 and 19). For instance, for the wing of aspect ratio 3 with a leading-edge radius of 0.25 percent chord (fig. 17(c)), the inflection lift coefficient $C_{L_{inf_s}}$ obtained at a constant Reynolds number of 4.06×10^6 was decreased from about 0.73 to 0.66 with an increase in Mach number from 0.10 to 0.20. The variation of inflection lift coefficient with

Reynolds number and Mach number as obtained at each tunnel pressure (figs. 20 to 22) indicate the interdependence of Mach number and Reynolds number effects. By comparing the inflection lifts at any Reynolds number, the effect of Mach number can be seen. Similarly, the effects of Reynolds number variation can be seen by comparing the inflection lift coefficients obtained at the two tunnel pressures at any given Mach number.

SUMMARY OF RESULTS

Force tests to determine the effects of changes of leading-edge radius from 0.89 to 0.25 percent chord on the low-speed longitudinal stability characteristics of wings having 45° sweepback and 9-percent-thick symmetrical airfoil sections were conducted at Reynolds numbers from 0.76×10^6 to 5.50×10^6 at atmospheric pressure and 1.74×10^6 to 8.20×10^6 at 33 pounds per square inch absolute; corresponding ranges of Mach number were 0.057 to 0.303 and 0.041 to 0.193, respectively.

In general, the results tend to indicate that, for sweepback of 45°, the boundary between leading-edge type of separation and trailing-edge type of separation (as expressed in terms of leading-edge radius and sweep angle) is somewhat broader than is indicated in NACA RM L52D16.

A decrease in leading-edge radius for either the aspect-ratio-3 wing or the aspect-ratio-5 wing (within limits of the investigation) hastened the changes in longitudinal stability characteristics associated with flow separation.

An increase in aspect ratio from 3 to 5 appeared to cause a trailing-edge type of separation over the tip sections before appreciable leading-edge separation developed.

For a given value of Mach number, the value of lift coefficient associated with marked changes of stability increased with Reynolds number, whereas an increase in Mach number for a constant Reynolds number had an adverse effect and tended to decrease the value of inflection lift.

Langley Aeronautical Laboratory,
National Advisory Committee for Aeronautics,
Langley Field, Va., May 26, 1955.

REFERENCES

1. Furlong, G. Chester, and McHugh, James G.: A Summary and Analysis of the Low-Speed Longitudinal Characteristics of Swept Wings at High Reynolds Number. NACA RM L52D16, 1952.

2. Stack, John, and Von Doenhoff, Albert E.: Tests of 16 Related Airfoils at High Speeds. NACA Rep. 492, 1934.

3. Sivells, James C., and Salmi, Rachel M.: Jet-Boundary Corrections for Complete and Semispan Swept Wings in Closed Circular Wind Tunnels. NACA TN 2454, 1951.

4. Cahill, Jones F., and Gottlieb, Stanley M.: Low-Speed Aerodynamic Characteristics of a Series of Swept Wings Having NACA 65A006 Airfoil Sections. NACA RM L50F16, 1950.

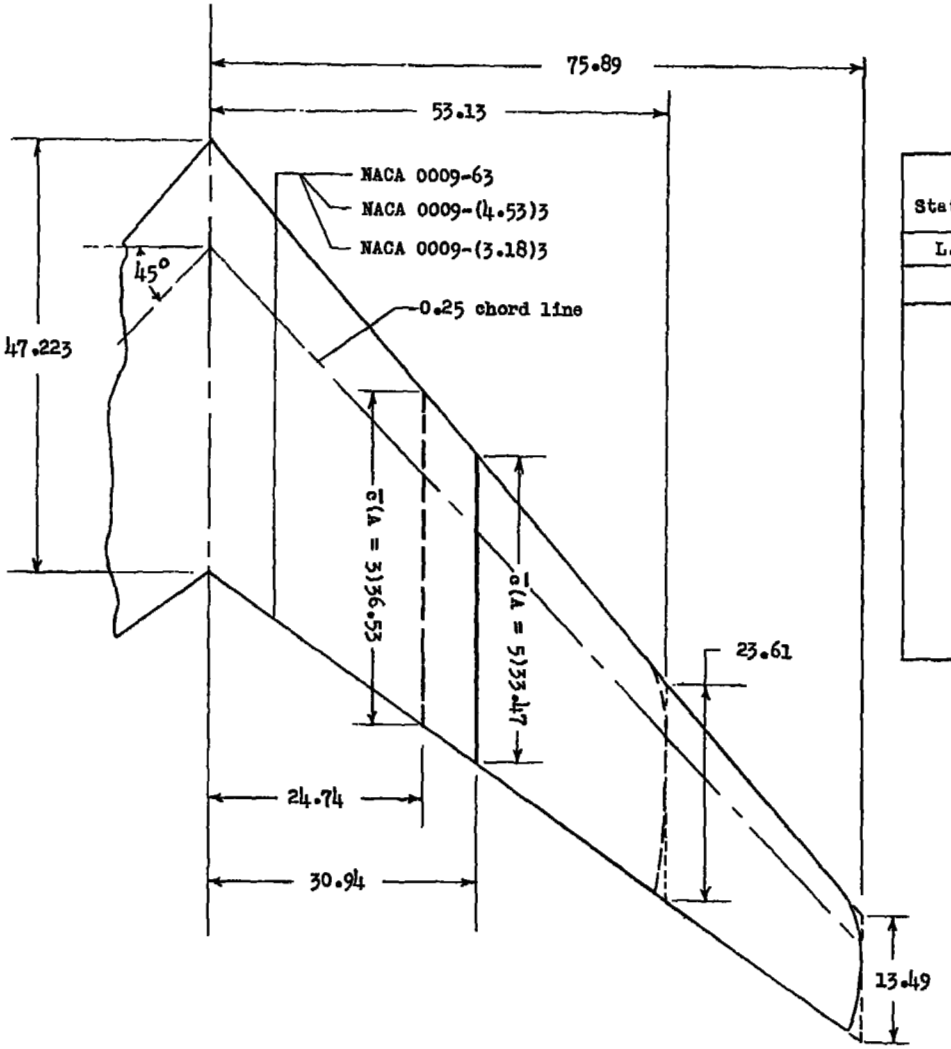

Ordinates of airfoils

Airfoil Station	0009-63	0009-(4.53)3	0009-(3.18)3
L. E. radius	0.0089c	0.0050c	0.0025c
x/c	z/c	z/c	z/c
0	0	0	0
.0125	.0144	.0120	.00994
.025	.0199	.0190	.01504
.0500	.0271	.0248	.02270
.0750	.0321	.0302	.02851
.1000	.0357	.0343	.03307
.1500	.0406	.0400	.03939
.2000	.0433	.0431	.04296
.3000	.0450	.0450	.04500
.4000		.0438	
.5000		.0406	
.6000		.0354	
.7000		.0286	
.8000		.0204	
.9000		.0111	
1.0000		.0009	

Figure 1.- Details of wings. All dimensions are in inches unless otherwise noted.

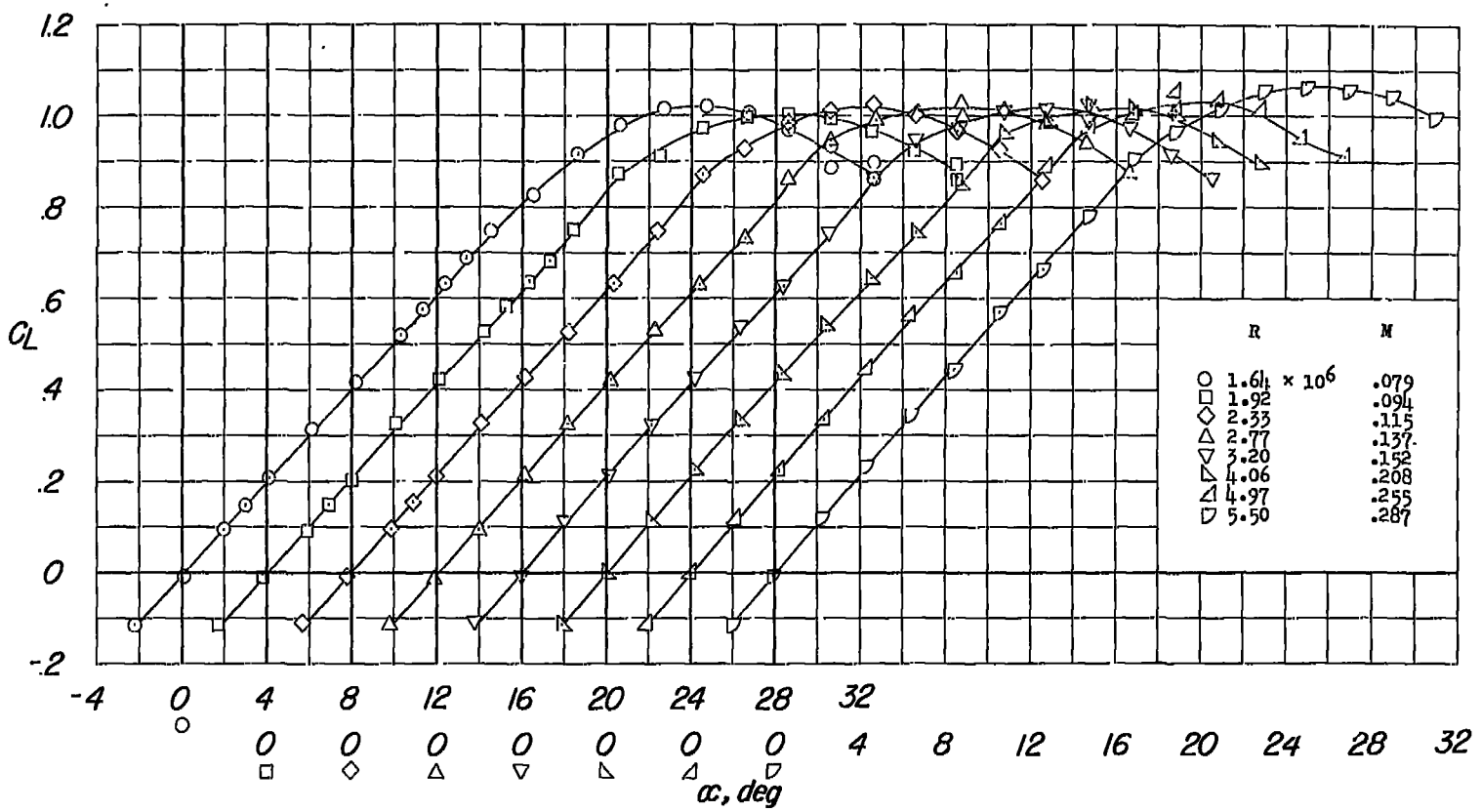

(a) C_L against α; atmospheric pressure.

Figure 2.- Variation of lift and pitching-moment coefficients with angle of attack of a 45° sweptback wing with an aspect ratio of 3 and a leading-edge radius of 0.0089c.

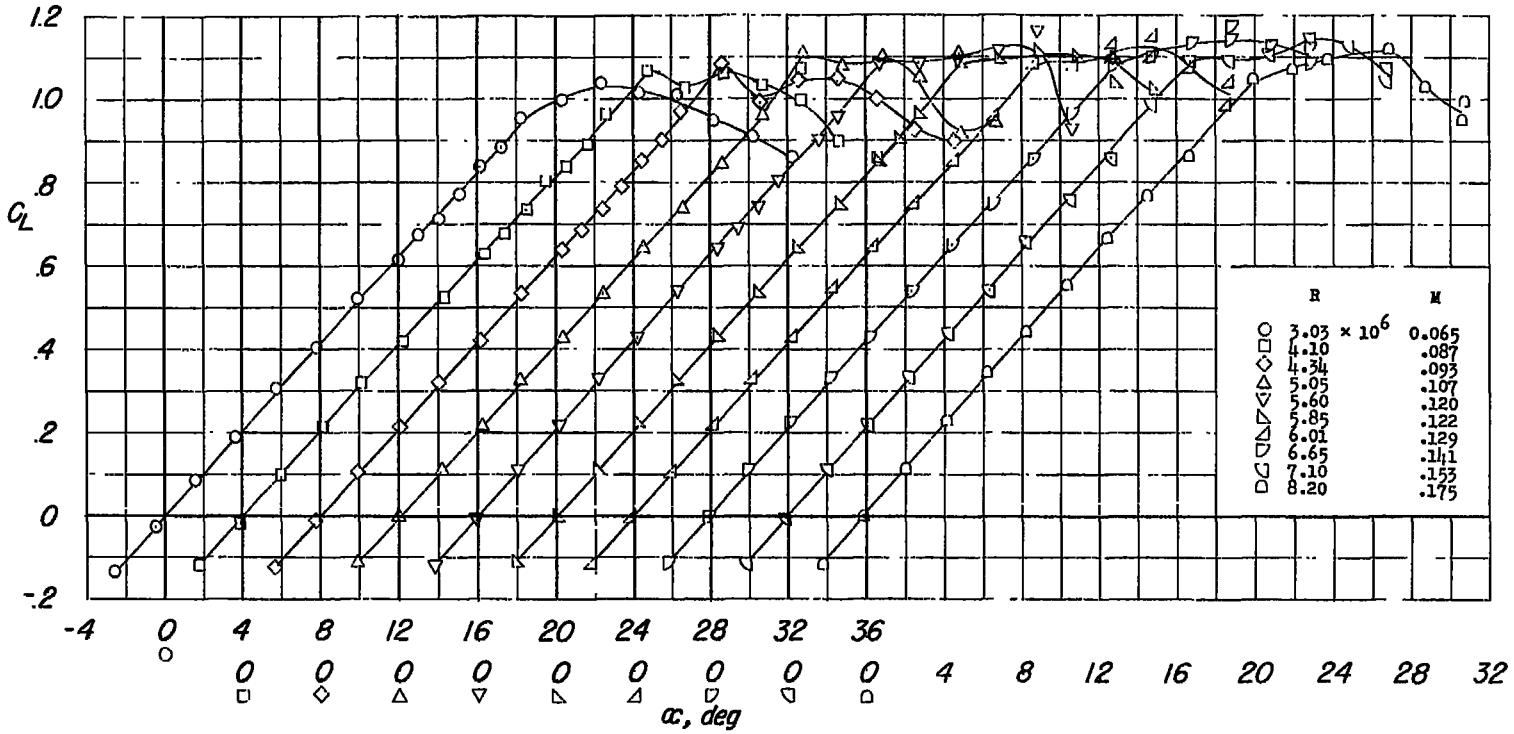

(b) C_L against α; pressure, 33 pounds per square inch.

Figure 2.- Continued.

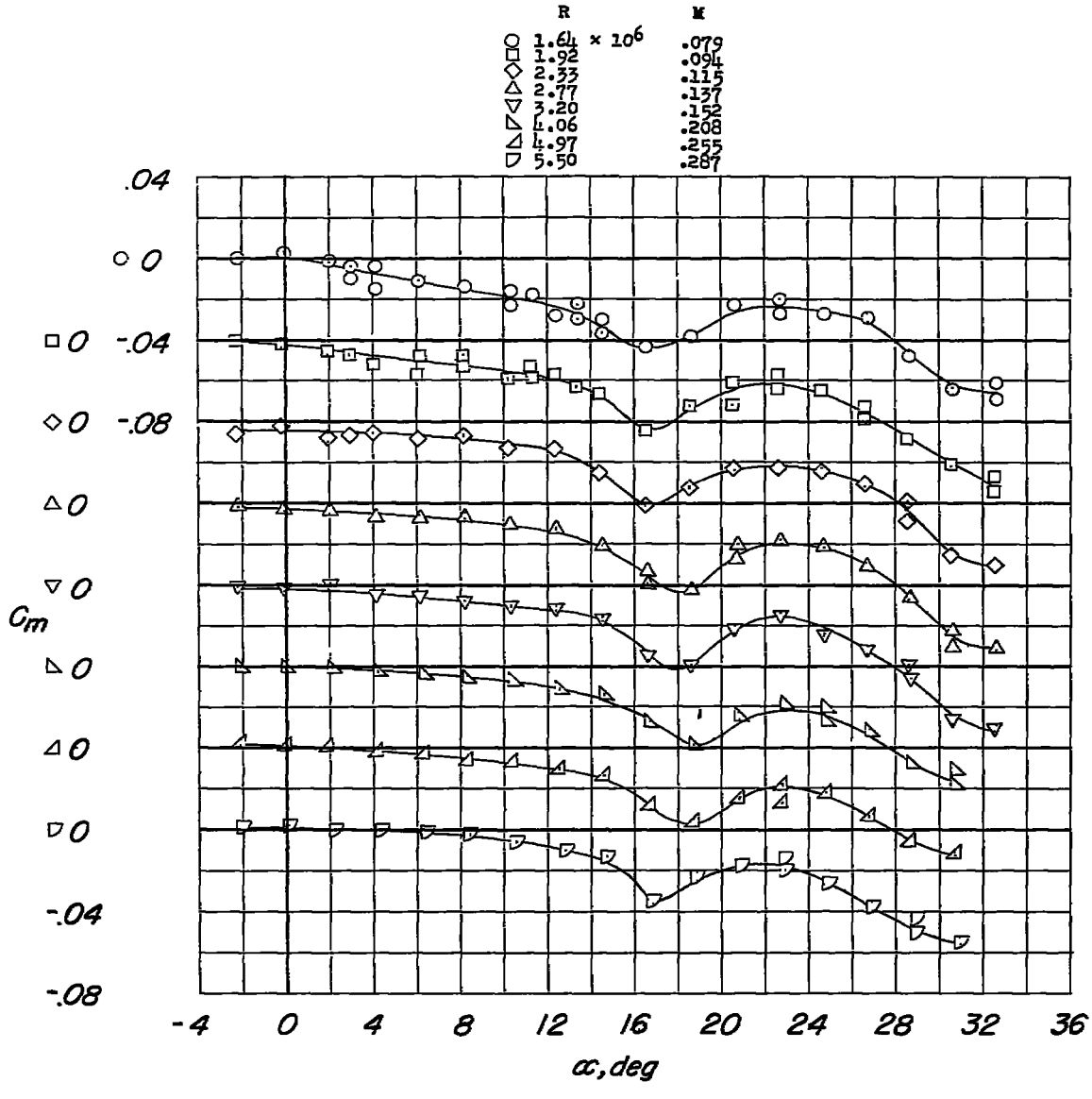

(c) C_m against α; atmospheric pressure.

Figure 2.- Continued.

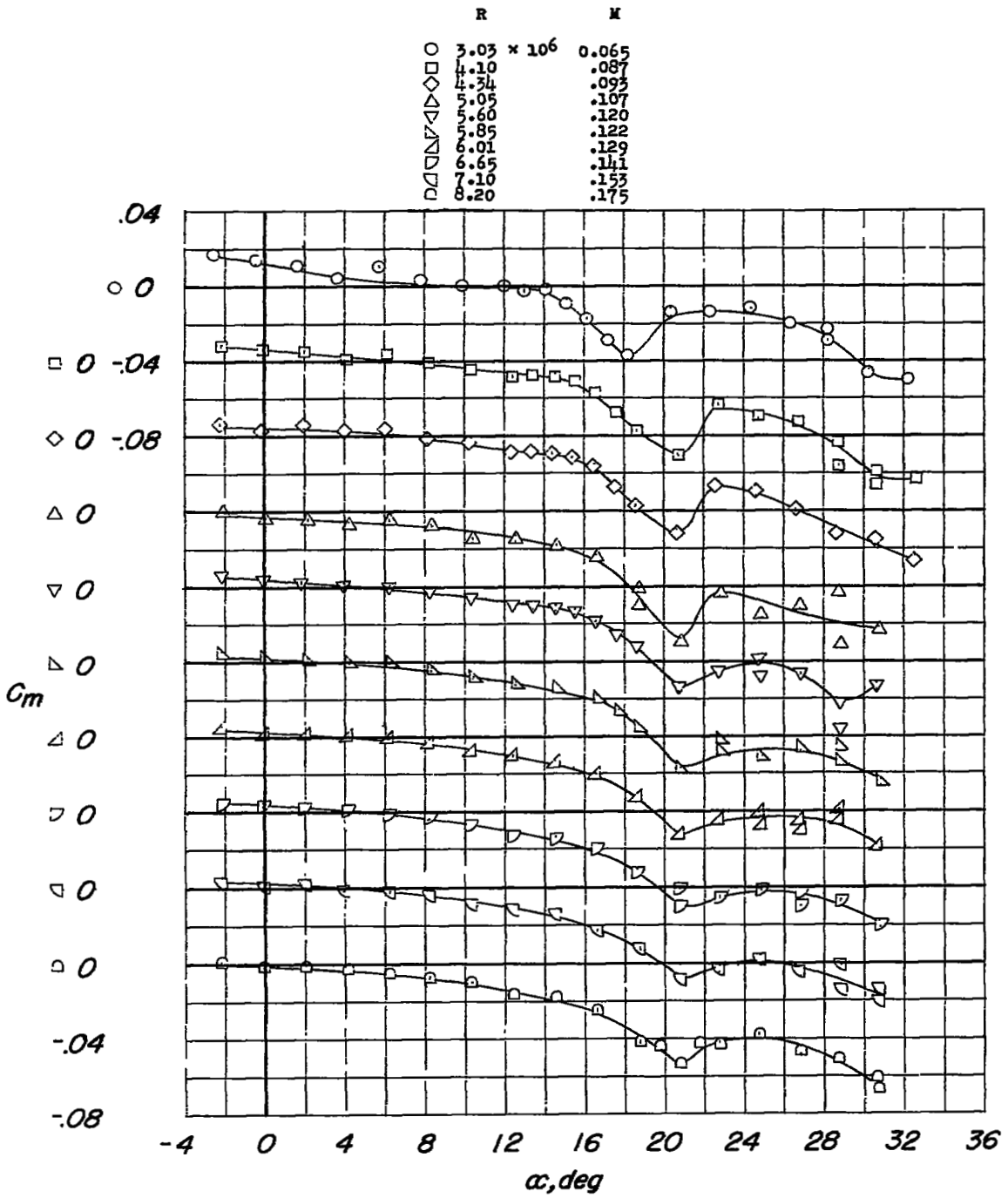

(d) C_m against α; pressure, 33 pounds per square inch.

Figure 2.- Concluded.

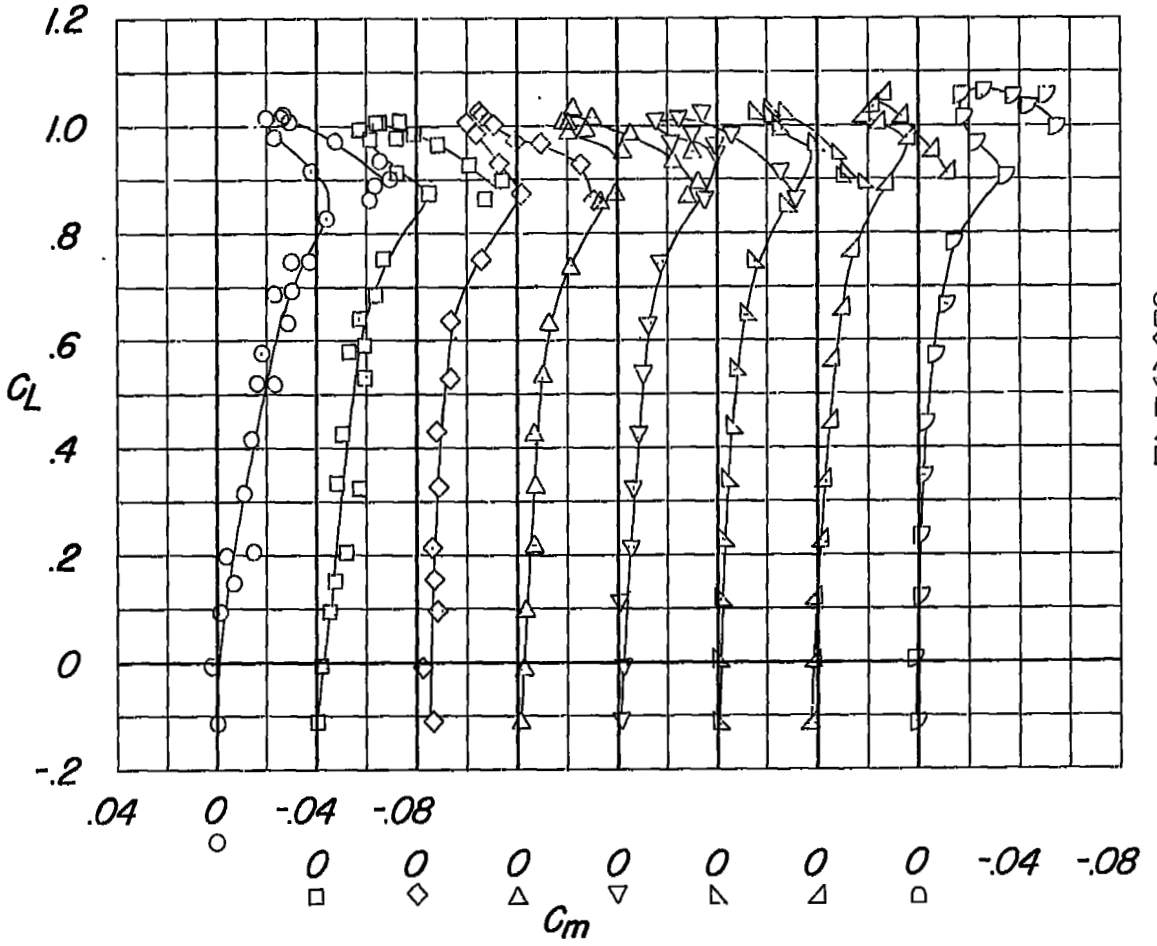

(a) Atmospheric pressure.

Figure 3.- Variation of pitching-moment coefficient with lift coefficient of a 45° sweptback wing with an aspect ratio of 3 and a leading-edge radius of 0.0089c.

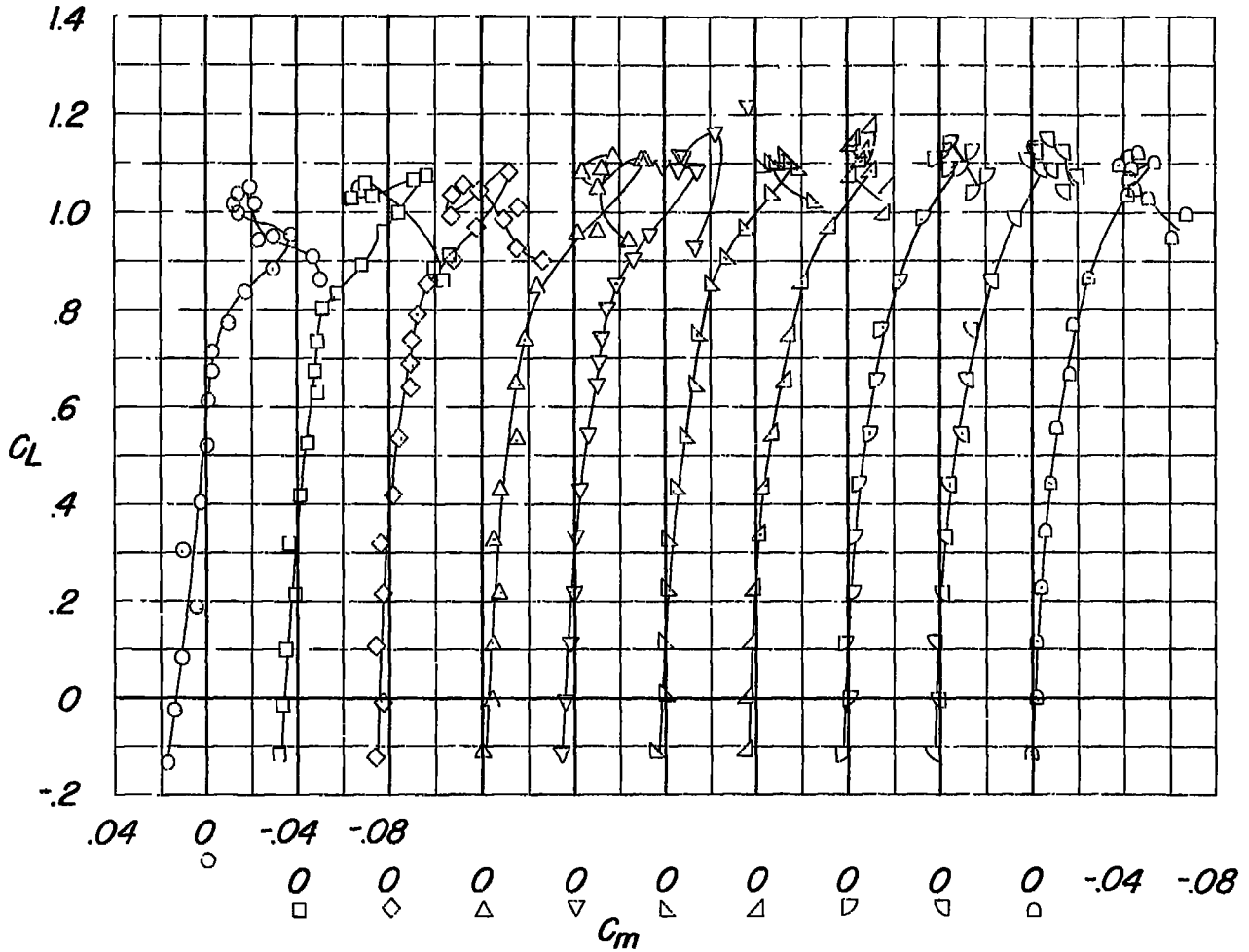

(b) Pressure, 33 pounds per square inch.

Figure 3.- Concluded.

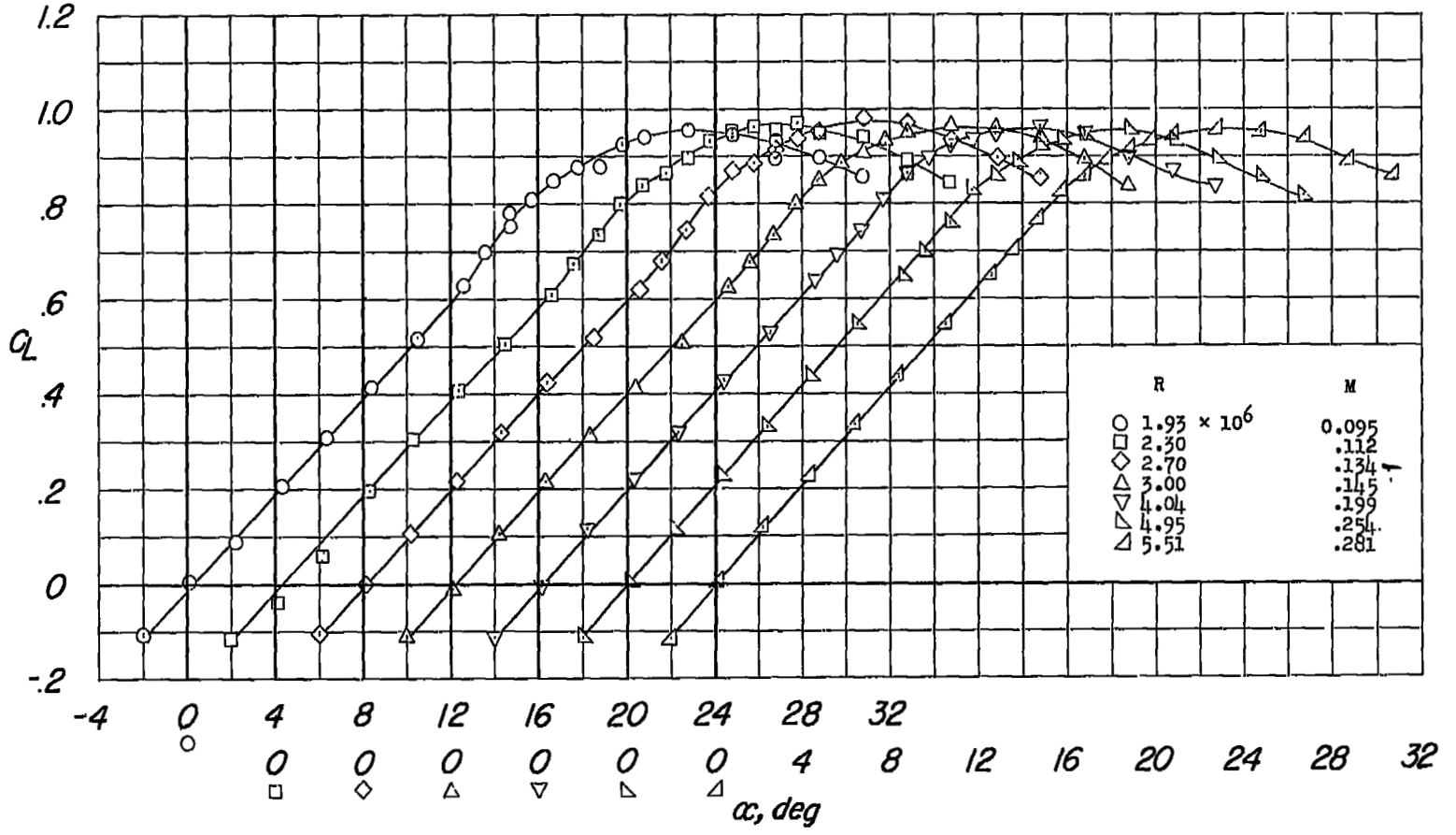

(a) C_L against α; atmospheric pressure.

Figure 4.- Variation of lift and pitching-moment coefficients with angle of attack of a 45° sweptback wing having an aspect ratio of 3 and a leading-edge radius of 0.0050c.

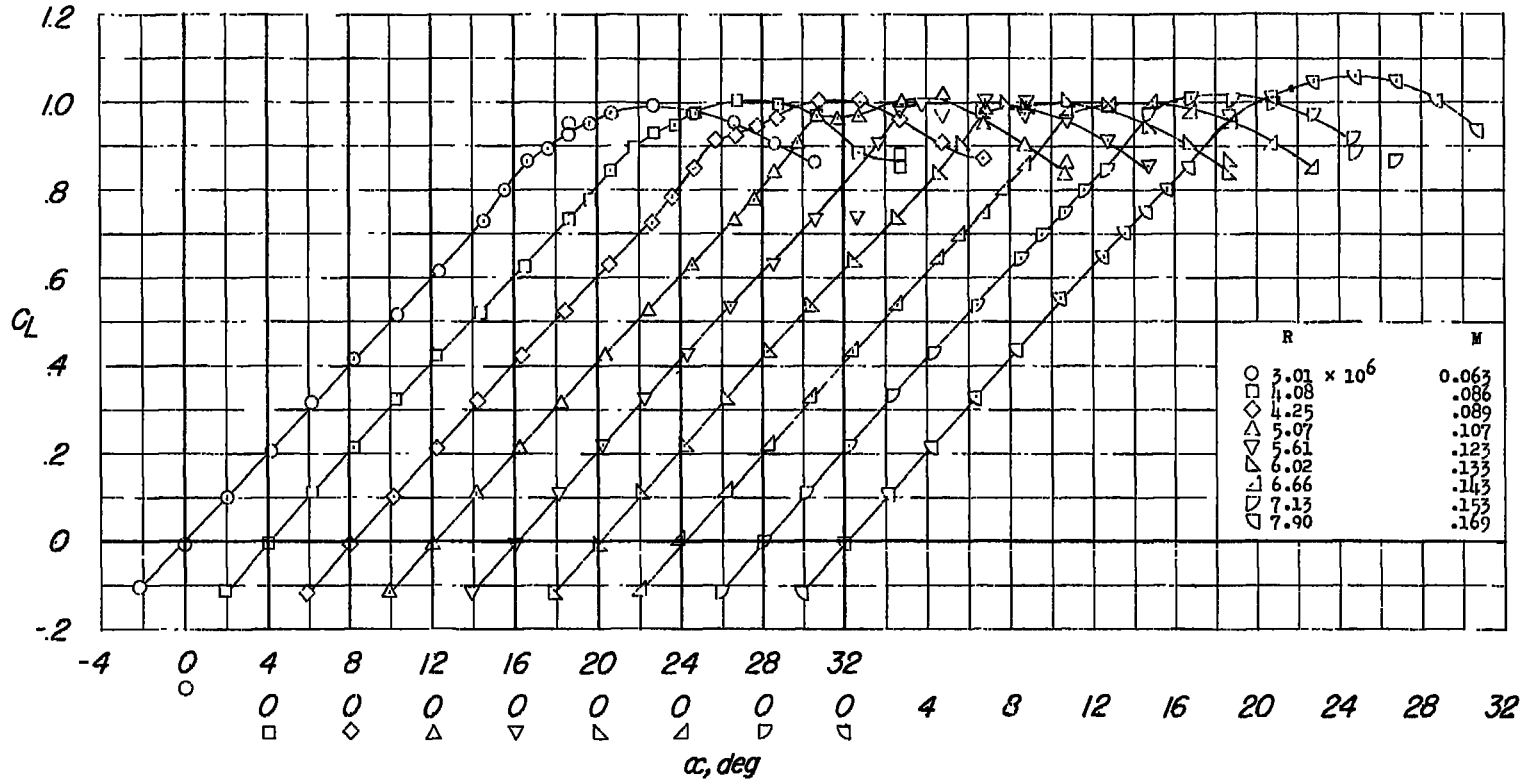

(b) C_L against α; pressure, 33 pounds per square inch.

Figure 4.- Continued.

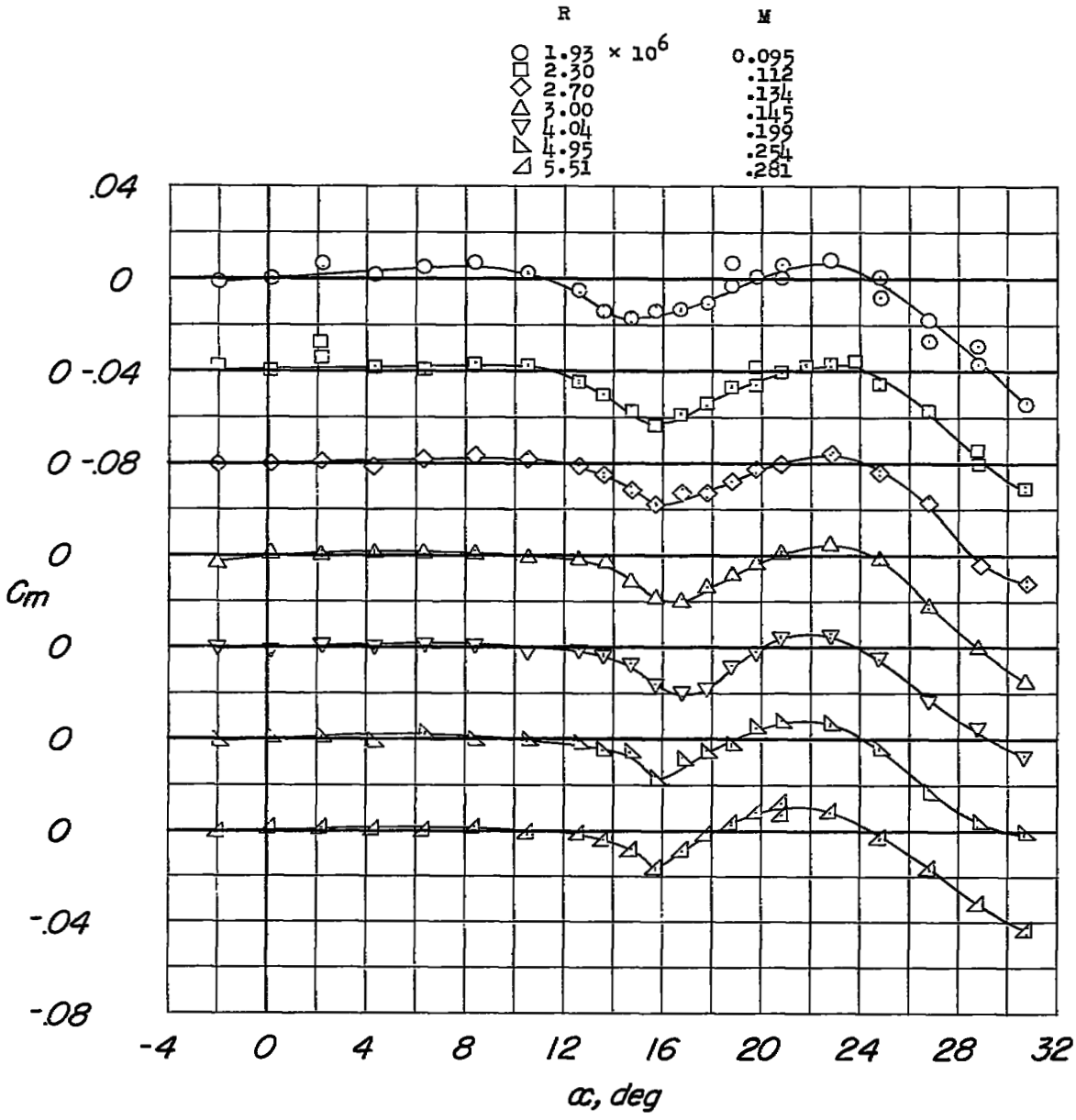

(c) C_m against α; atmospheric pressure.

Figure 4.- Continued.

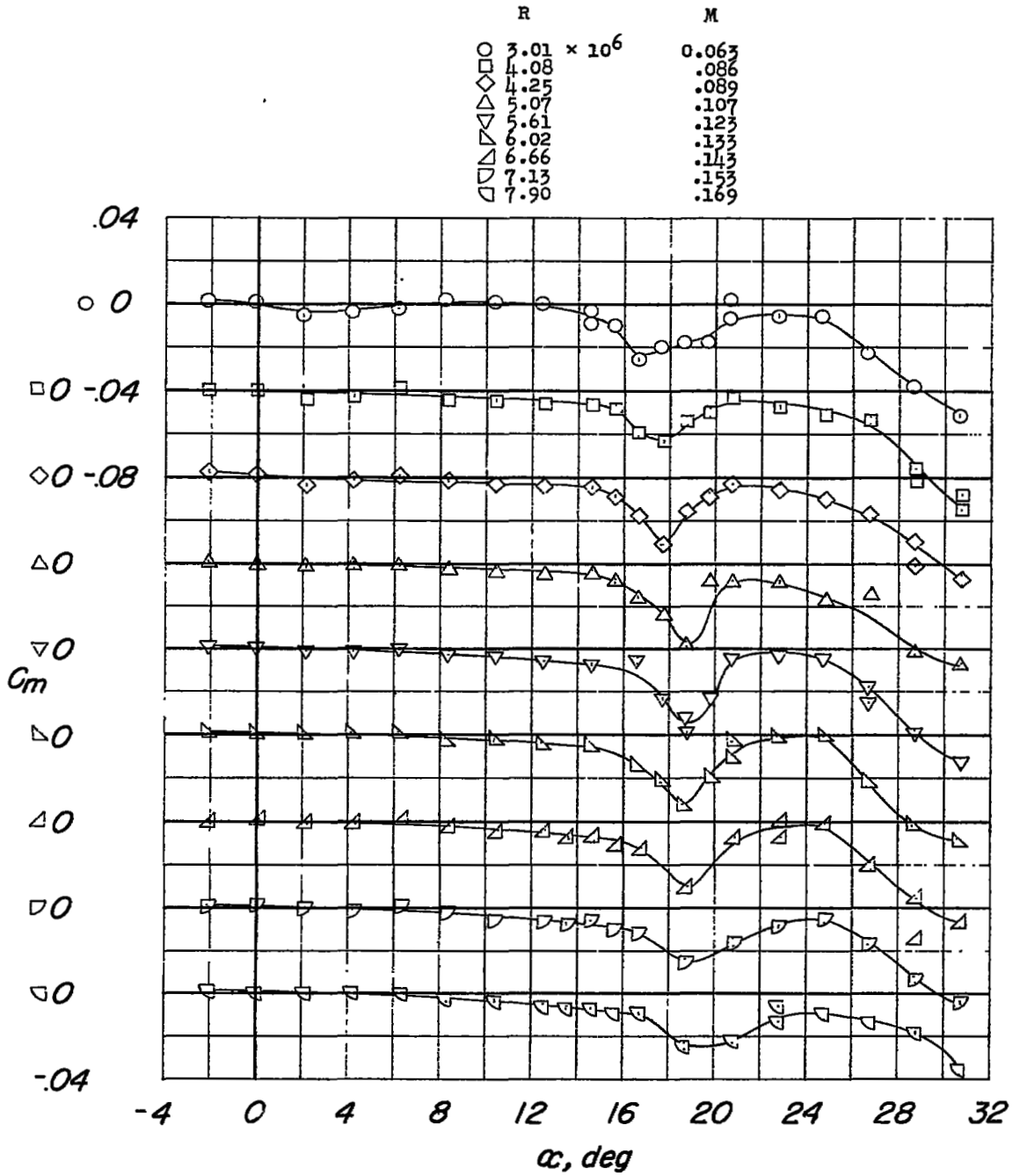

(d) C_m against α; pressure, 33 pounds per square inch.

Figure 4.- Concluded.

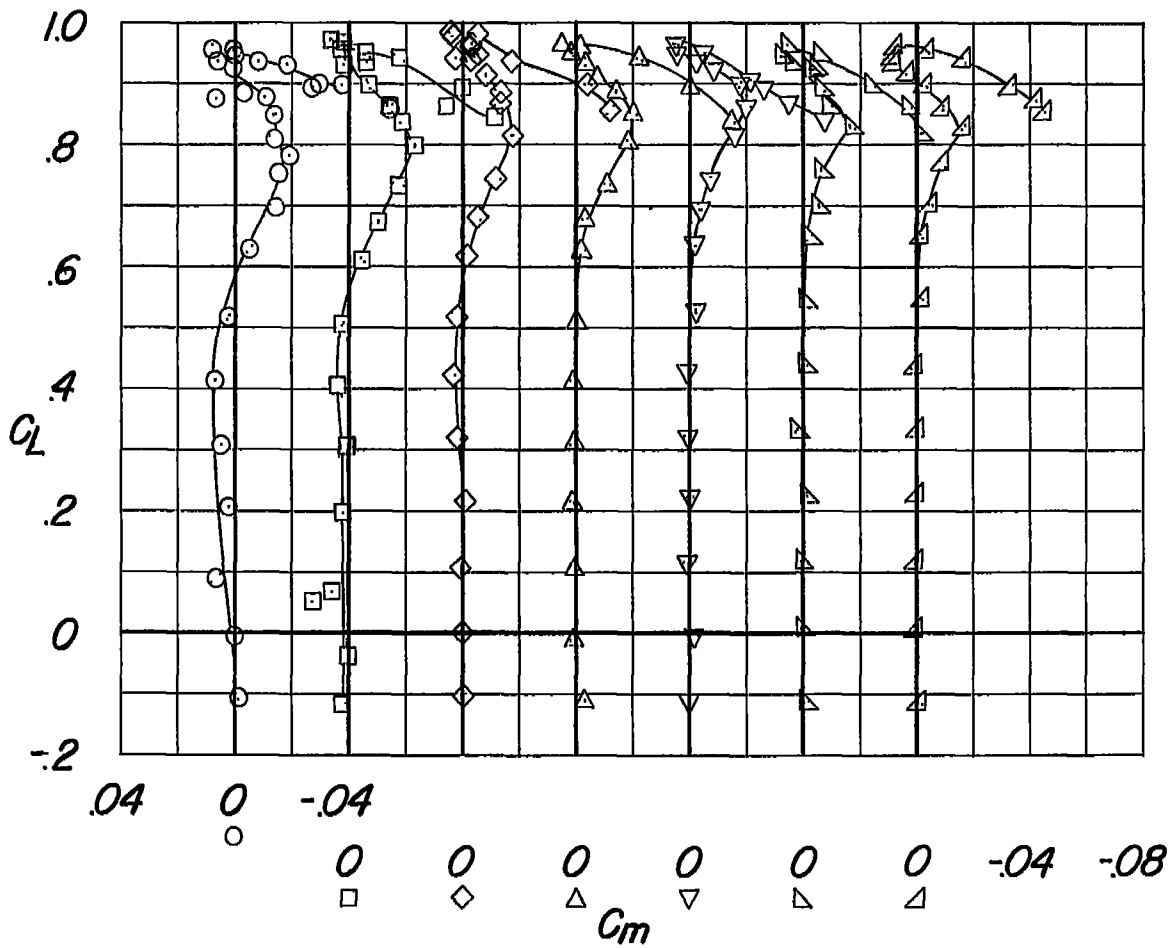

(a) Atmospheric pressure.

Figure 5.- Variation of pitching-moment coefficient with lift coefficient of a 45° sweptback wing having an aspect ratio of 3 and a leading-edge radius of 0.0050c.

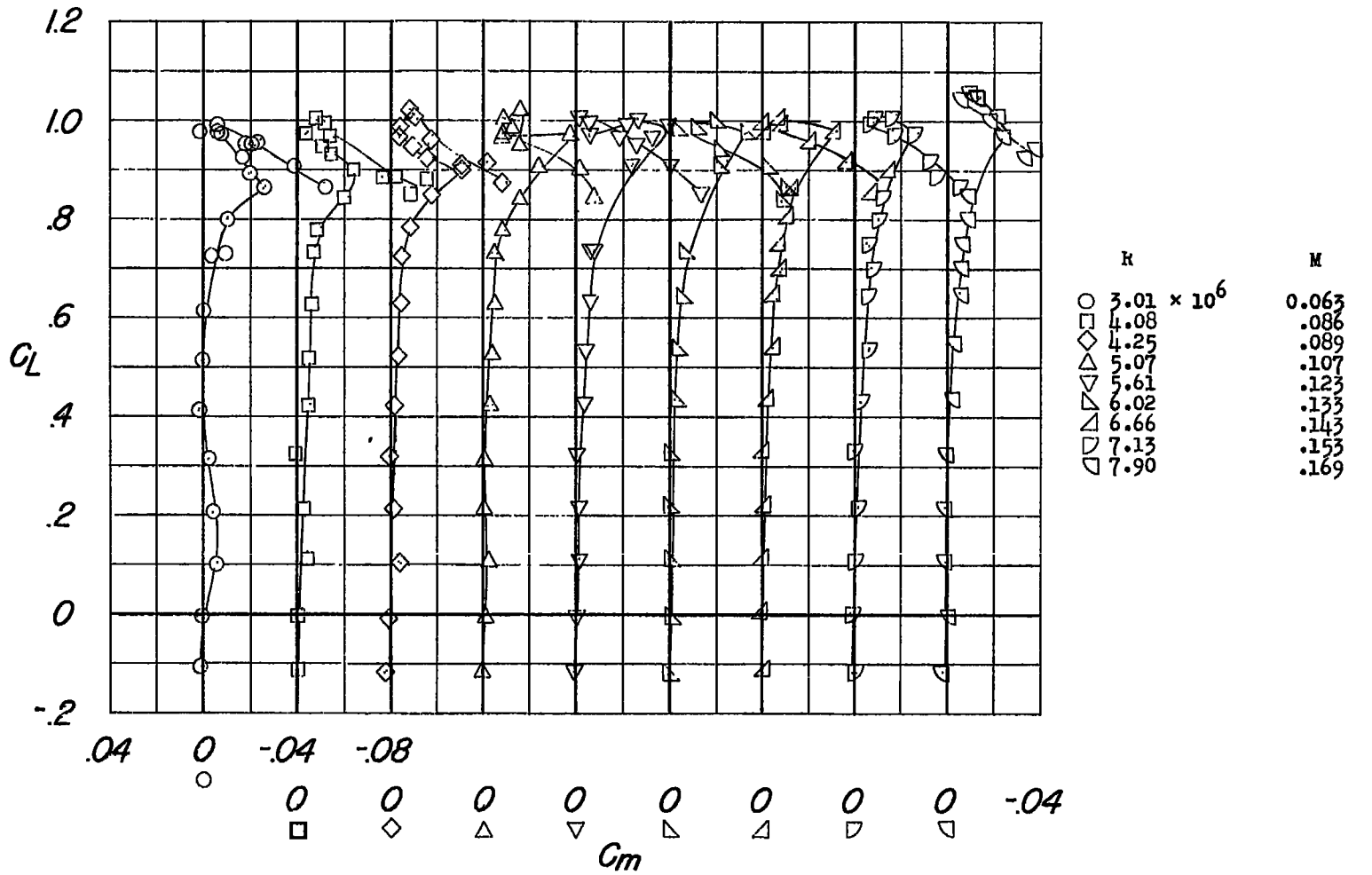

(b) Pressure, 33 pounds per square inch.

Figure 5.- Concluded.

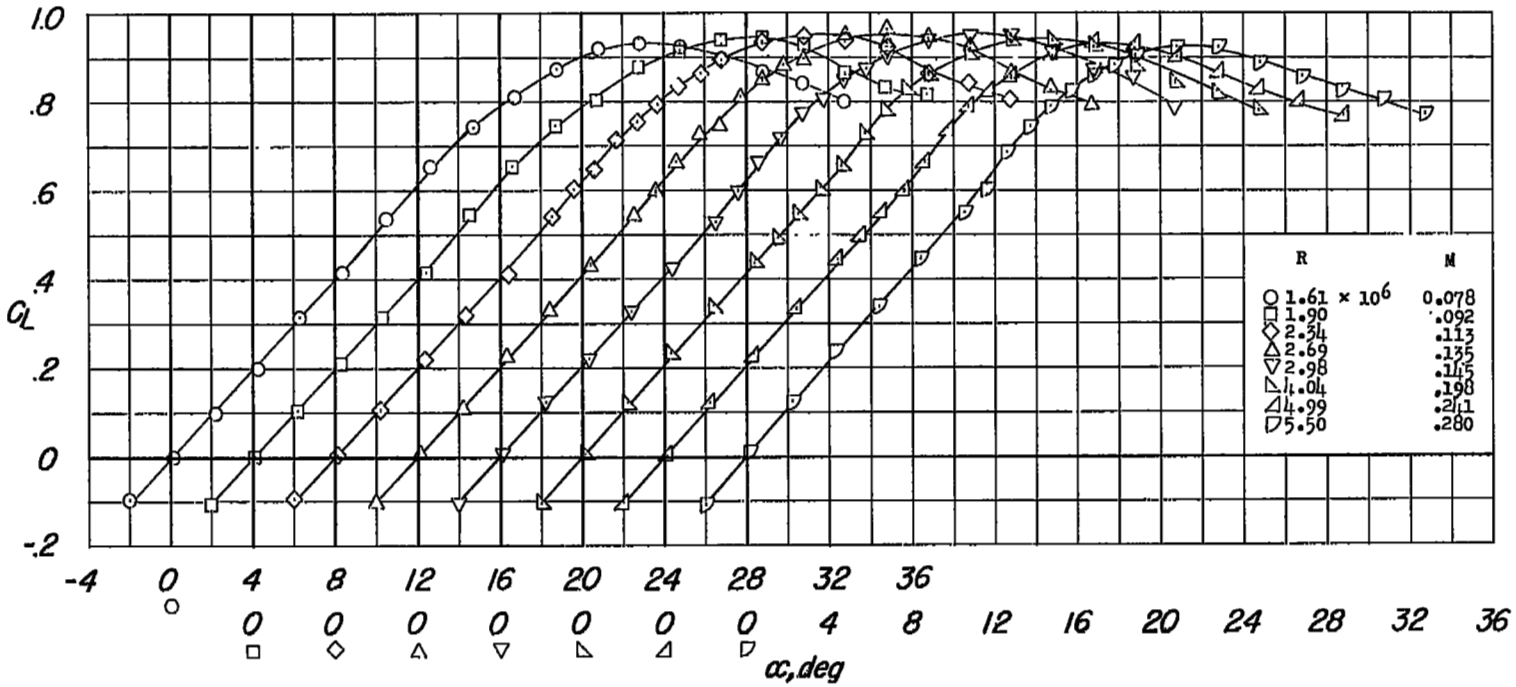

(a) C_L against α; atmospheric pressure.

Figure 6.- Variation of lift and pitching-moment coefficient with angle of attack of a 45° sweptback wing having an aspect ratio of 3 and a leading-edge radius of 0.0025c.

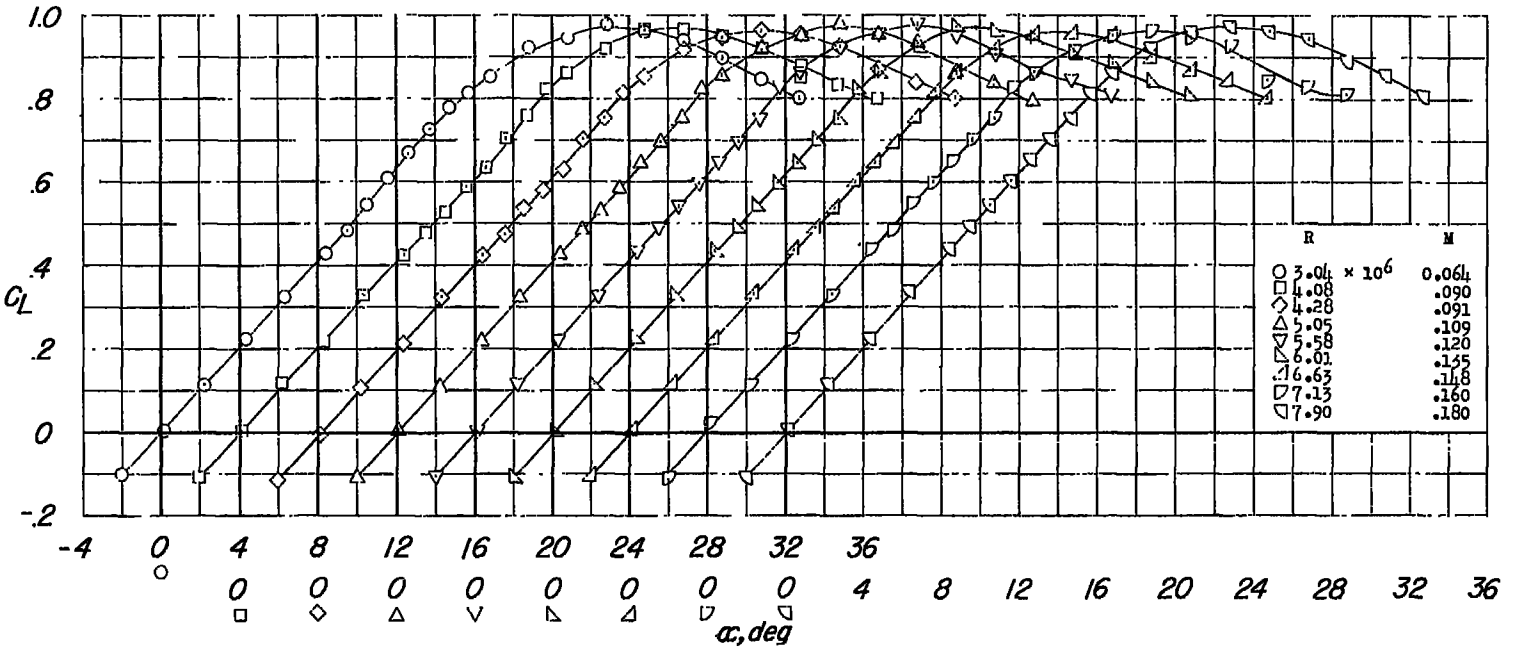

(b) C_L against α; 33 pounds per square inch.

Figure 6.- Continued.

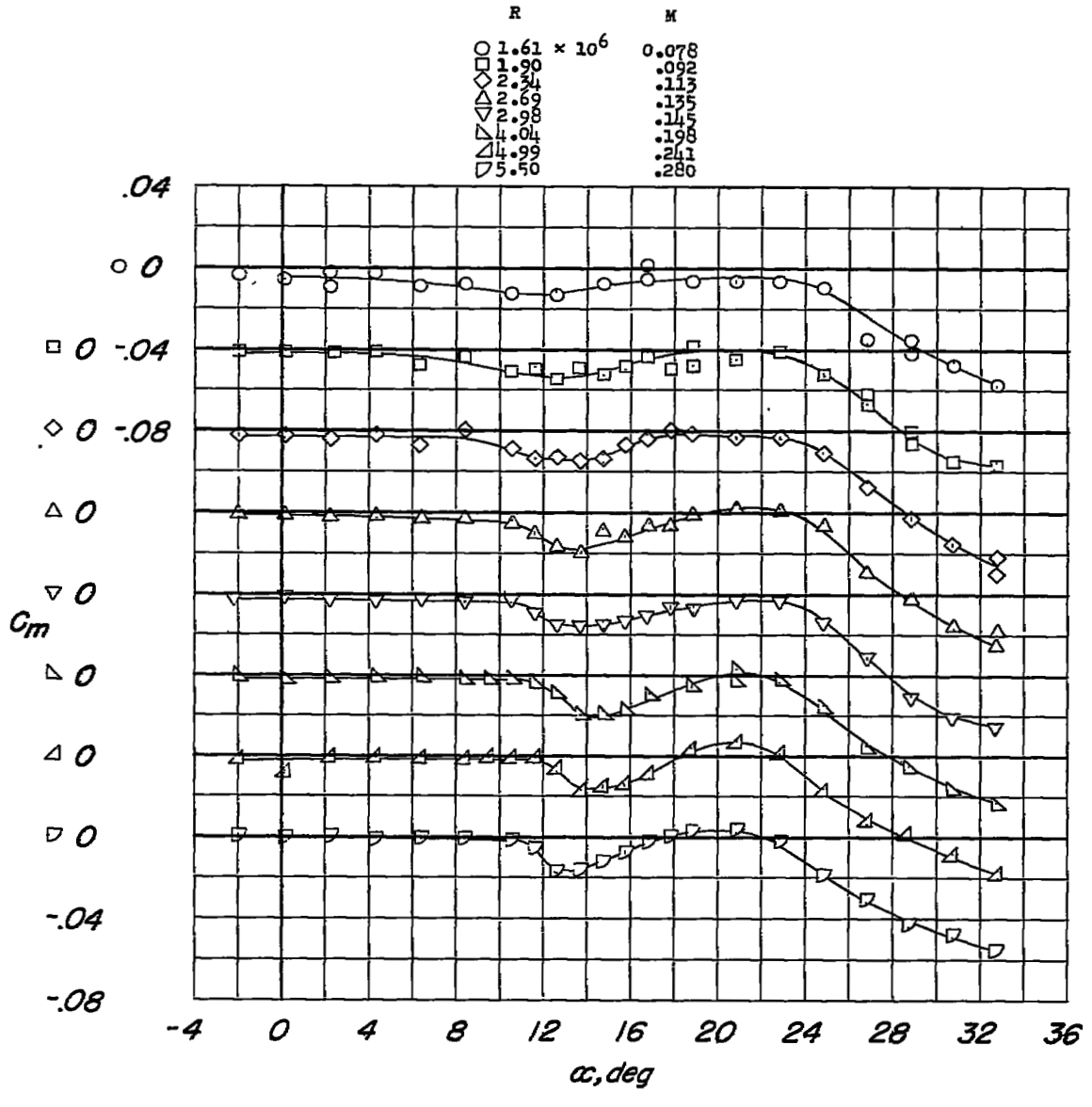

(c) C_m against α; atmospheric pressure.

Figure 6.- Continued.

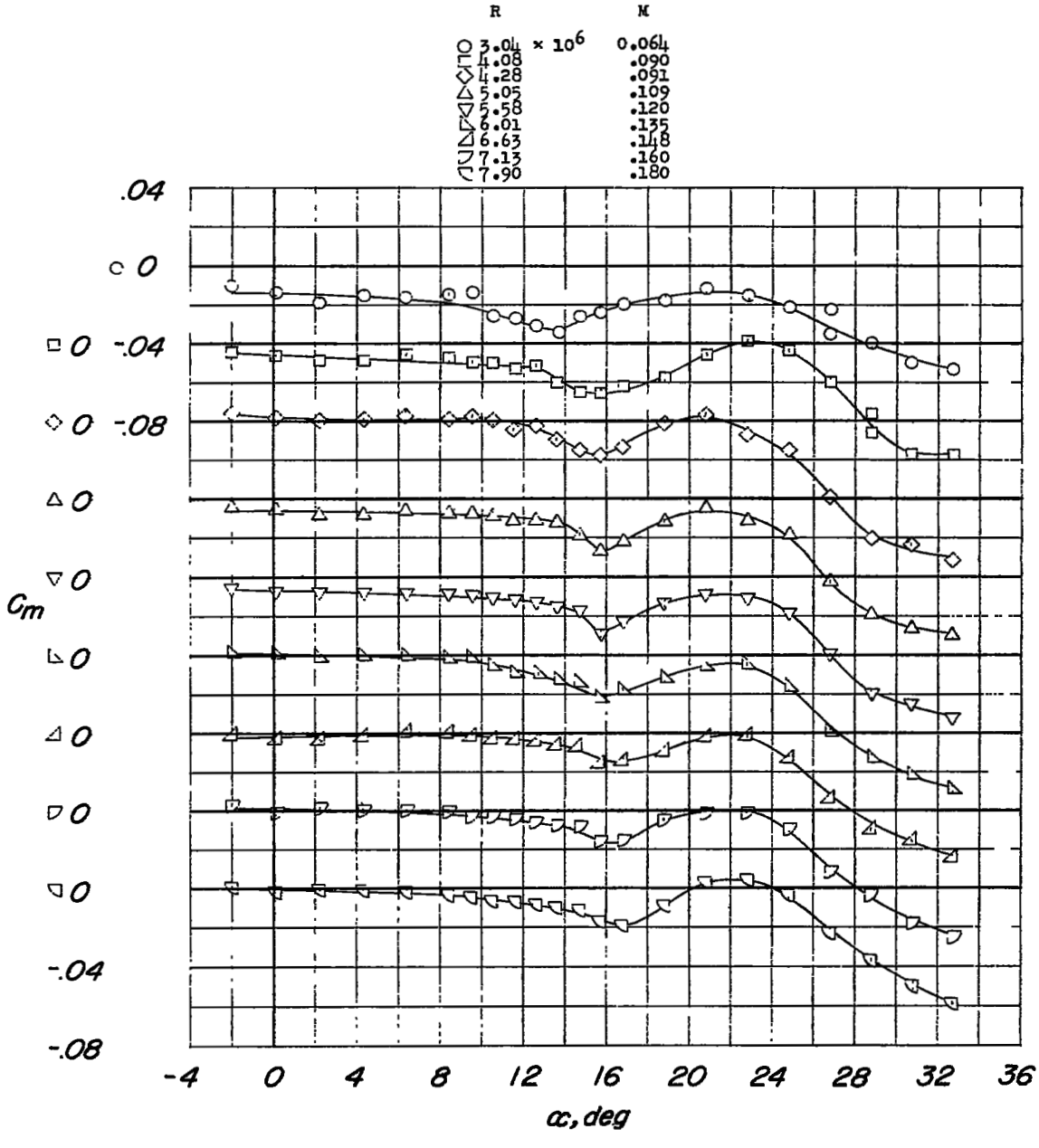

(d) C_m against α; 33 pounds per square inch.

Figure 6.- Concluded.

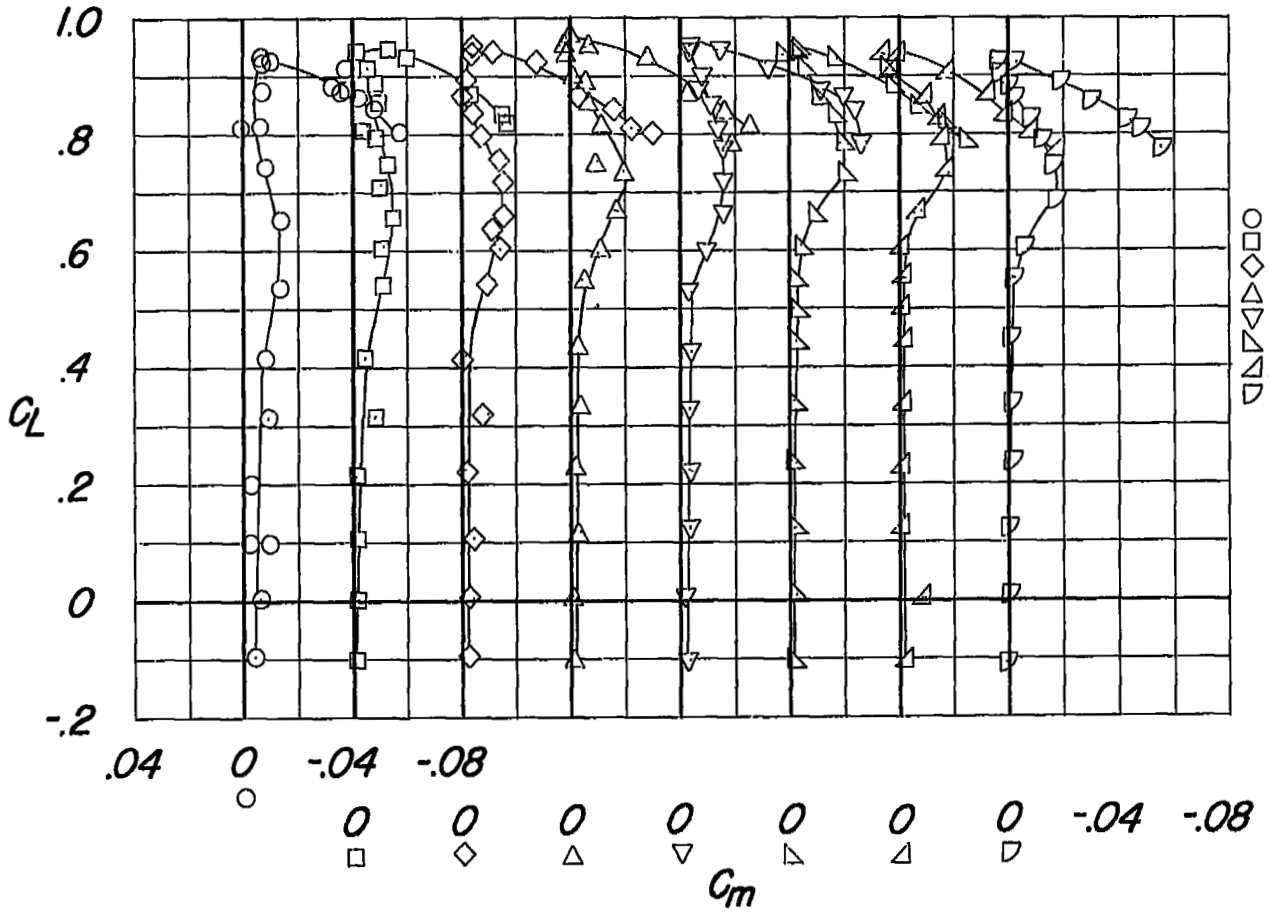

(a) Atmospheric pressure.

Figure 7.- Variation of pitching-moment coefficient with lift coefficient of a 45° sweptback wing having an aspect ratio of 3 and a leading-edge radius of 0.0025c.

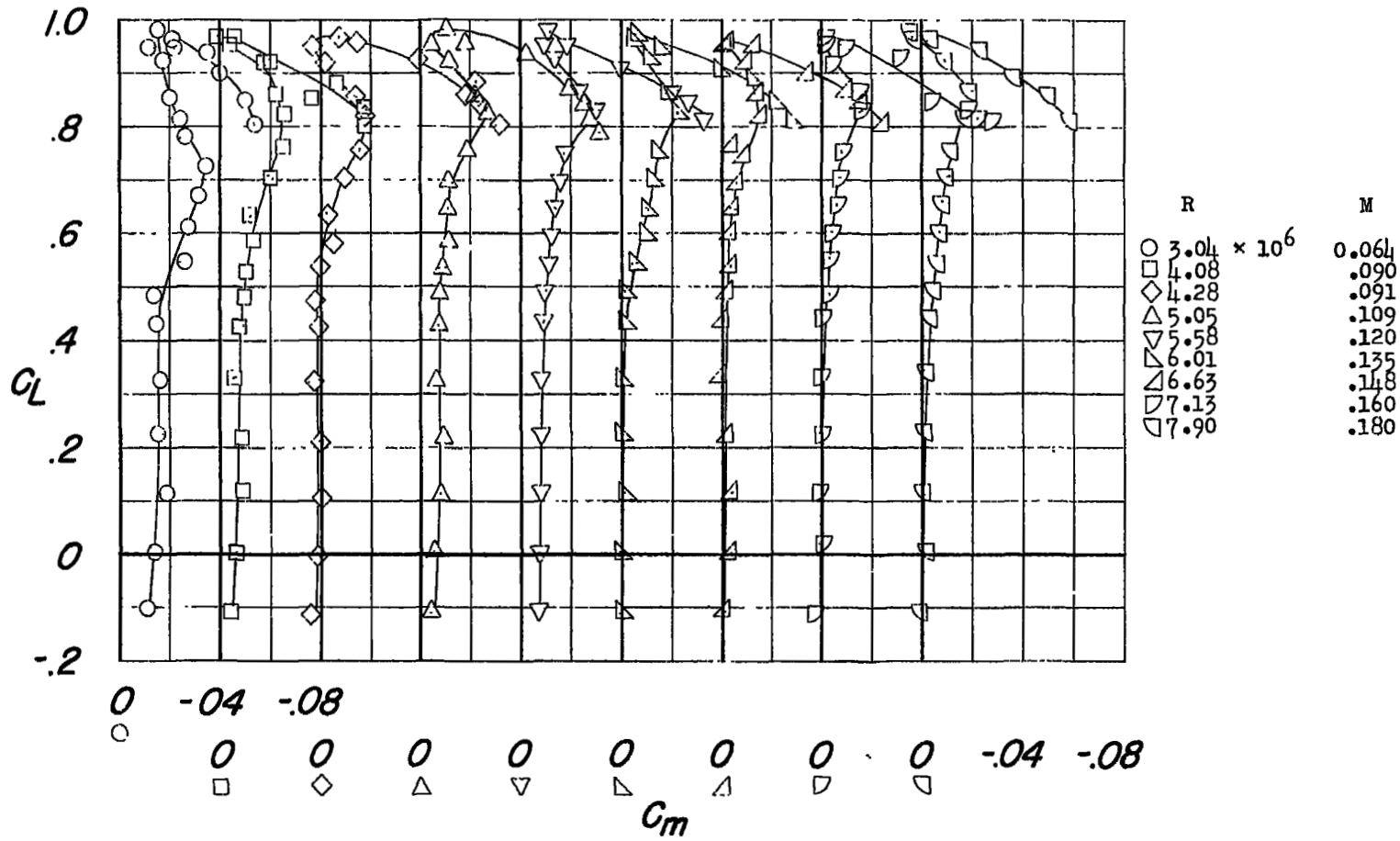

(b) Pressure, 33 pounds per square inch.

Figure 7.- Concluded.

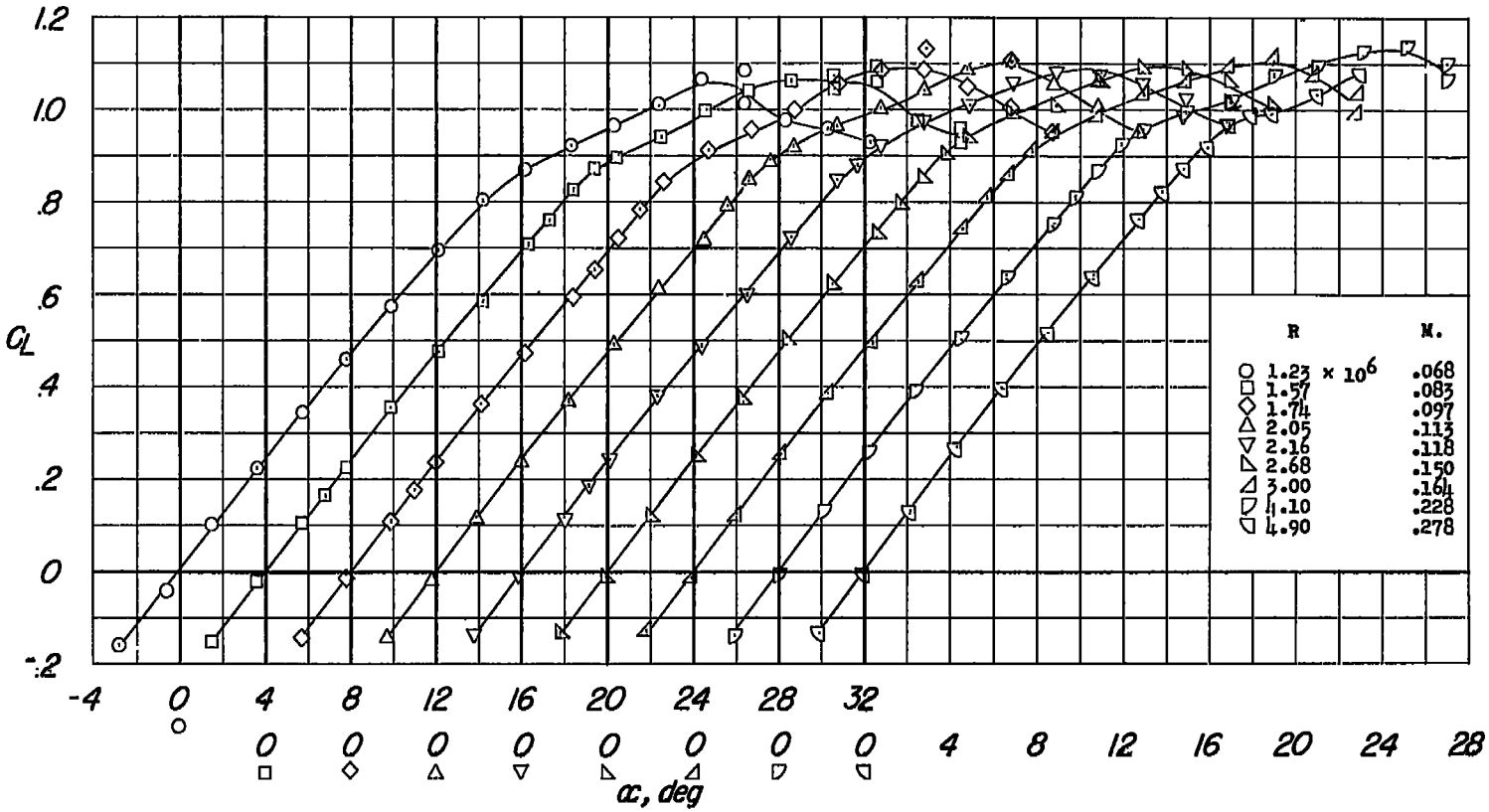

(a) C_L against α; atmospheric pressure.

Figure 8.- Variation of lift and pitching-moment coefficients with angle of attack of a 45° sweptback wing having an aspect ratio of 5 and a leading-edge radius of 0.0089c.

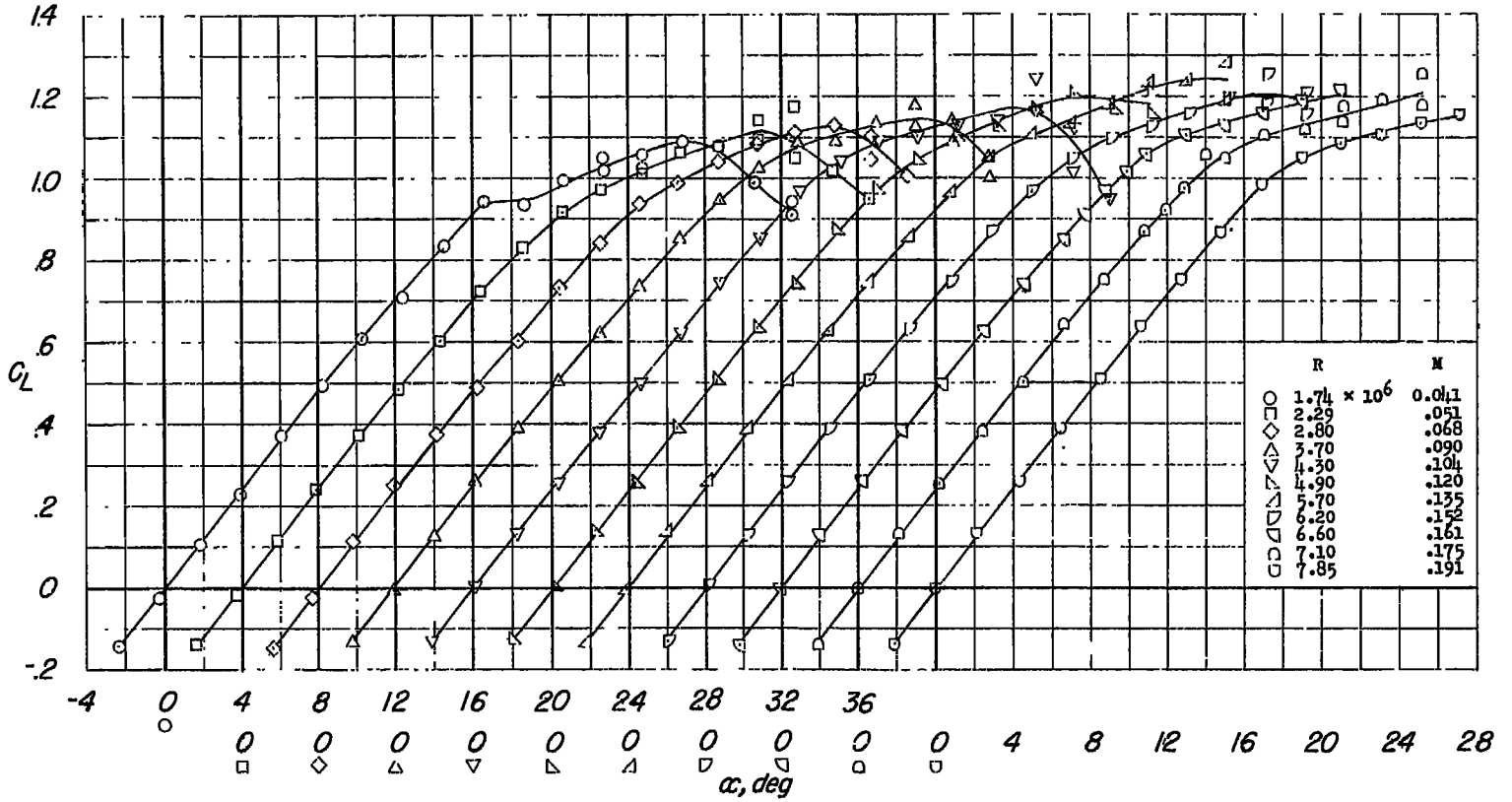

(b) C_L against α; pressure, 33 pounds per square inch.

Figure 8.- Continued.

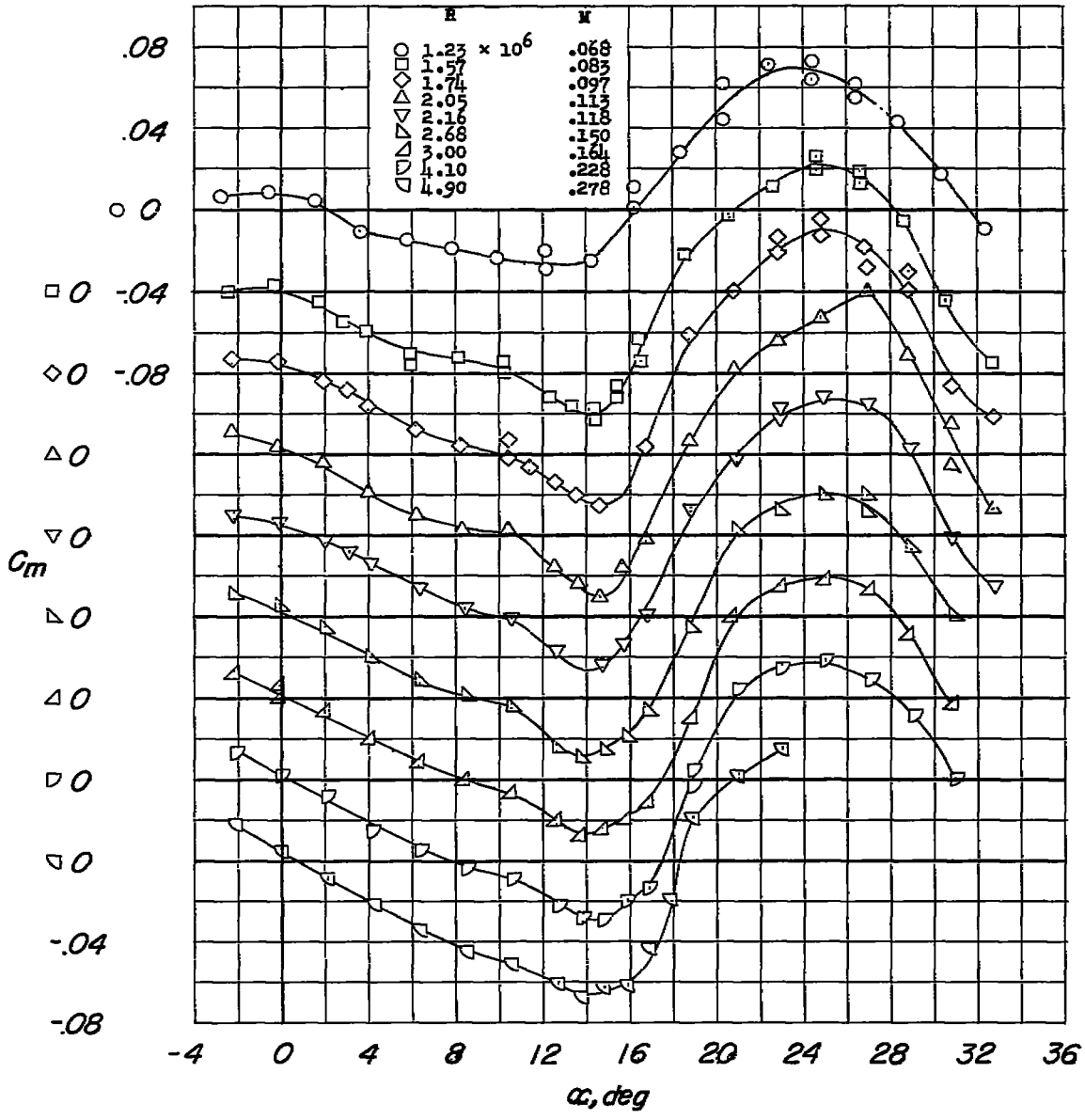

(c) C_m against α; atmospheric pressure.

Figure 8.- Continued.

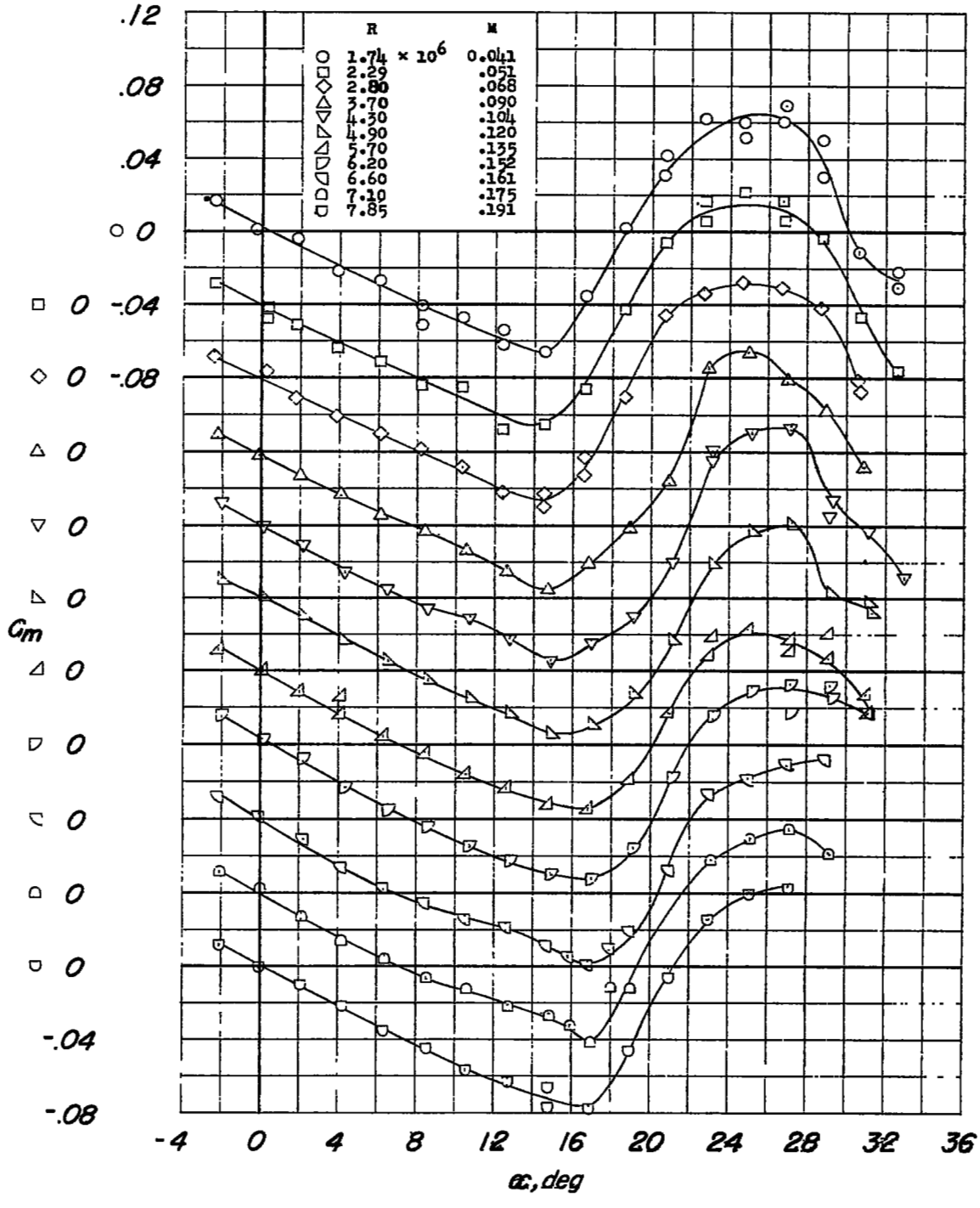

(d) C_m against α; pressure, 33 pounds per square inch.

Figure 8.- Concluded.

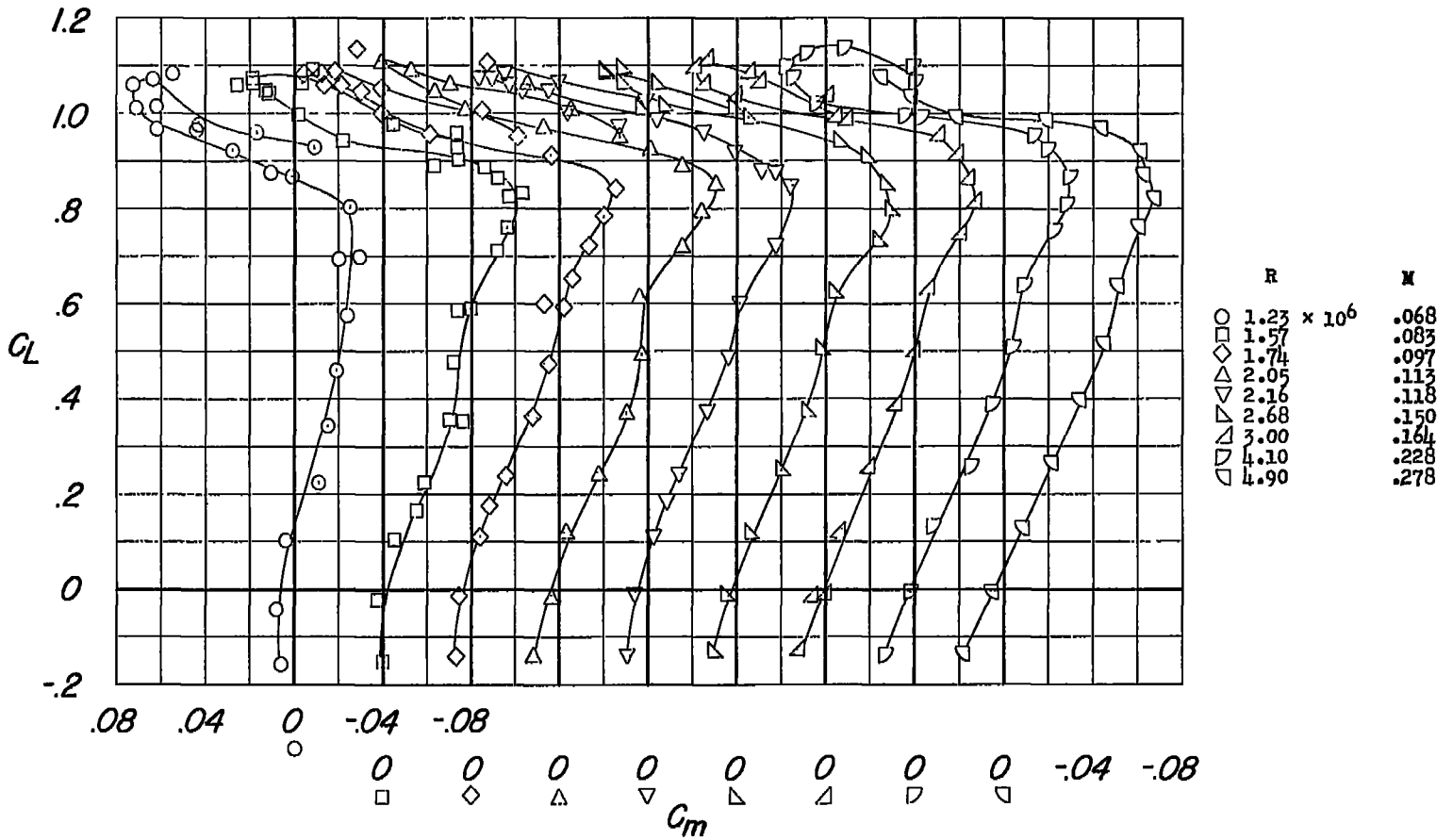

(a) Atmospheric pressure.

Figure 9.- Variation of pitching-moment coefficient with lift coefficient of a 45° sweptback wing having an aspect ratio of 5 and a leading-edge radius of 0.0089c.

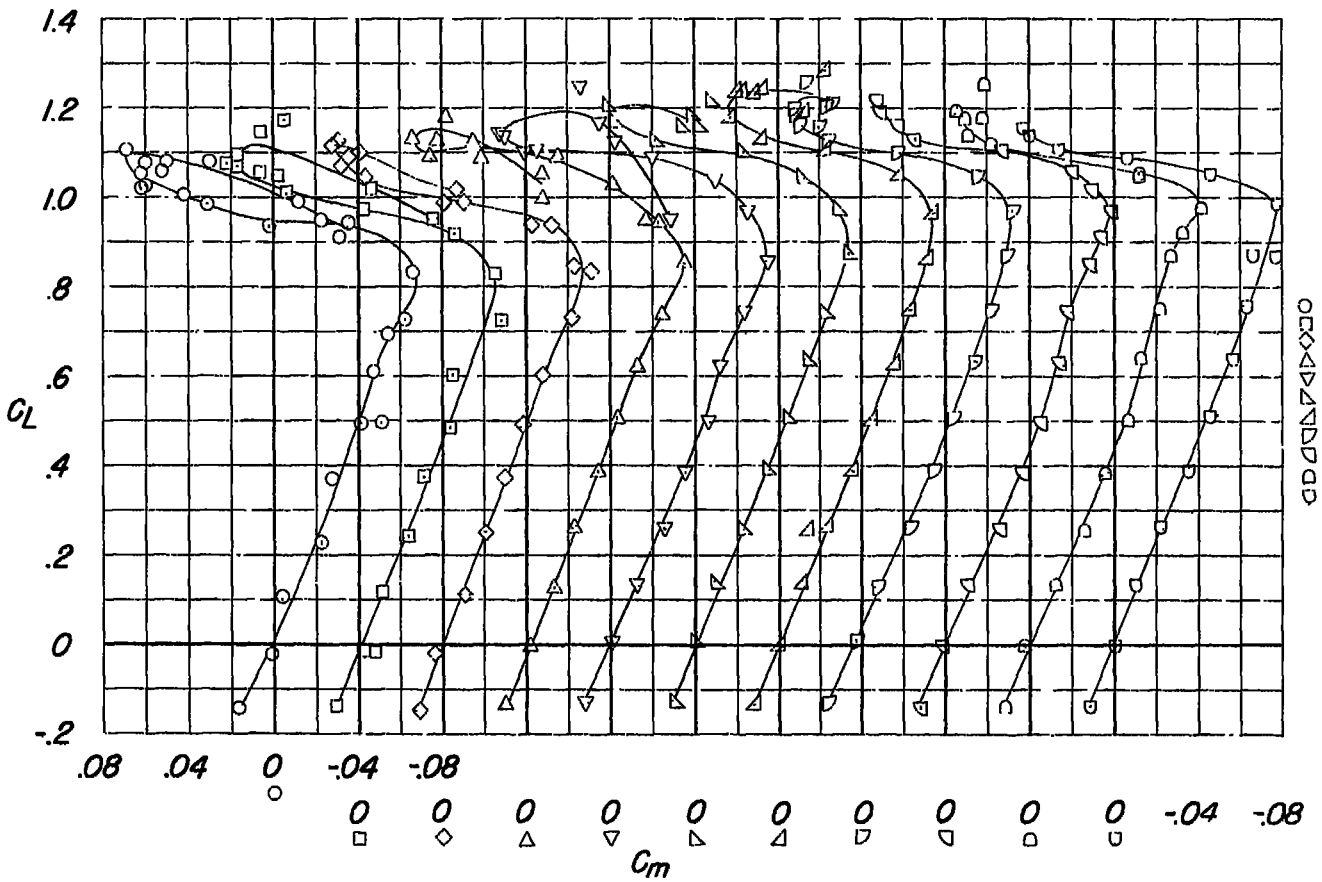

(b) Pressure, 33 pounds per square inch.

Figure 9.- Concluded.

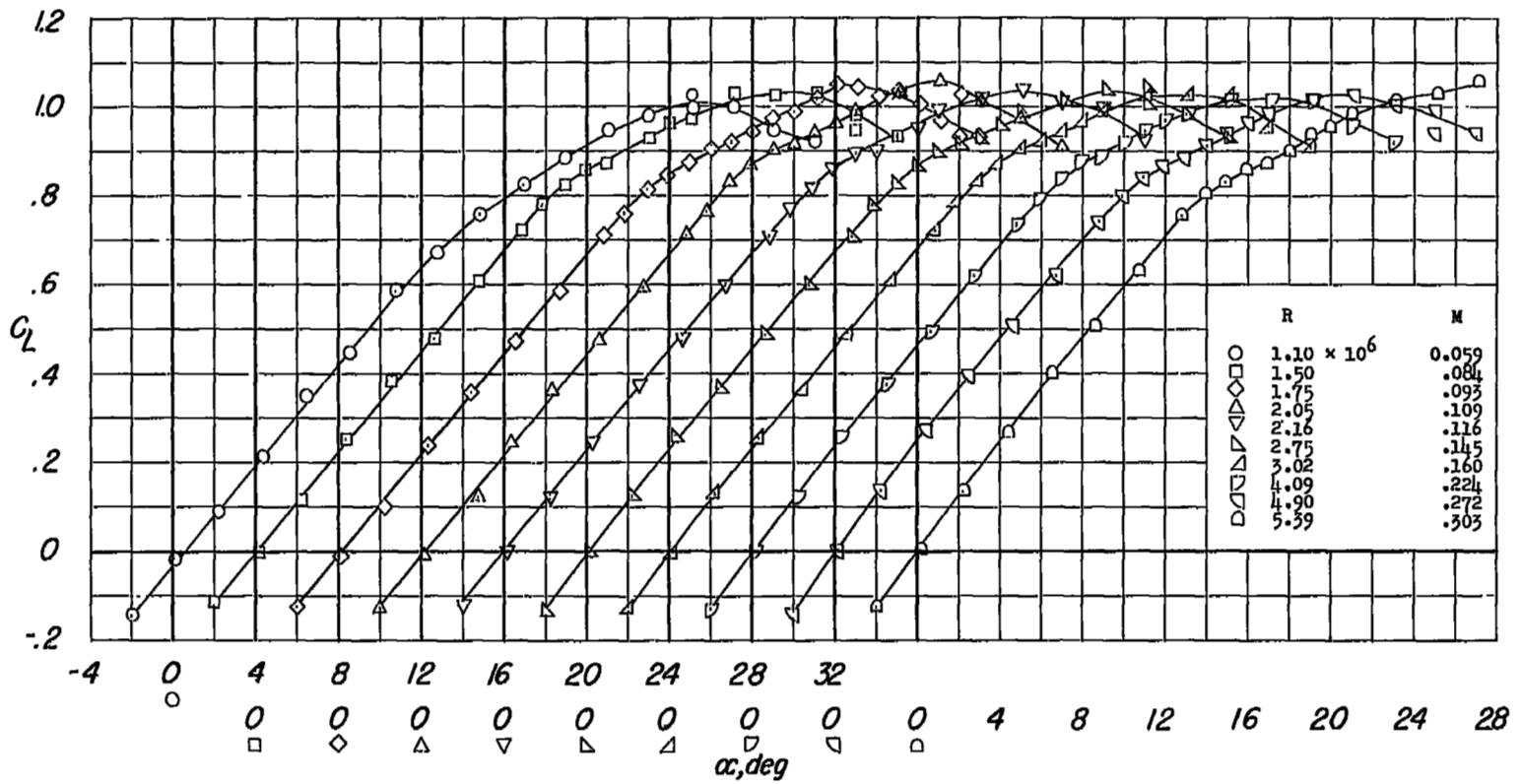

(a) C_L against α; atmospheric pressure.

Figure 10.- Variation of lift and pitching-moment coefficients with angle of attack of a 45° sweptback wing having an aspect ratio of 5 and a leading-edge radius of 0.0050c.

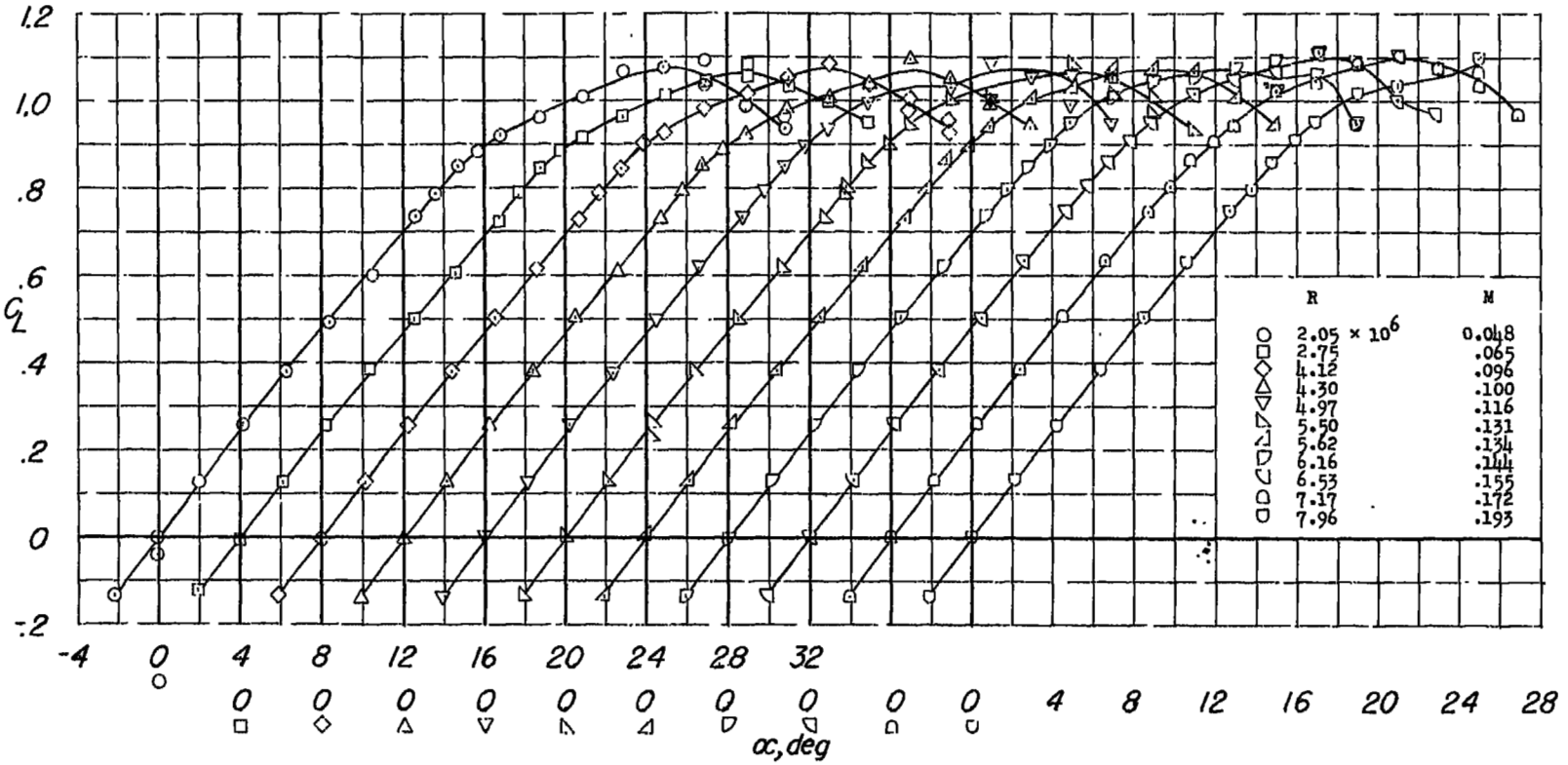

(b) C_L against α; pressure, 33 pounds per square inch.

Figure 10.- Continued.

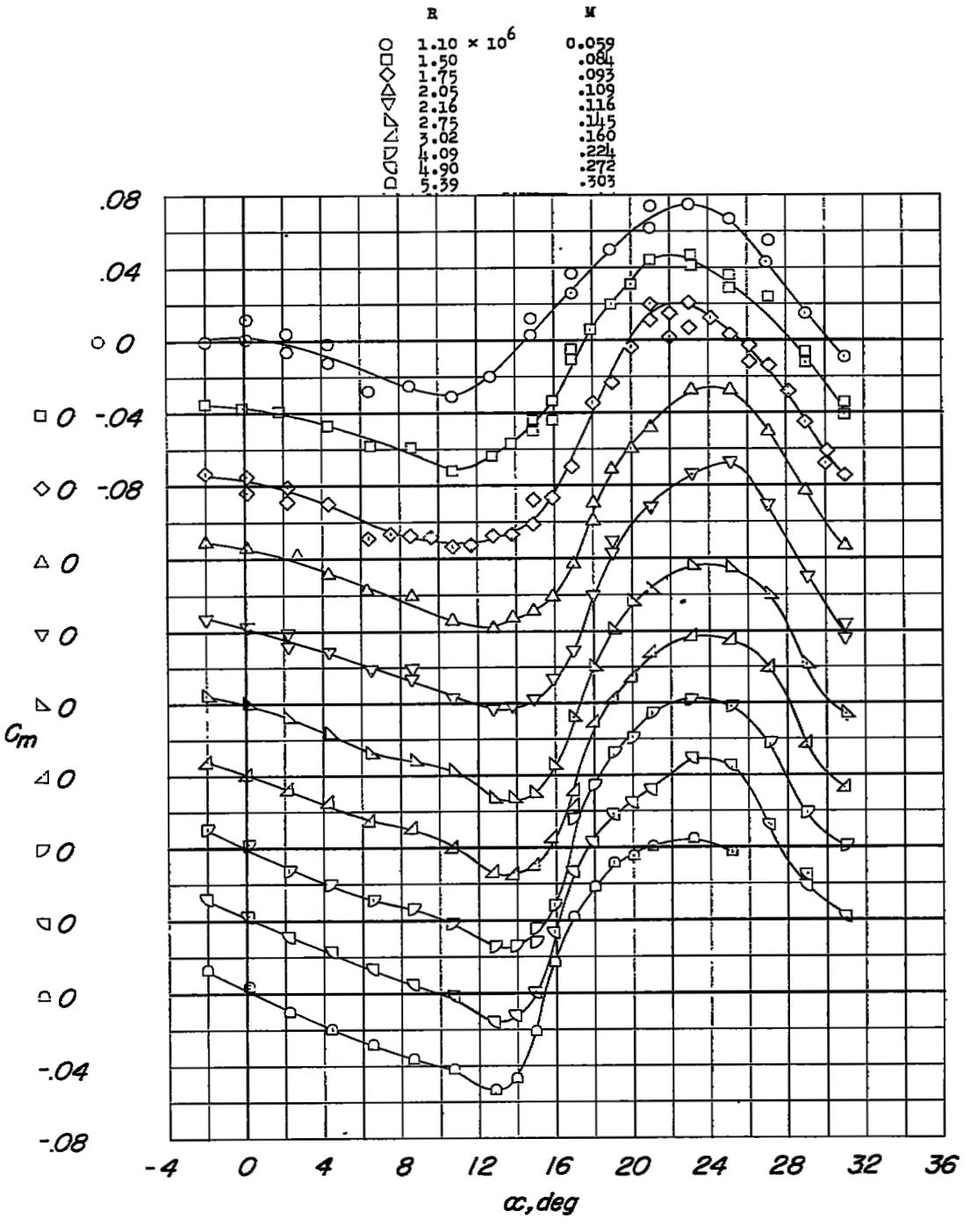

(c) C_m against α; atmospheric pressure.

Figure 10.- Continued.

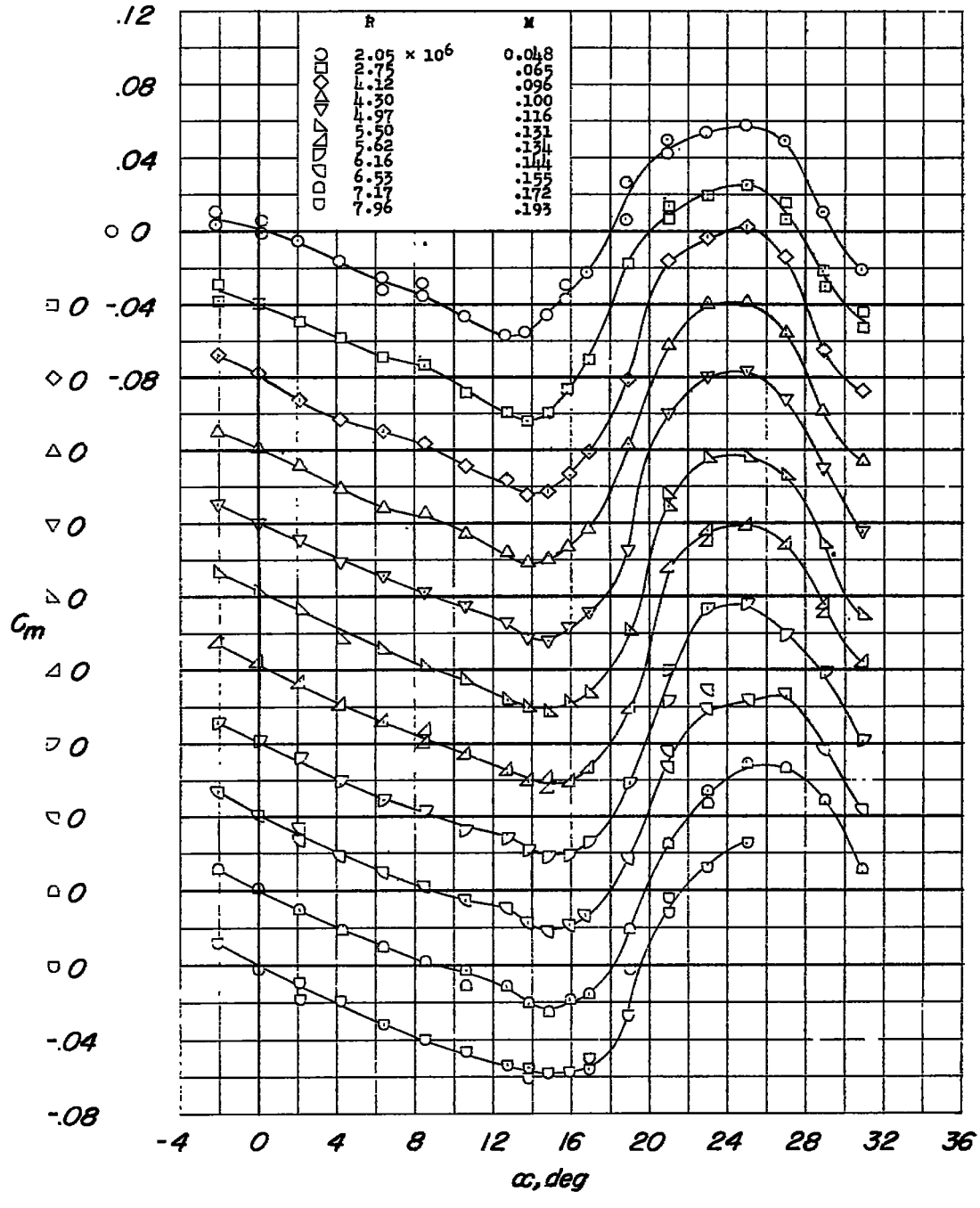

(d) C_m against α; pressure, 33 pounds per square inch.

Figure 10.- Concluded.

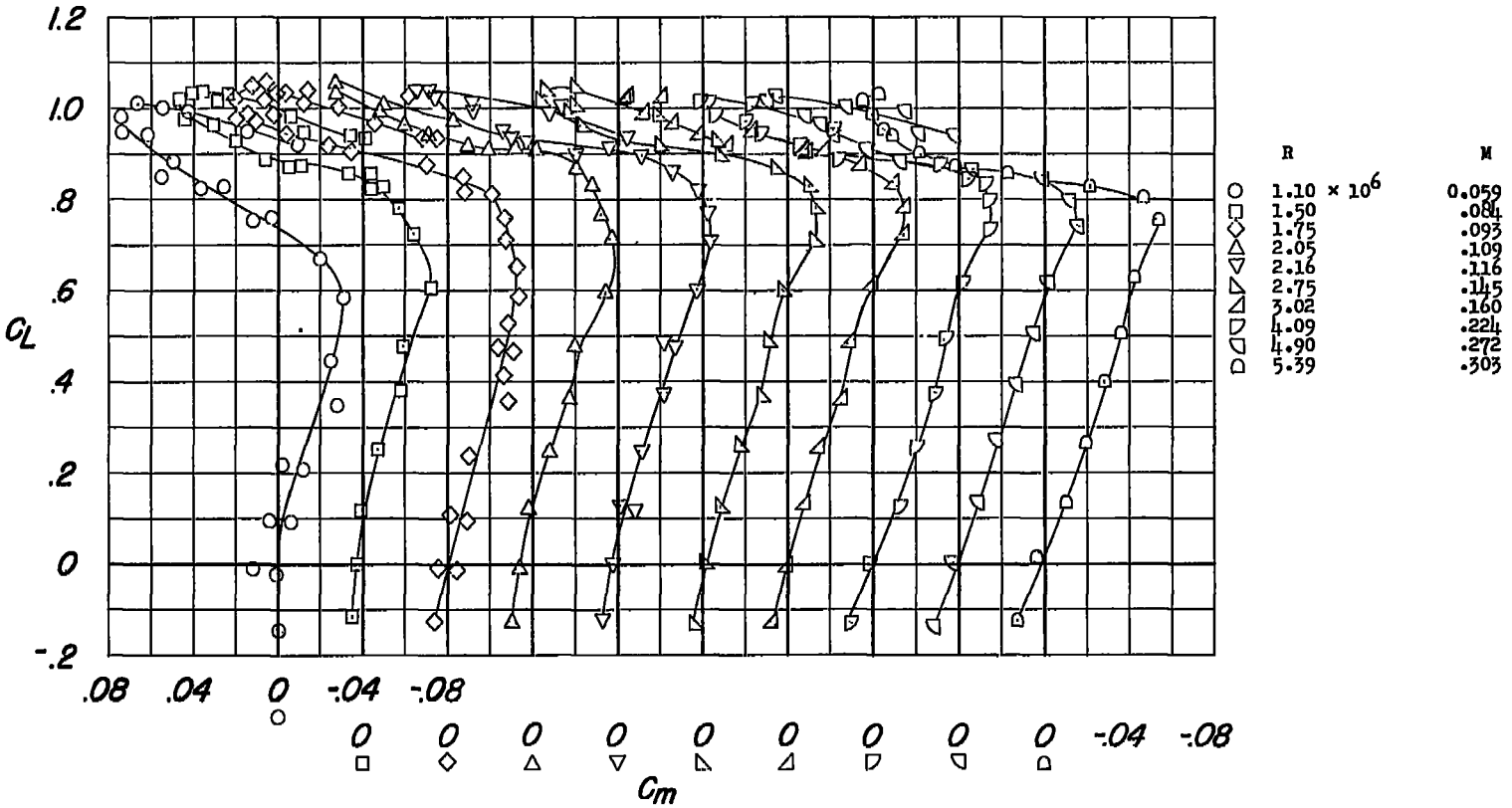

(a) Atmospheric pressure.

Figure 11.- Variation of pitching-moment coefficient with lift coefficient of a 45° sweptback wing having an aspect ratio of 5 and a leading-edge radius of 0.0050c.

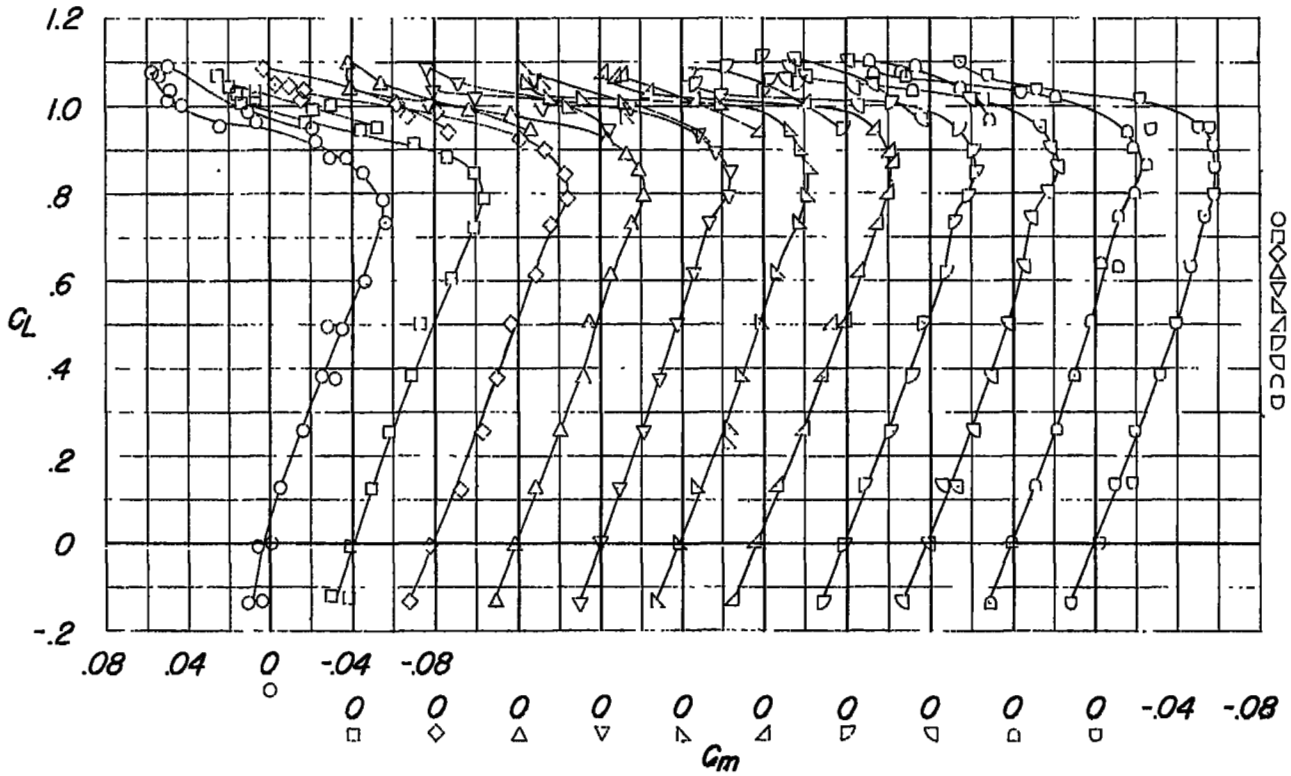

(b) Pressure, 33 pounds per square inch.

Figure 11.- Concluded.

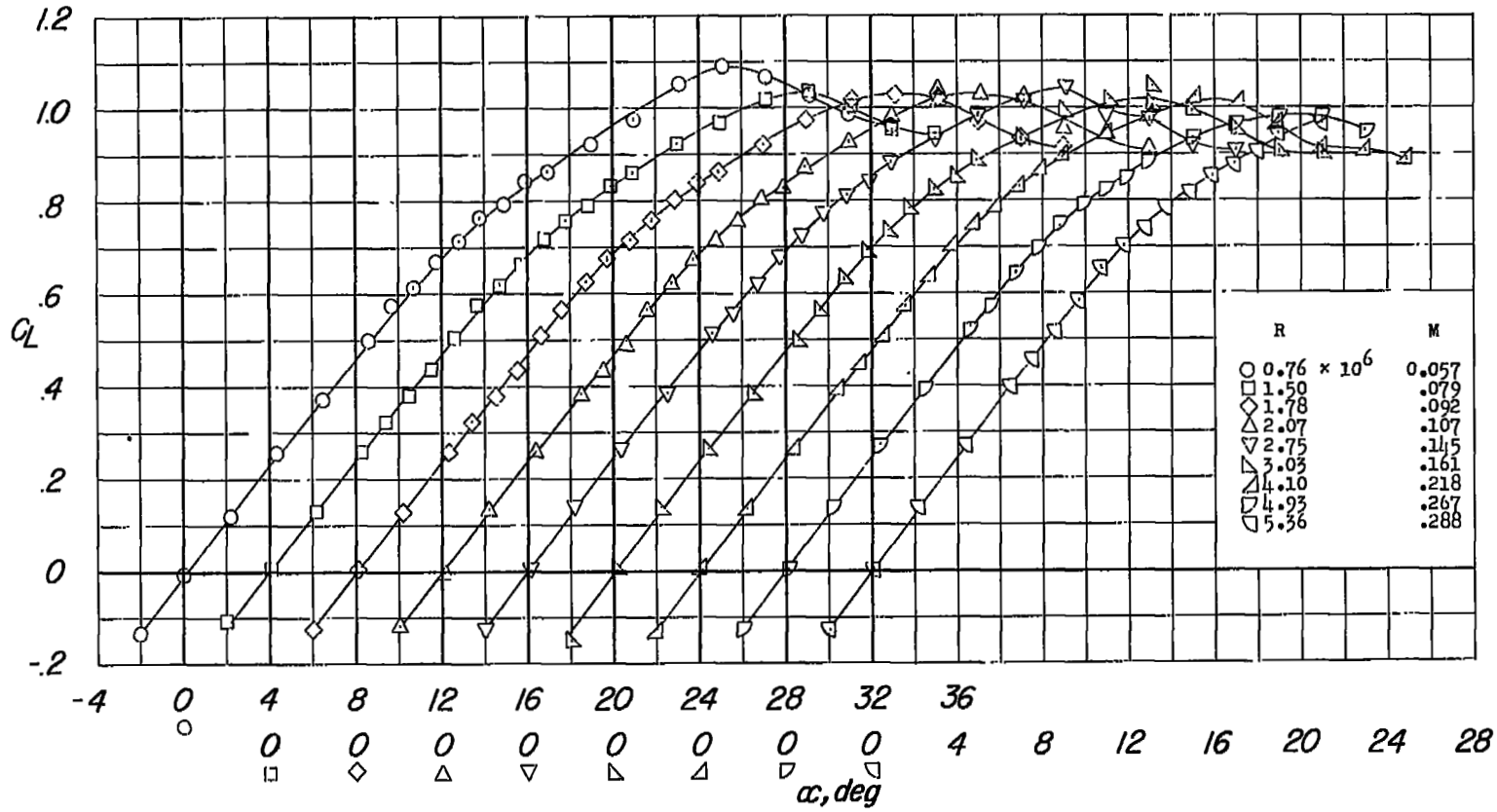

(a) C_L against α; atmospheric pressure.

Figure 12.- Variation of lift and pitching-moment coefficients with angle of attack of a 45° sweptback wing having an aspect ratio of 5 and a leading-edge radius of 0.0025c.

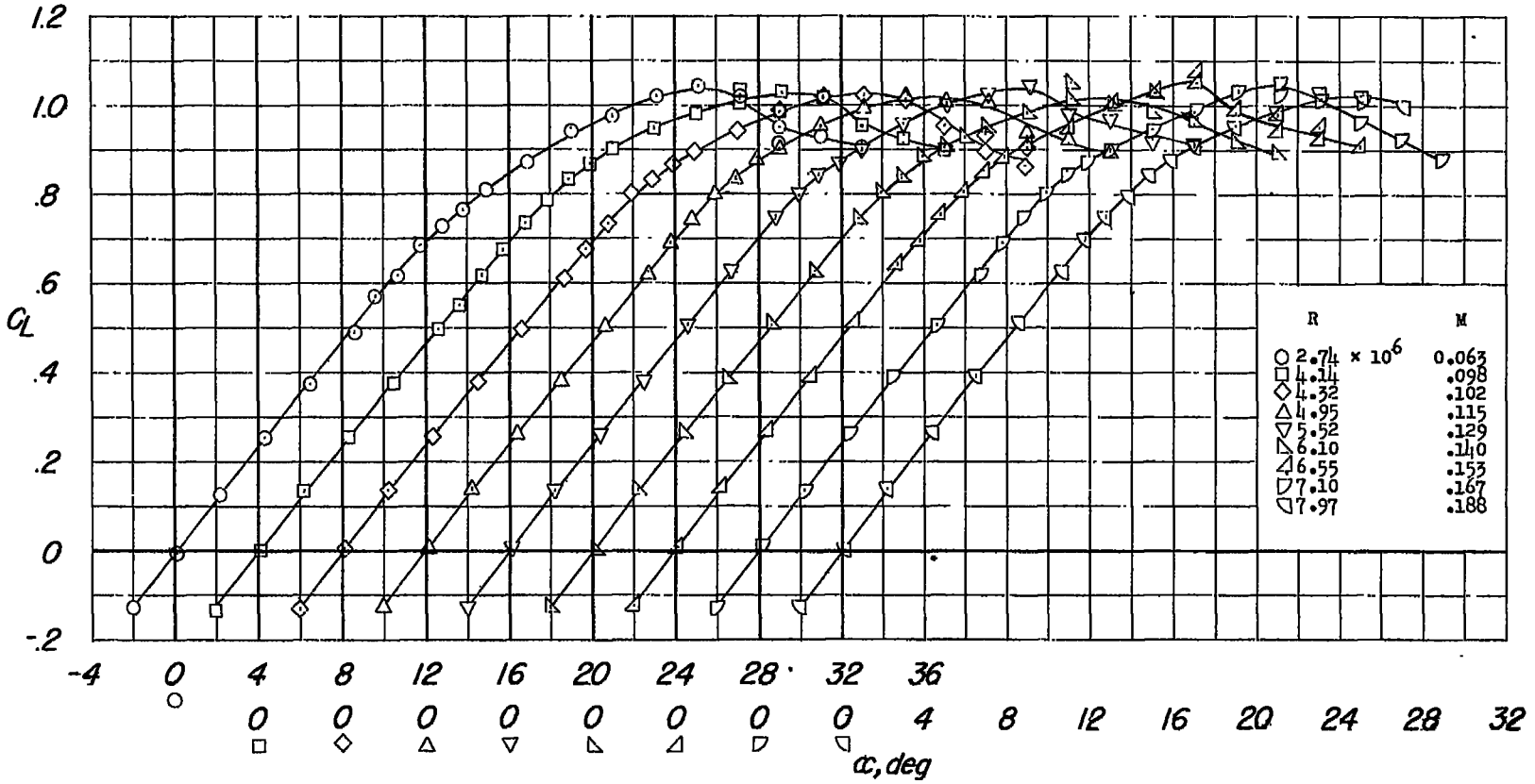

(b) C_L against α; 33 pounds per square inch.

Figure 12.- Continued.

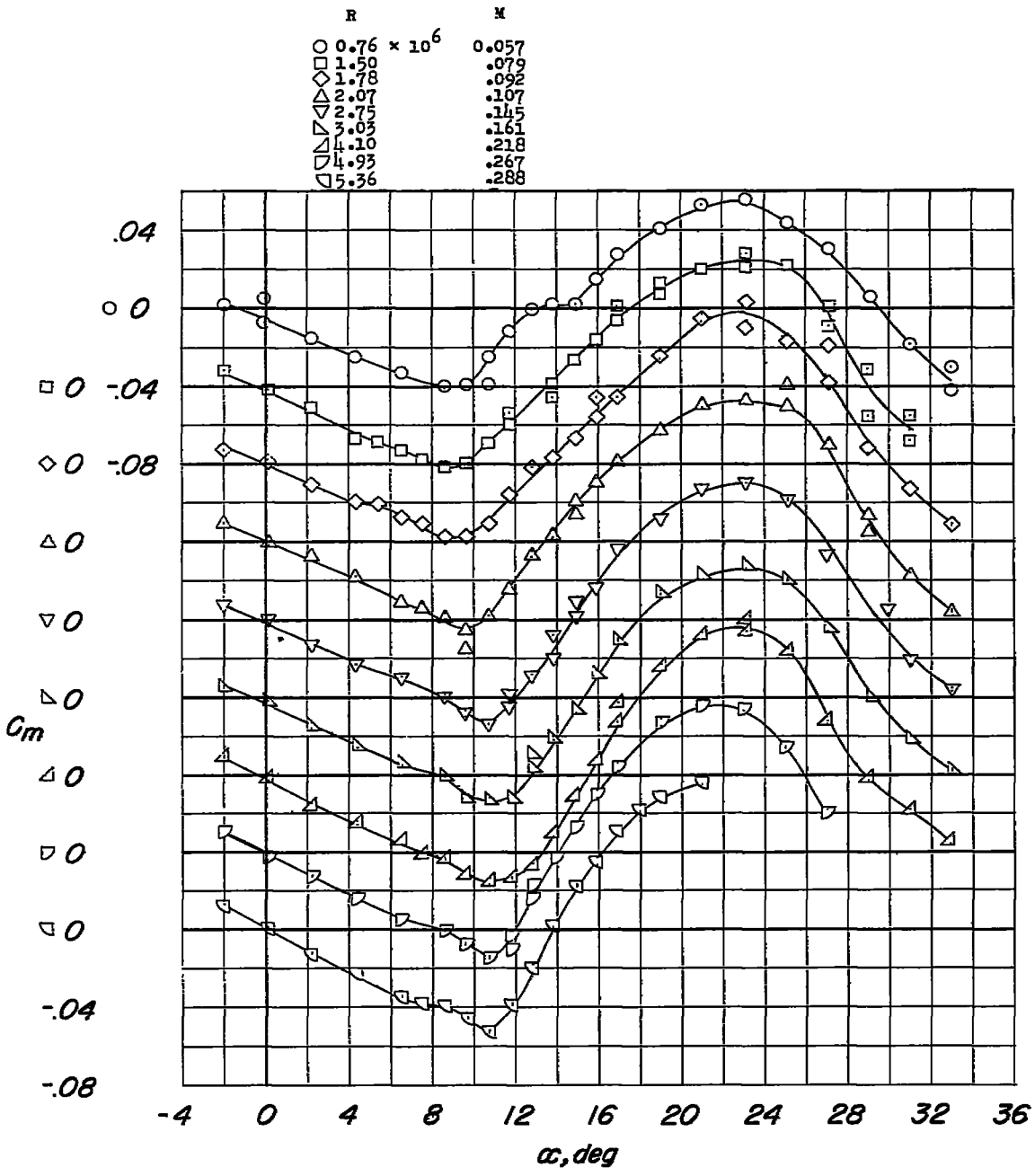

(c) C_m against α; atmospheric pressure.

Figure 12.- Continued.

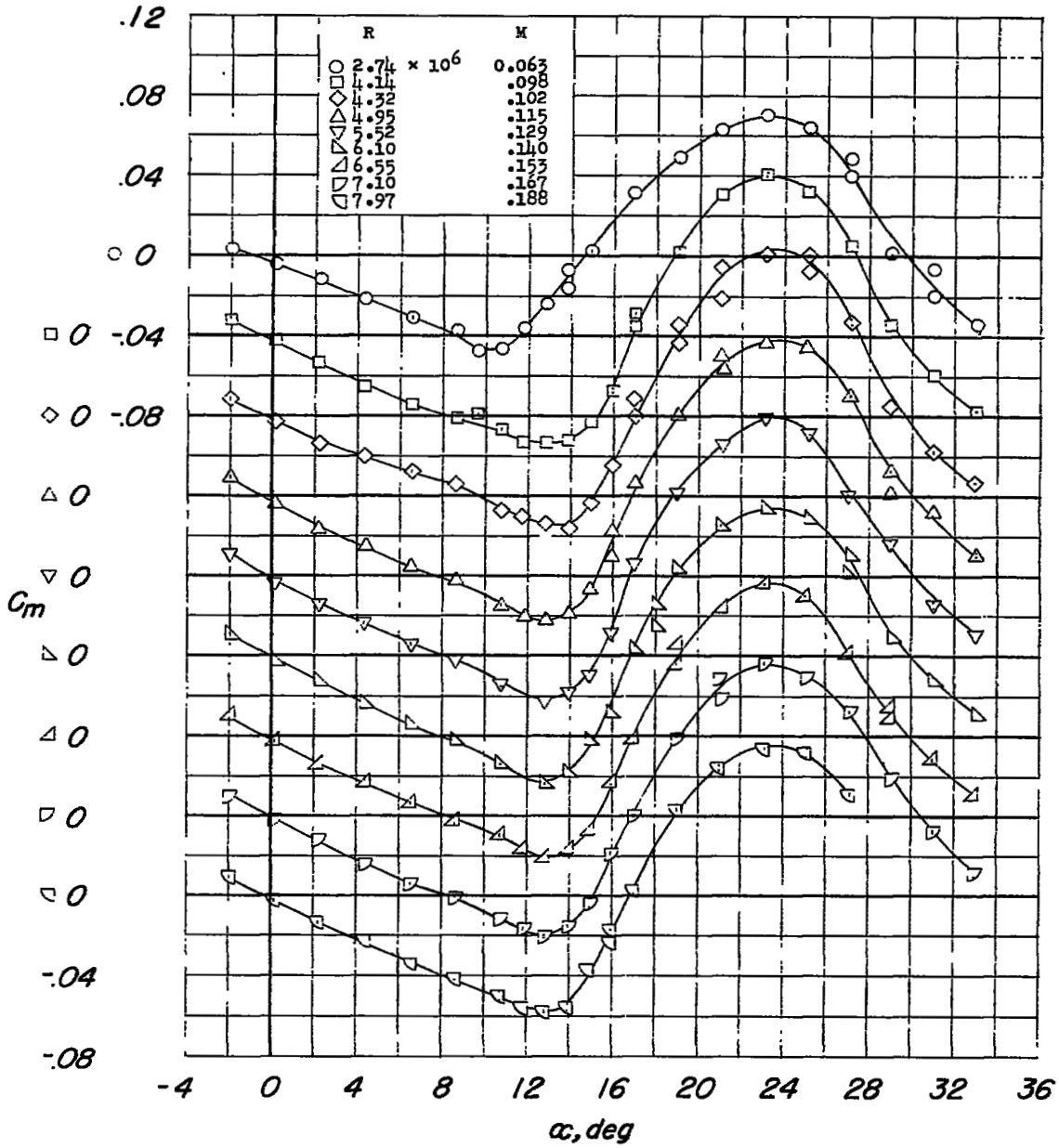

(d) C_m against α; 33 pounds per square inch.

Figure 12.- Concluded.

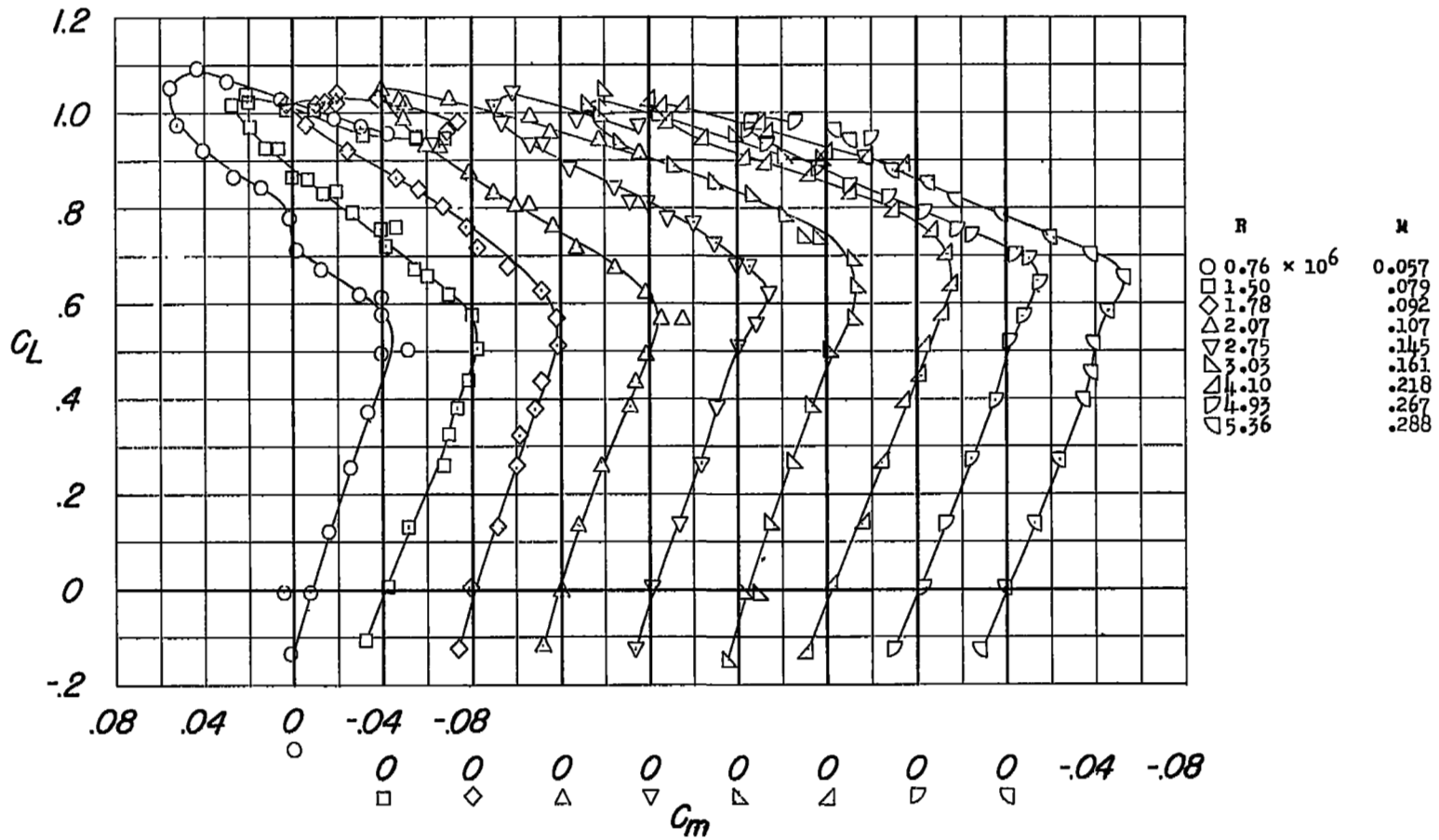

(a) Atmospheric pressure.

Figure 13.- Variation of pitching-moment coefficient with lift coefficient of a 45° sweptback wing having an aspect ratio of 5 and a leading-edge radius of 0.0025c.

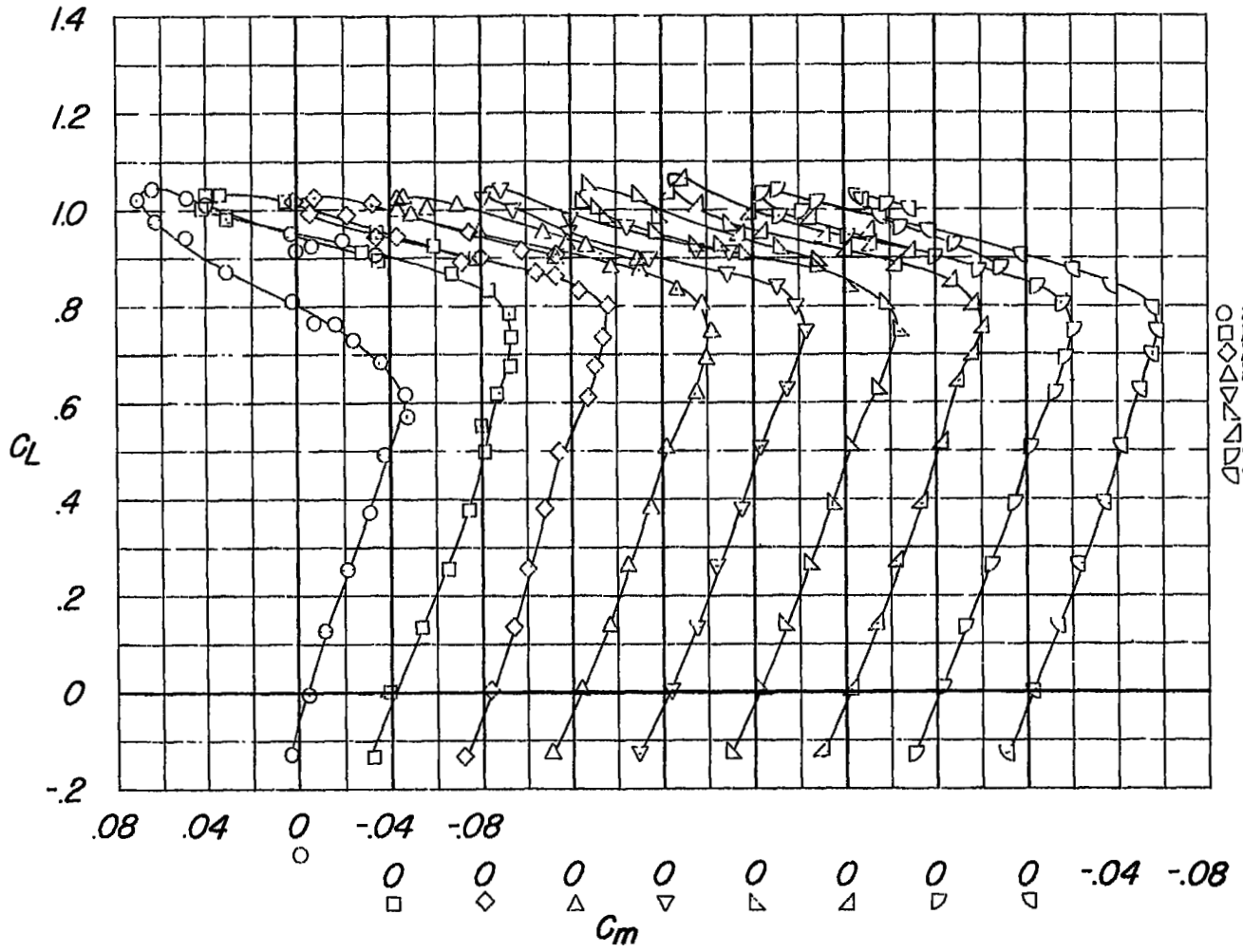

(b) Pressure, 33 pounds per square inch.

Figure 13.- Concluded.

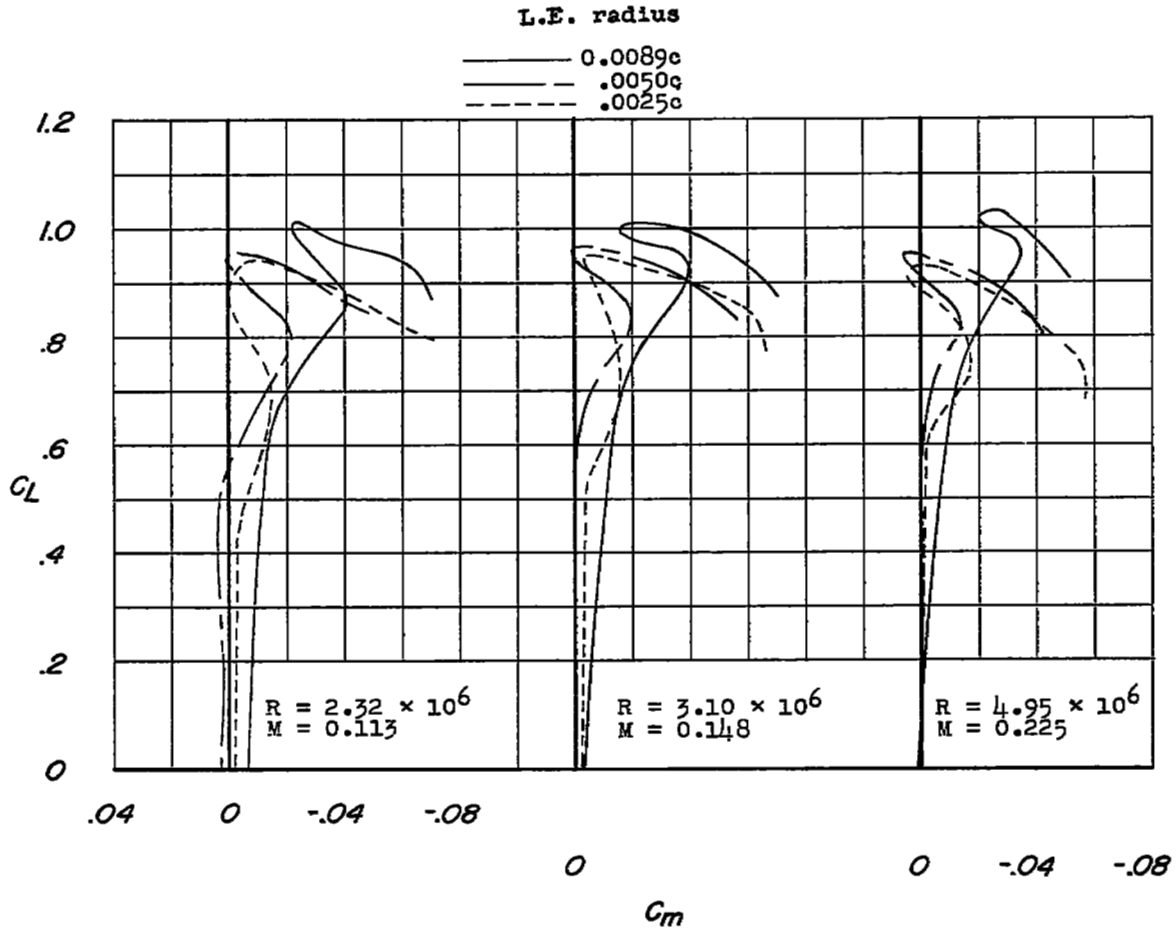

(a) Atmospheric pressure.

Figure 14.- Effect of leading-edge radius on the pitching-moment characteristics of a wing having 45° sweepback and an aspect ratio of 3.

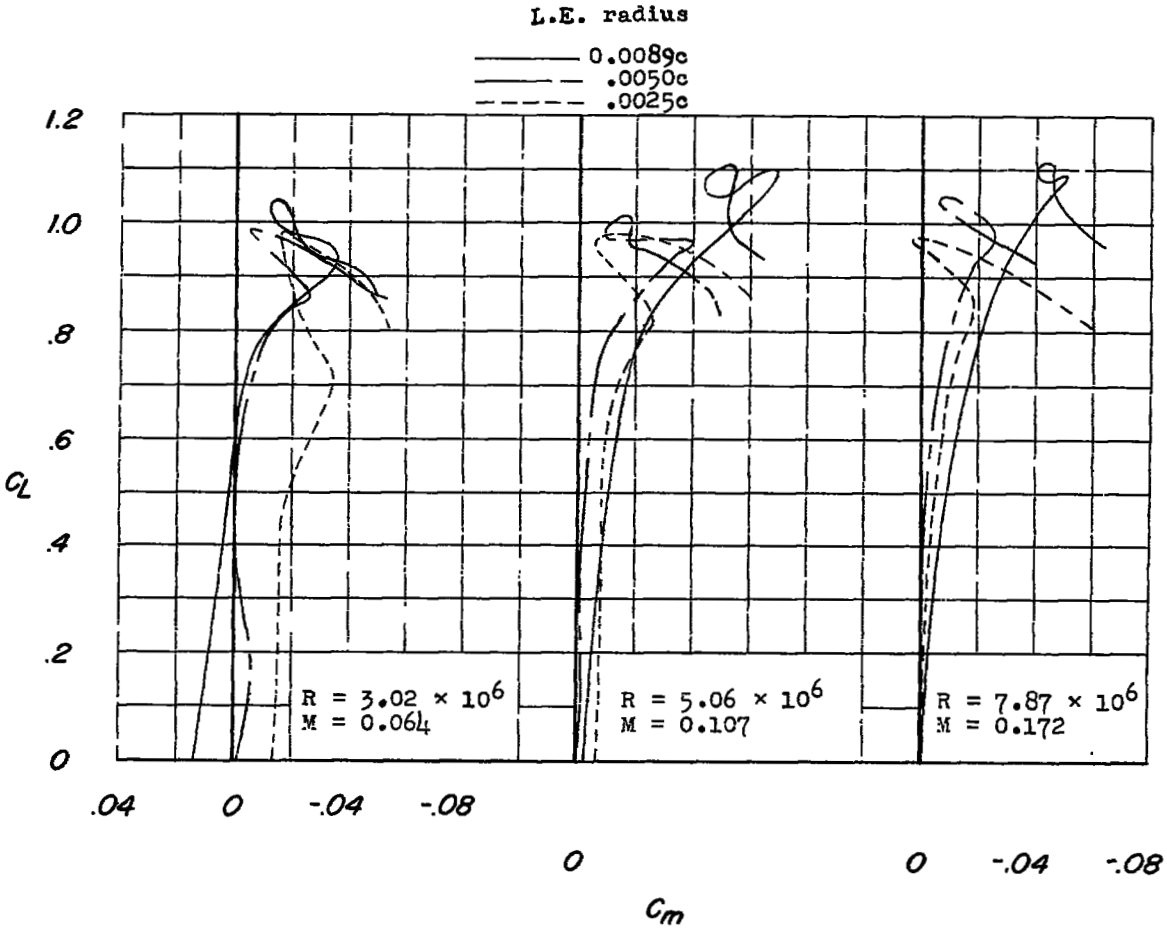

(b) Pressure, 33 pounds per square inch.

Figure 14.- Concluded.

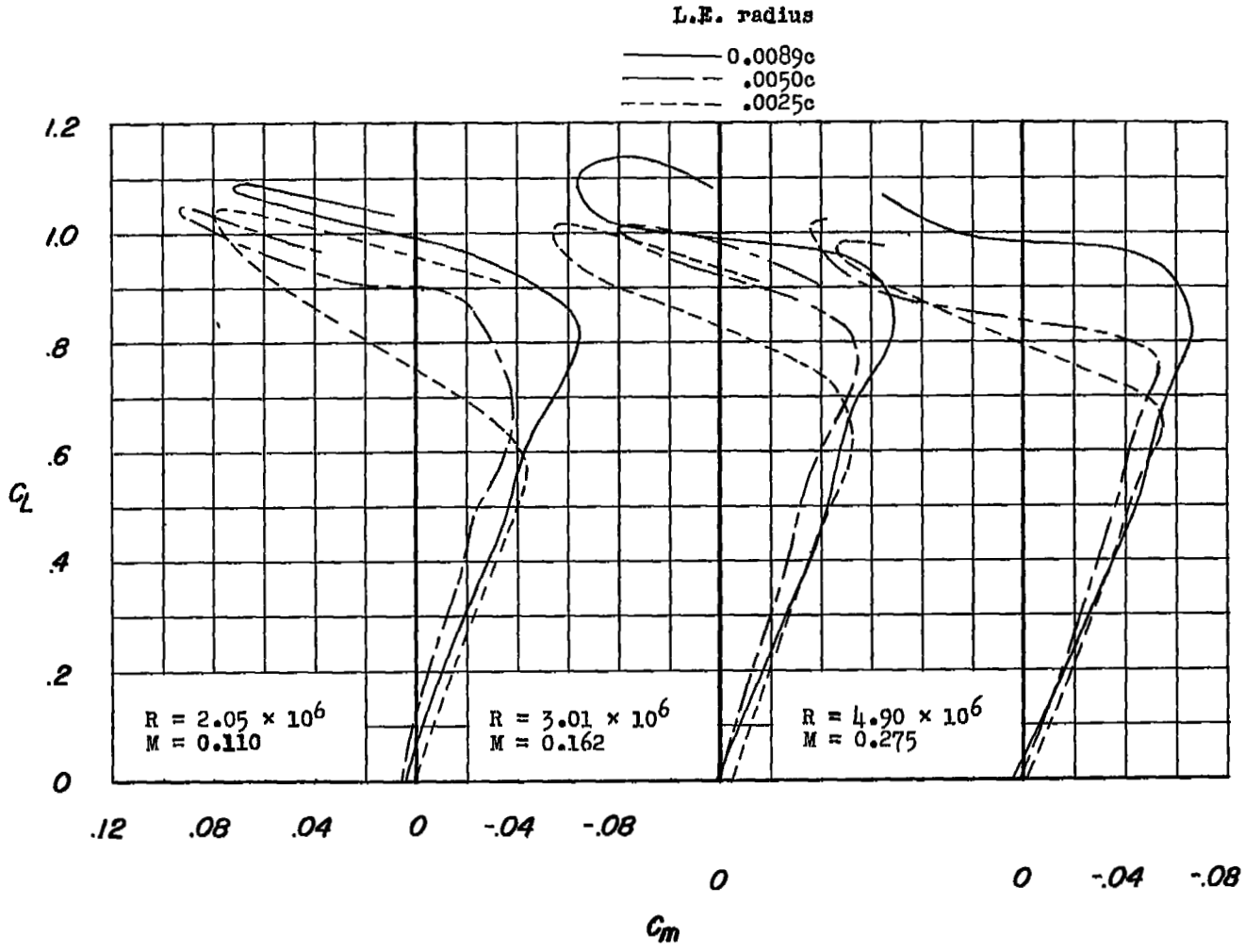

(a) Atmospheric pressure.

Figure 15.- Effect of leading-edge radius on the pitching-moment characteristics of a wing having 45° sweepback and an aspect ratio of 5.

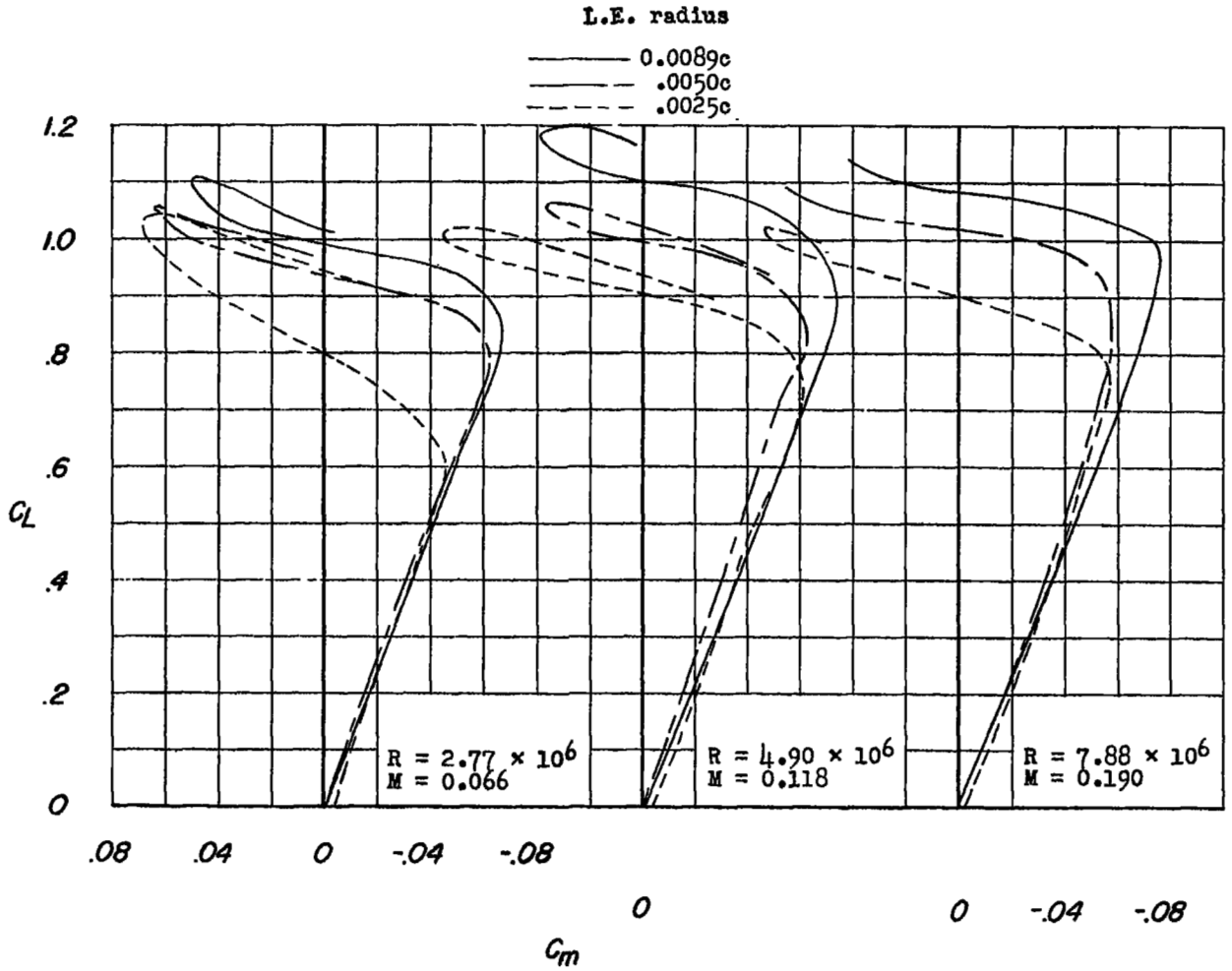

(b) Pressure, 33 pounds per square inch.

Figure 15.- Concluded.

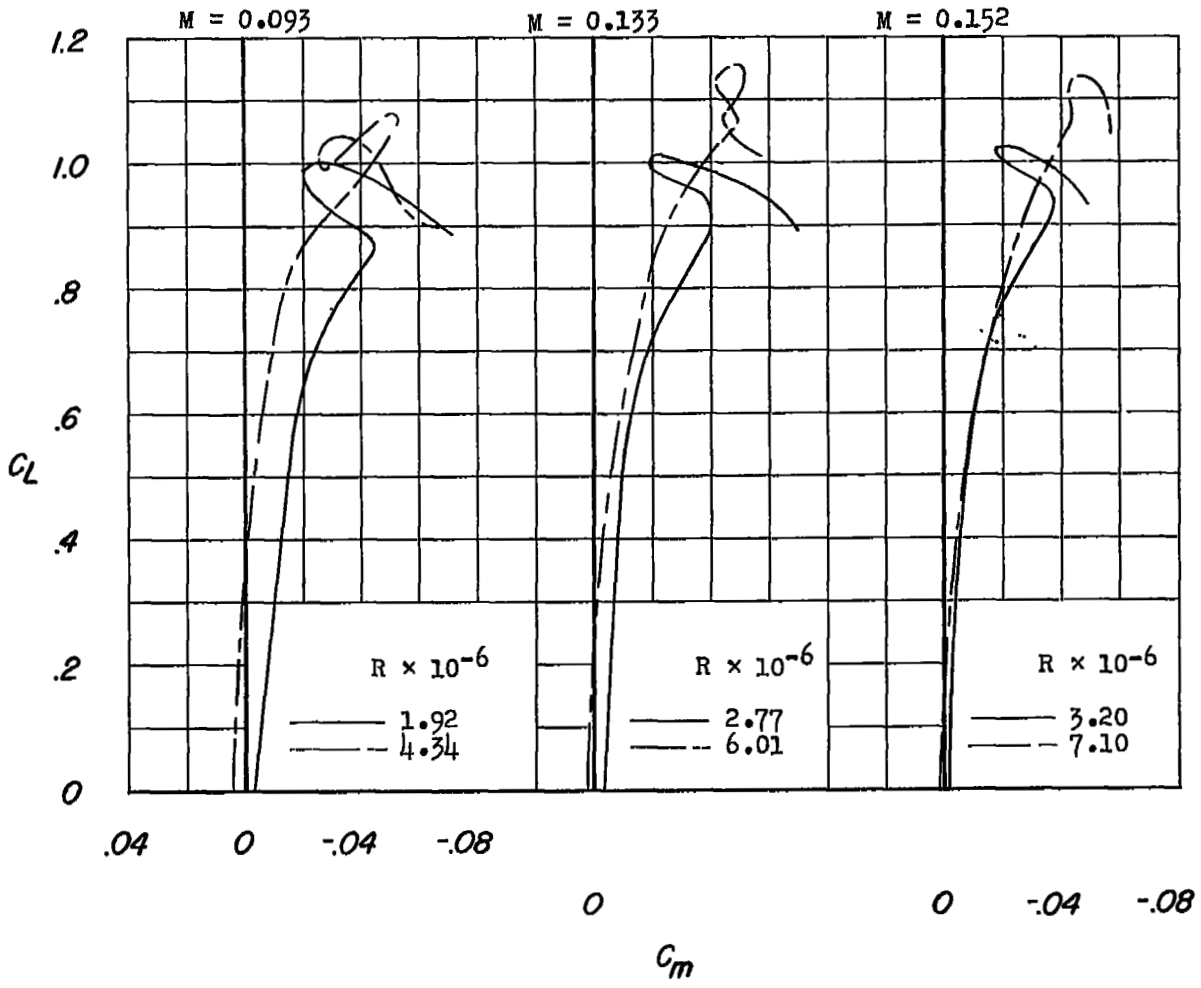

(a) Leading-edge radius 0.0089c.

Figure 16.- Effect of Reynolds number on the pitching-moment characteristics of a wing having 45° sweepback and an aspect ratio of 3.

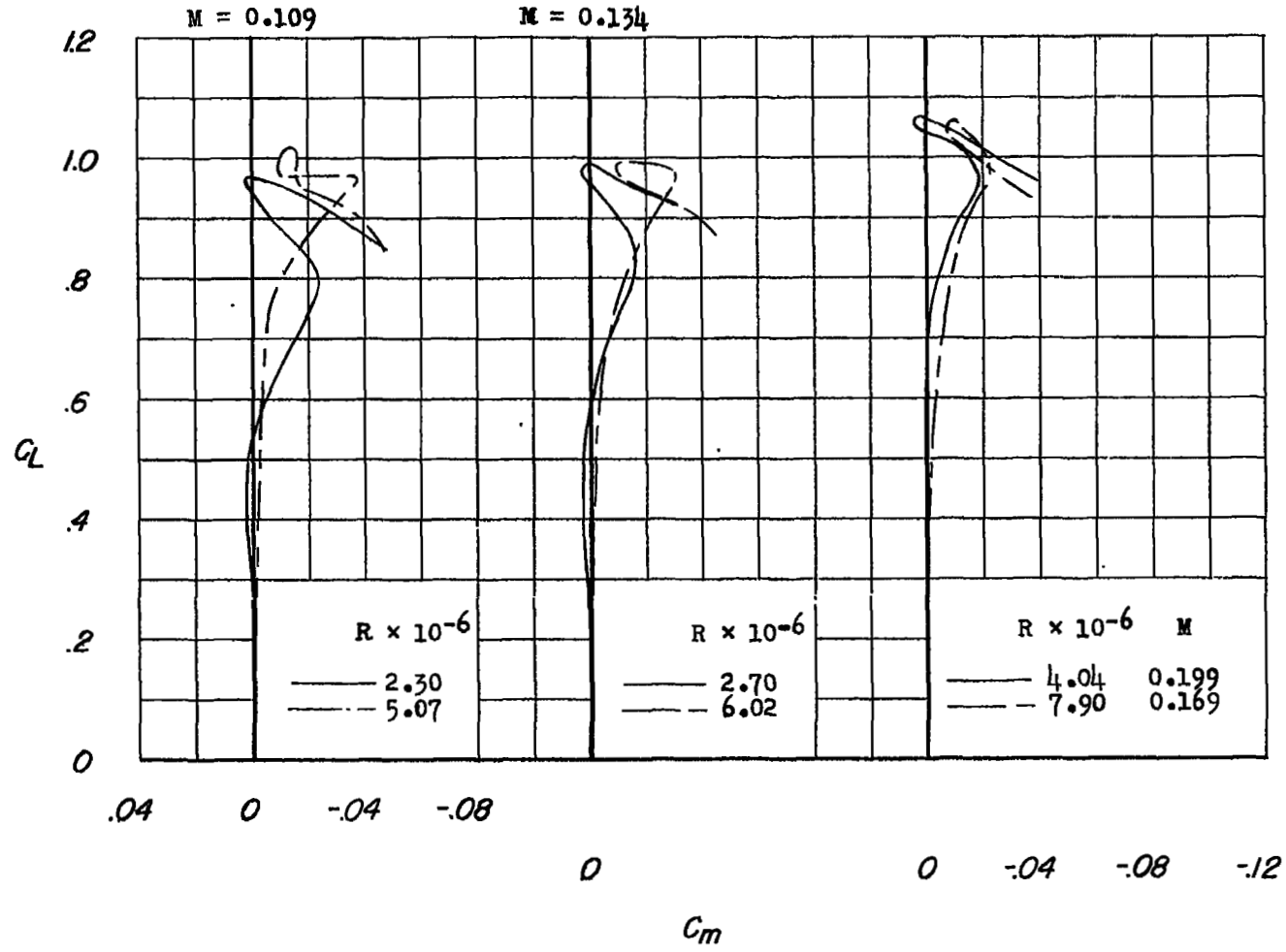

(b) Leading-edge radius of 0.0050c.

Figure 16.- Continued.

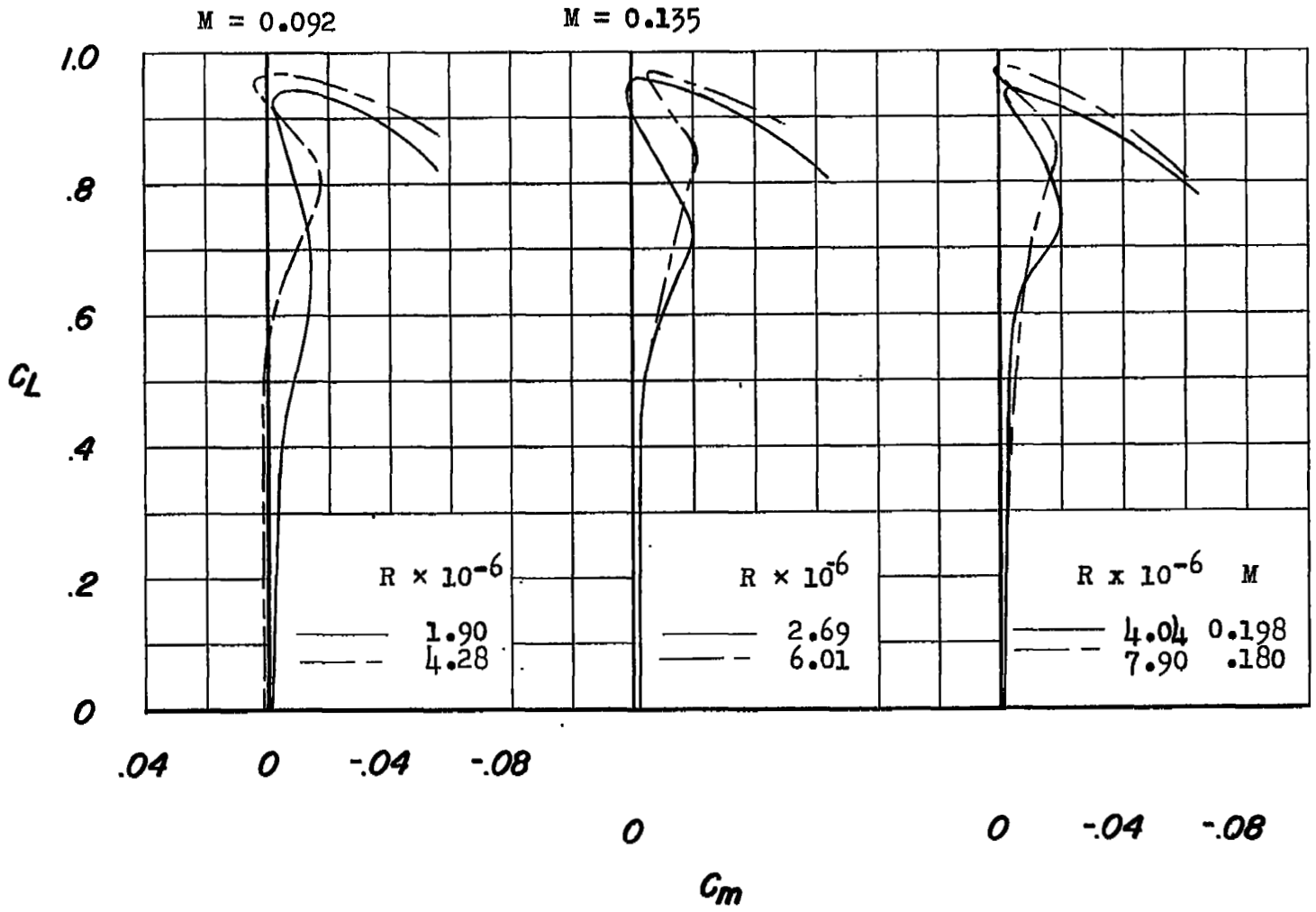

(c) Leading-edge radius of 0.0025c.

Figure 16.- Concluded.

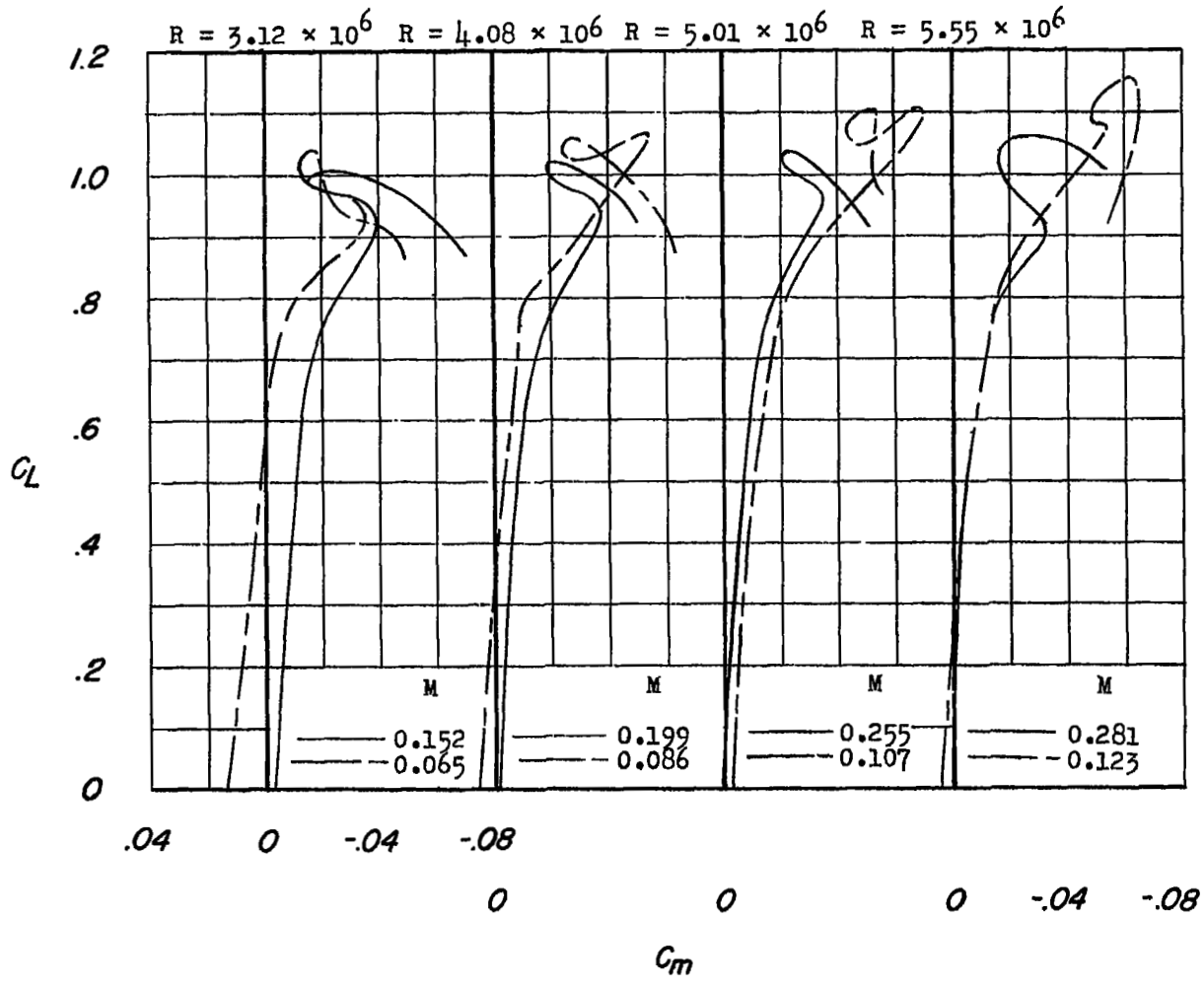

(a) Leading-edge radius of 0.0089c.

Figure 17.- Effect of Mach number on the pitching-moment characteristics of a wing having 45° sweepback and an aspect ratio of 3.

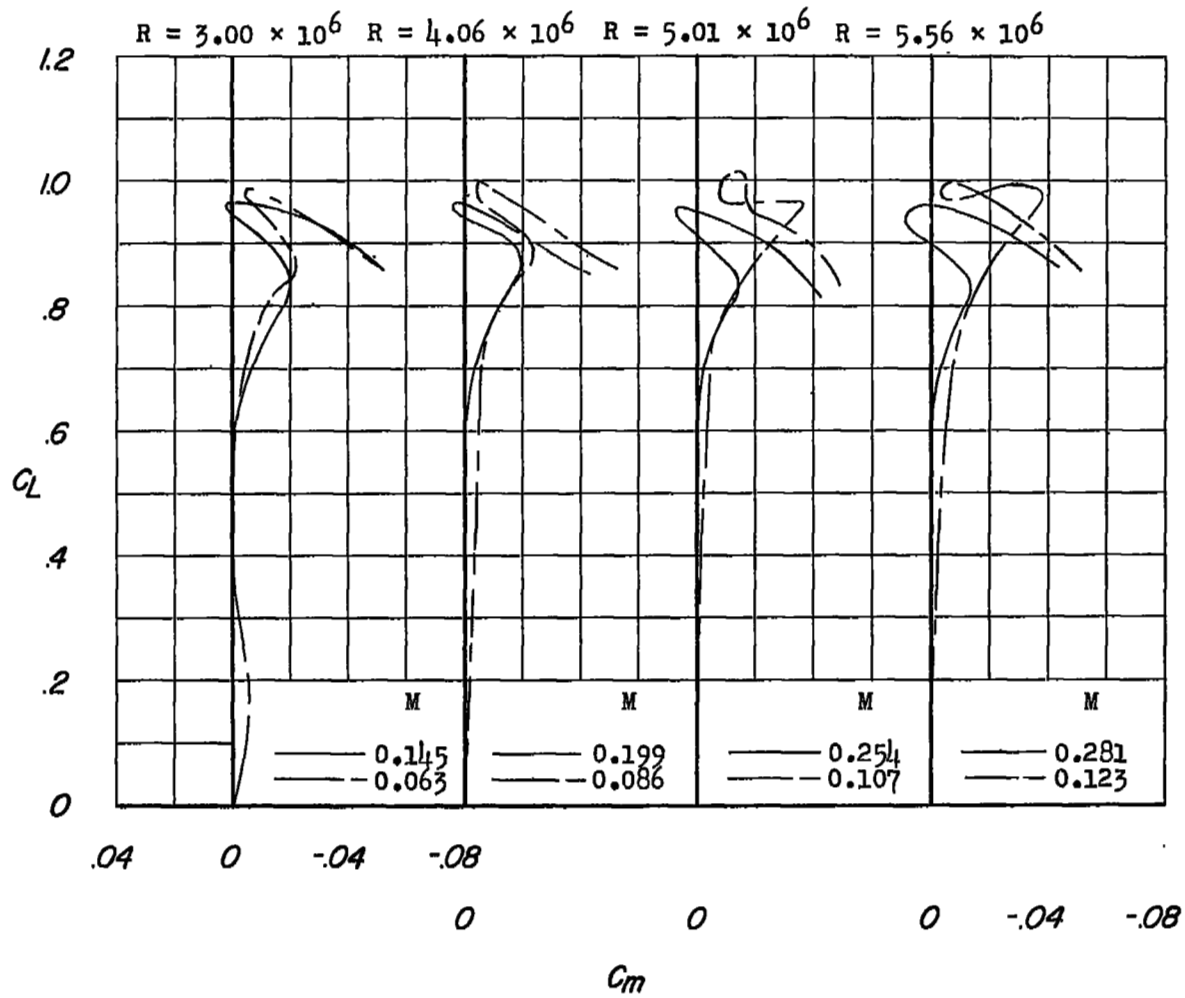

(b) Leading-edge radius of 0.0050c.

Figure 17.- Continued.

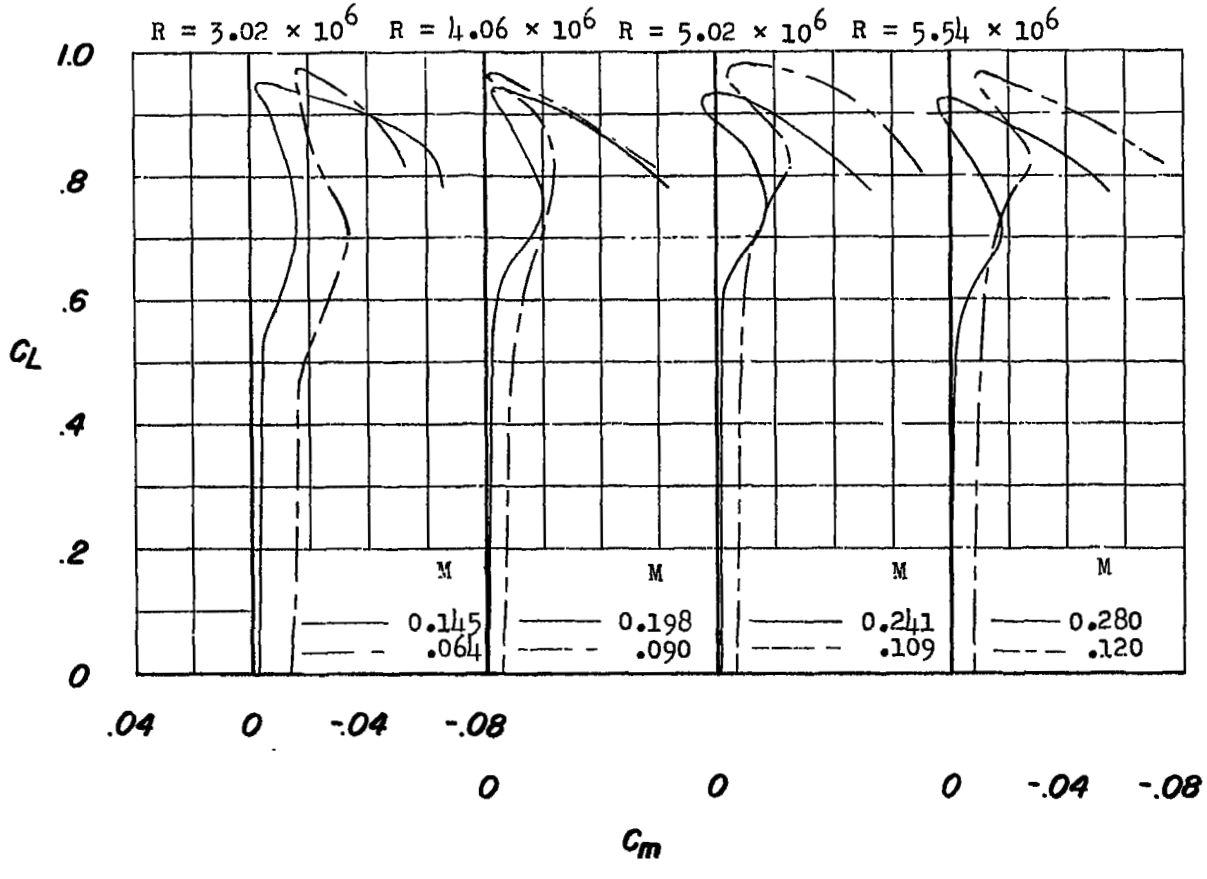

(c) Leading-edge radius of 0.0025c.

Figure 17.- Concluded.

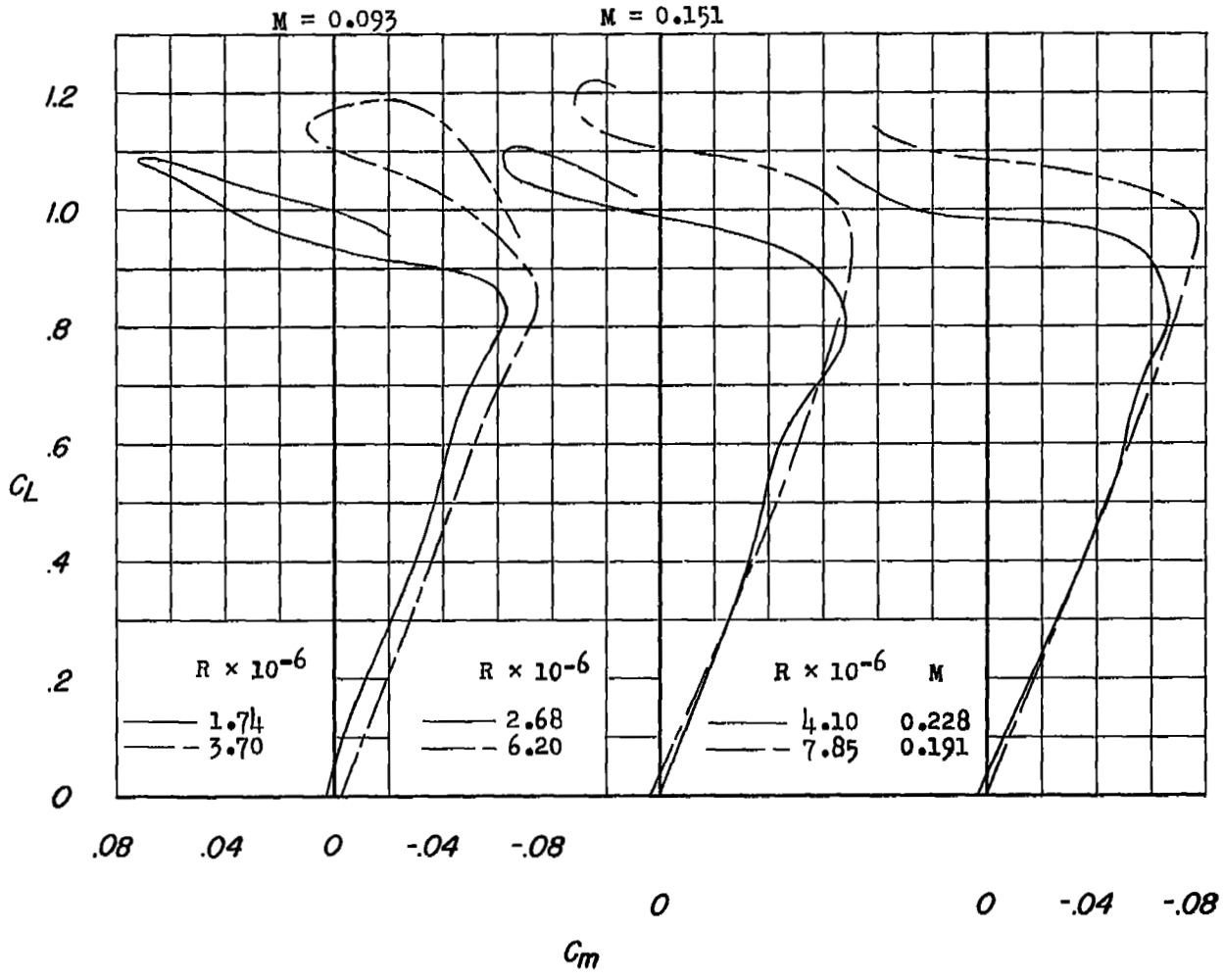

(a) Leading-edge radius of 0.0089c.

Figure 18.- Effect of Reynolds number on the pitching-moment characteristics of a wing having 45° sweepback and an aspect ratio of 5.

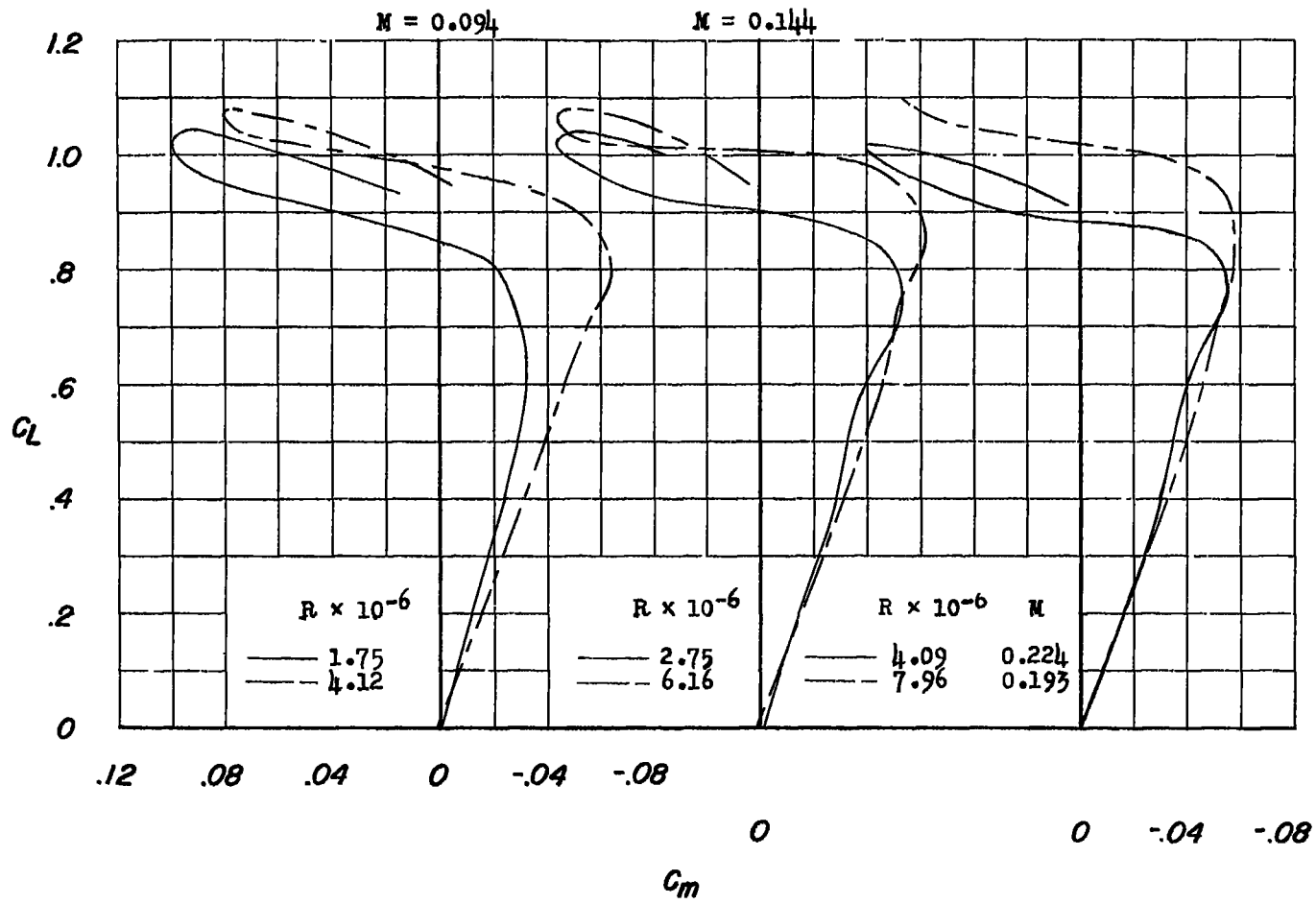

(b) Leading-edge radius of 0.0050c.

Figure 18.- Continued.

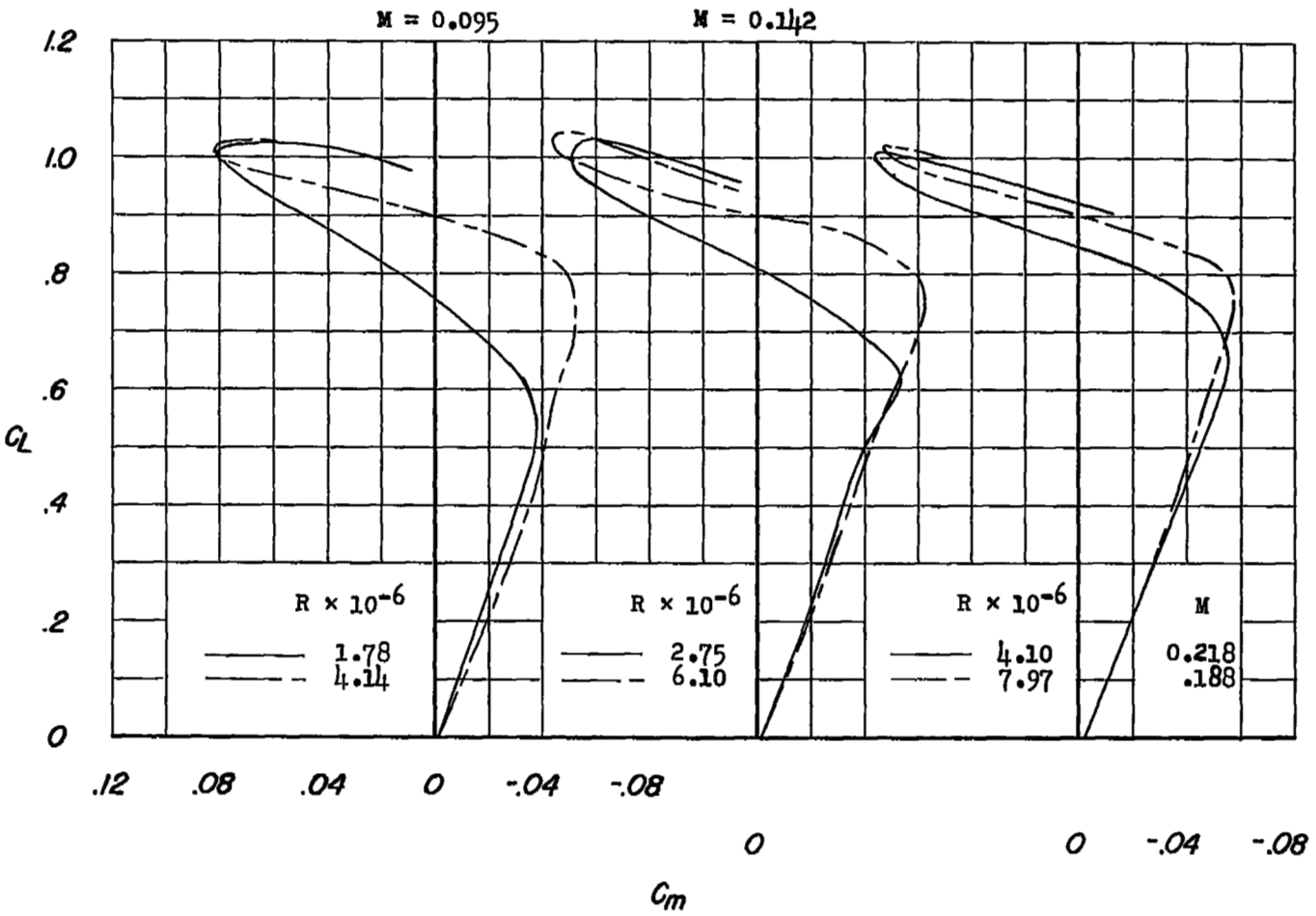

(c) Leading-edge radius of 0.0025c.

Figure 18.- Concluded.

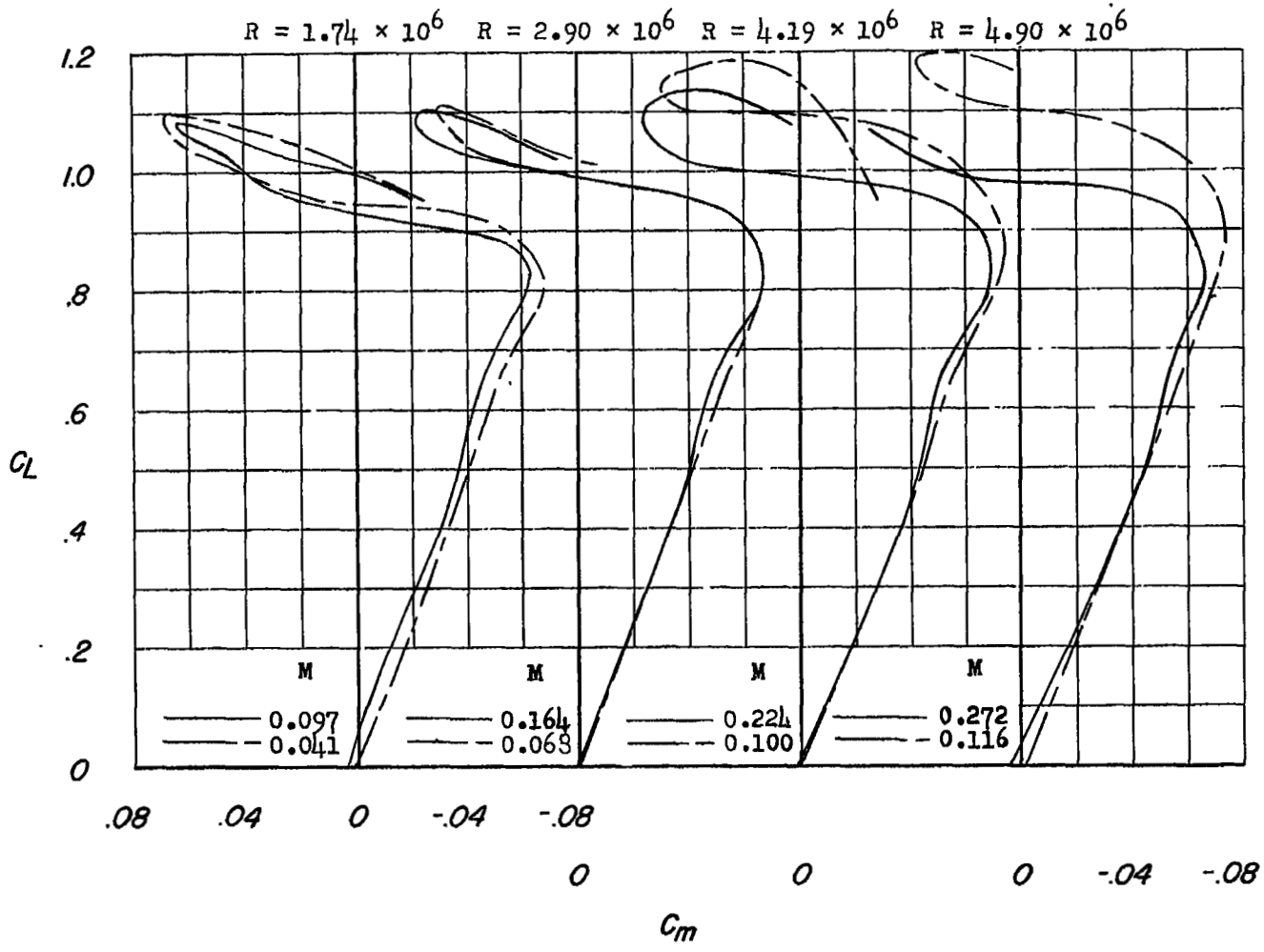

(a) Leading-edge radius of 0.0089c.

Figure 19.- Effect of Mach number on the pitching-moment characteristics of a wing having 45° sweepback and an aspect ratio of 5.

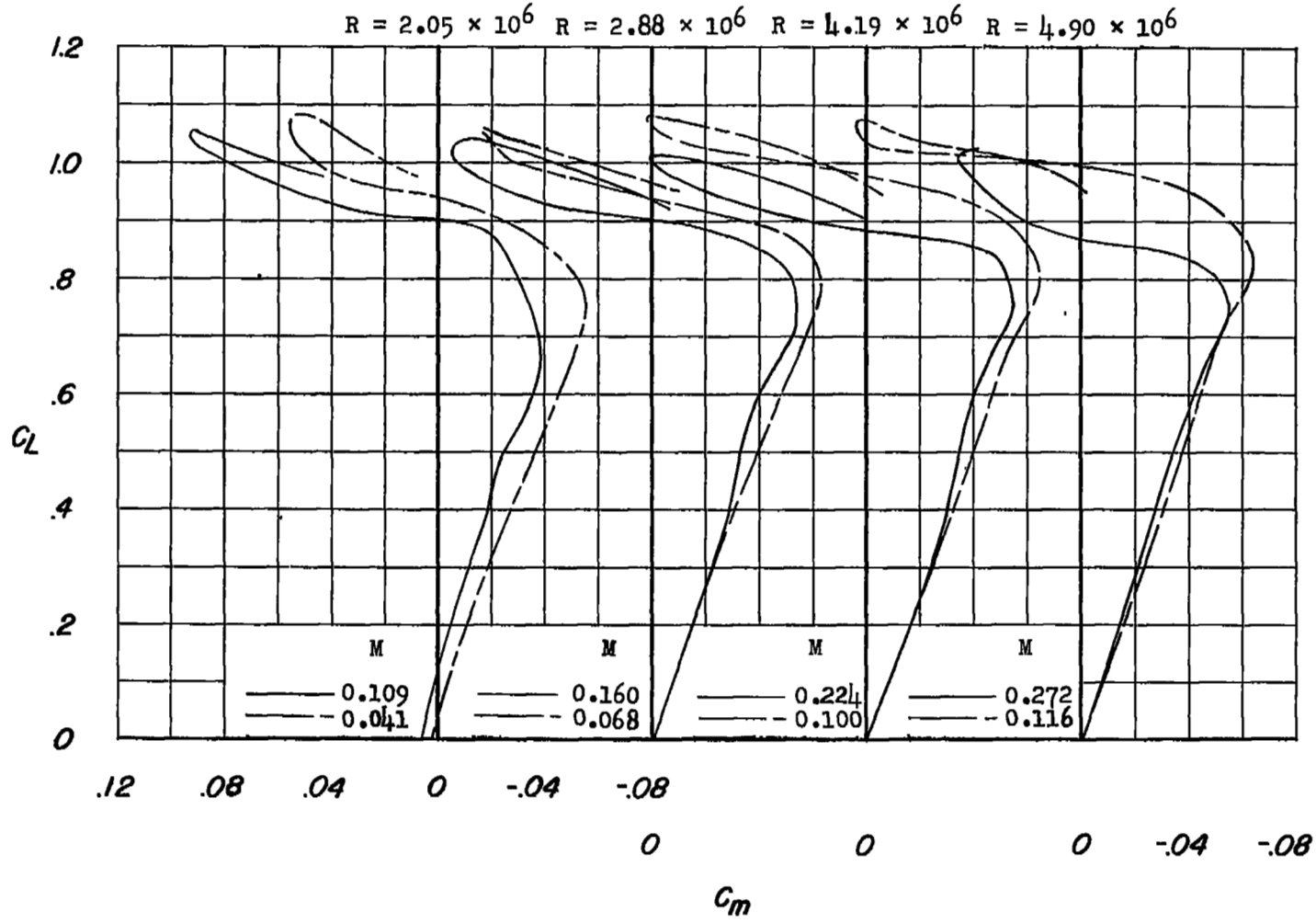

(b) Leading-edge radius of 0.0050c.

Figure 19.- Continued.

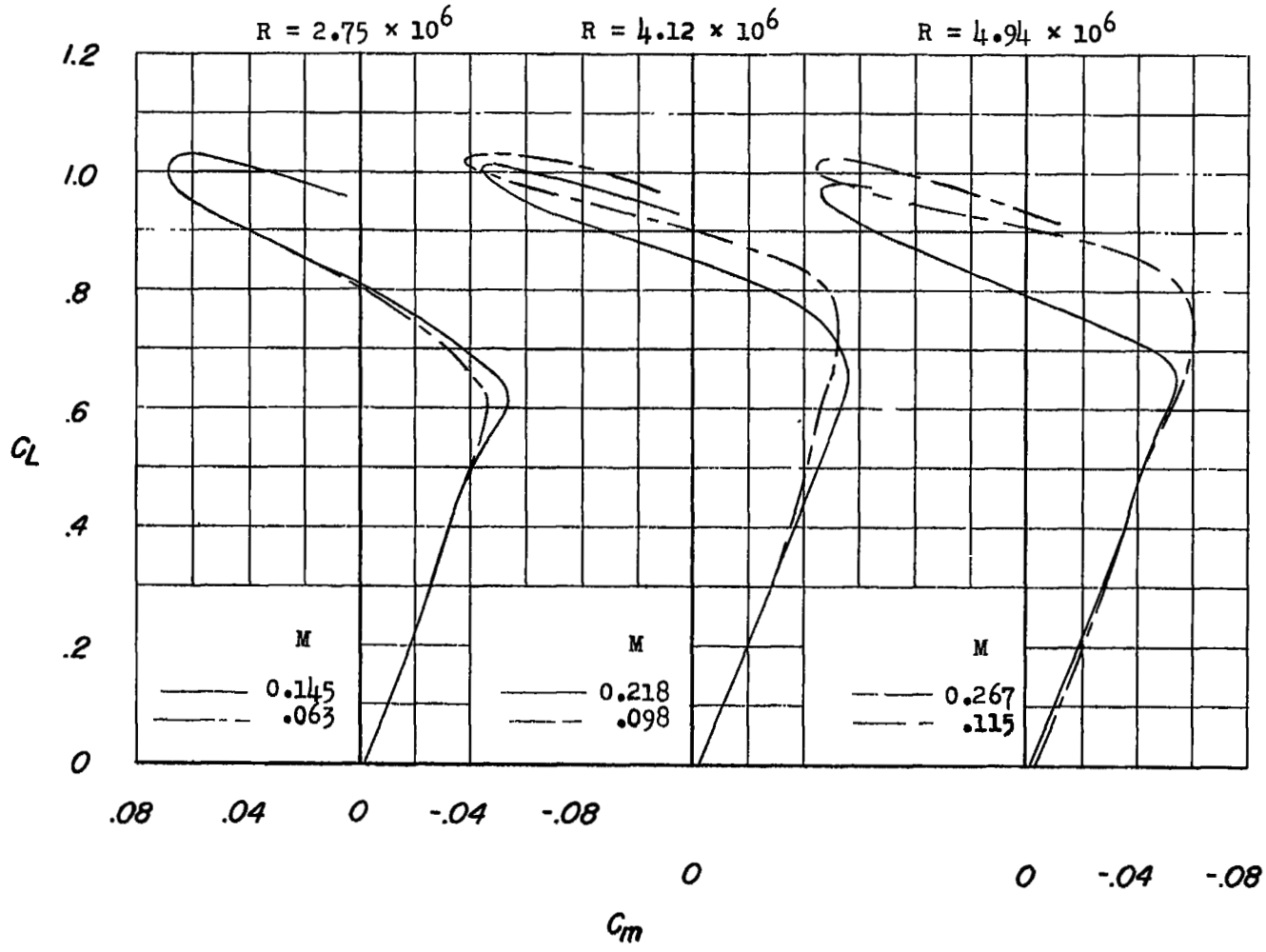

(c) Leading-edge radius of 0.0025c.

Figure 19.- Concluded.

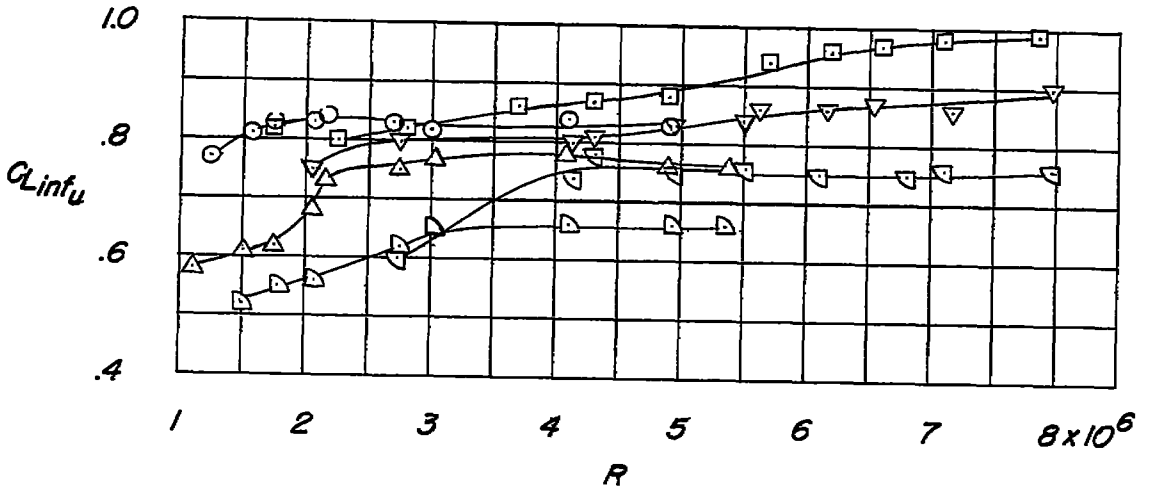

(a) Mach number effect at any Reynolds number through the Reynolds number range.

L.E. radius		
○	0.0089c	atmospheric pressure,
□	.0089c	33 pounds per square inch
△	.0050c	atmospheric pressure,
▽	.0050c	33 pounds per square inch
▷	.0025c	atmospheric pressure,
◁	.0025c	33 pounds per square inch

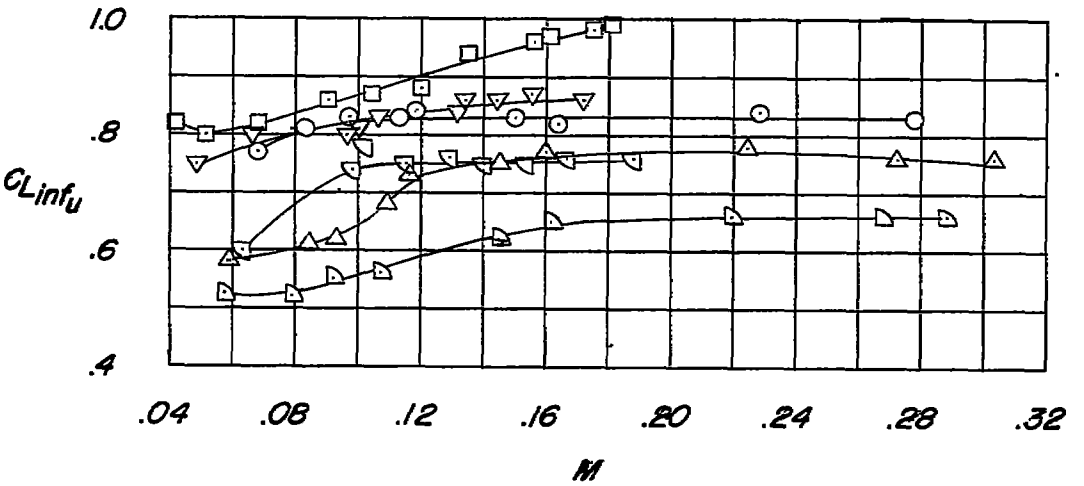

(b) Reynolds number effect at any Mach number through the Mach number range.

Figure 20.- Effect of leading-edge radius on the variation of inflection lift coefficient with Reynolds number and Mach number. Aspect ratio 5.

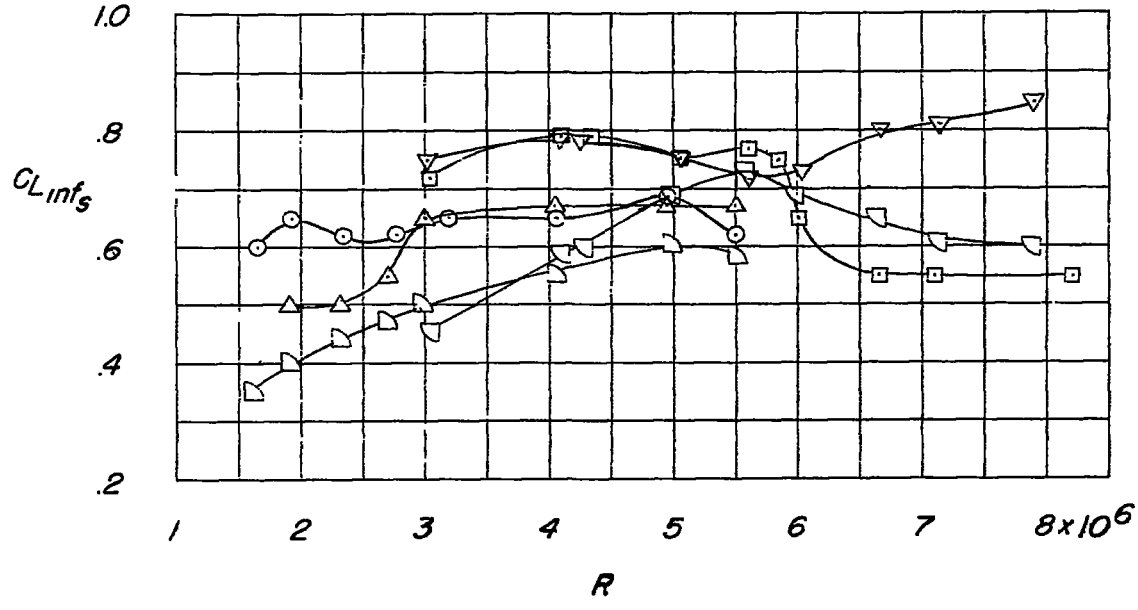

(a) Mach number effect at any Reynolds number through the Reynolds number range.

L.E. radius		
○	0.0089c	atmospheric pressure,
□	.0089c	33 pounds per square inch
△	.0050c	atmospheric pressure,
▽	.0050c	33 pounds per square inch
◺	.0025c	atmospheric pressure,
◿	.0025c	33 pounds per square inch

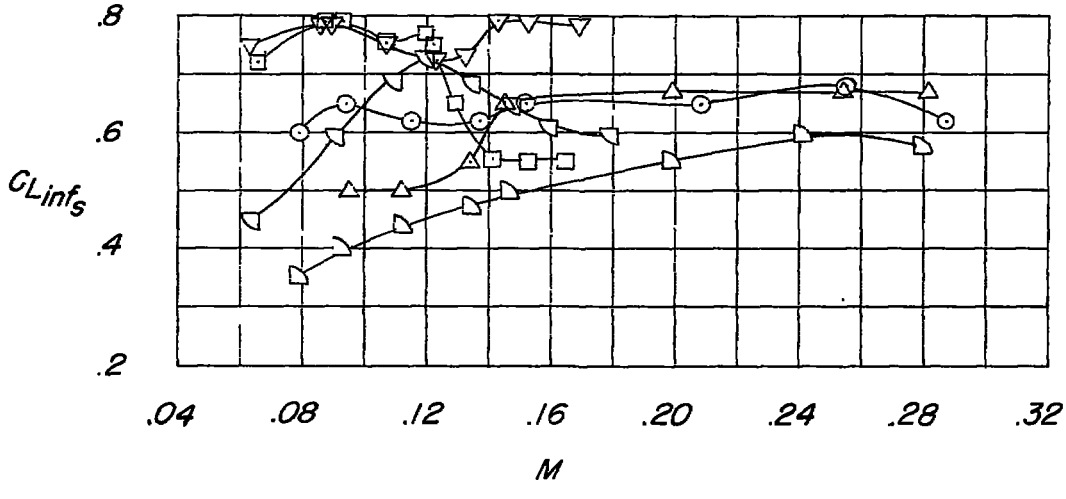

(b) Reynolds number effect at any Mach number through the Mach number range.

Figure 21.- Effect of leading-edge radius of the variation of inflection lift coefficient with Reynolds number and Mach number. Aspect ratio 3.

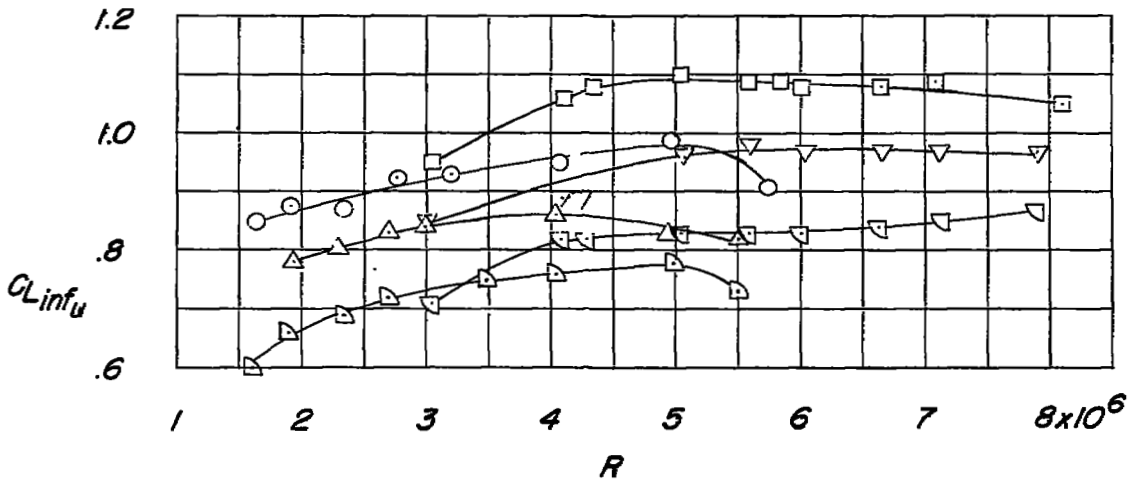

(a) Mach number effect at any Reynolds number through the Reynolds number range.

L.E. radius		
○	0.0089c	atmospheric pressure,
□	.0089c	33 pounds per square inch
△	.0050c	atmospheric pressure,
▽	.0050c	33 pounds per square inch
▷	.0025c	atmospheric pressure,
◁	.0025c	33 pounds per square inch

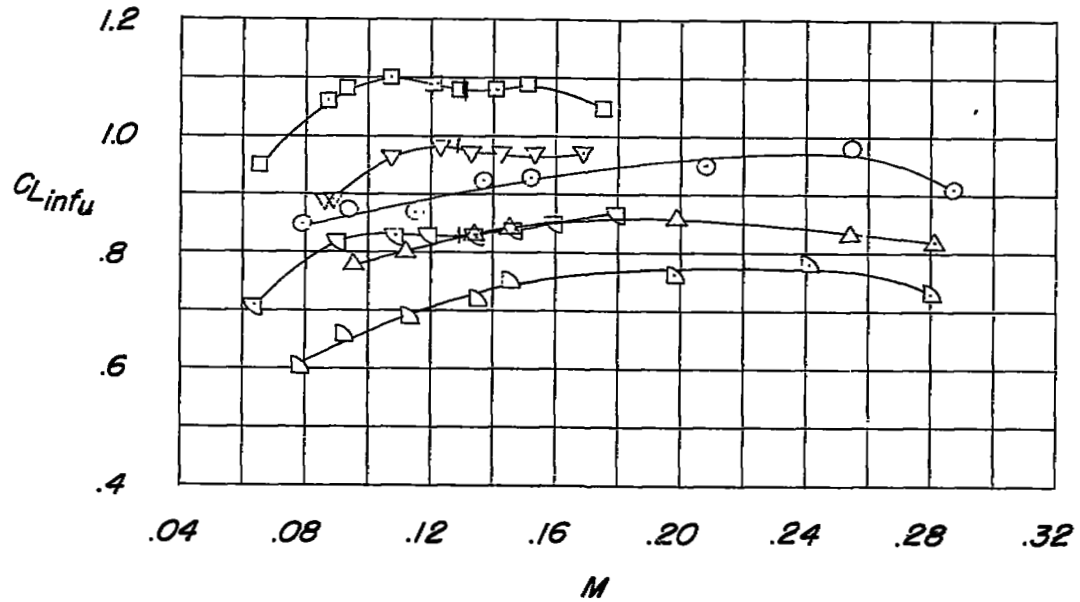

(b) Reynolds number effect at any Mach number through the Mach number range.

Figure 22.- Effect of leading-edge radius on the variation of inflection lift coefficient with Reynolds number and Mach number. Aspect ratio 3.